AD-A118 724 PANAMETRICS INC WALTHAM MASS F/G 7/4
OPERATION OF THE RAPID SCAN PARTICLE SPECTROMETER SCS ON THE SC--ETC(U)
JUN 82 F A HANSER, B SELLERS F19628-79-C-0099
UNCLASSIFIED AFGL-TR-82-0164 NL

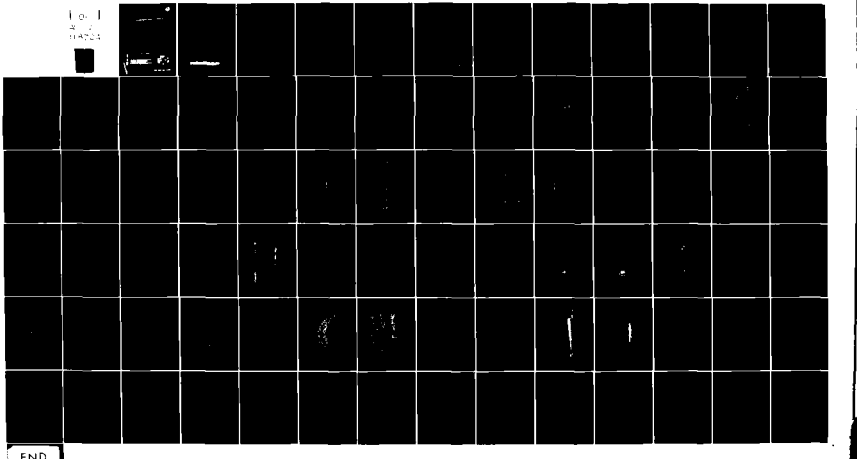

END
DATE FILMED
9 82
DTIC

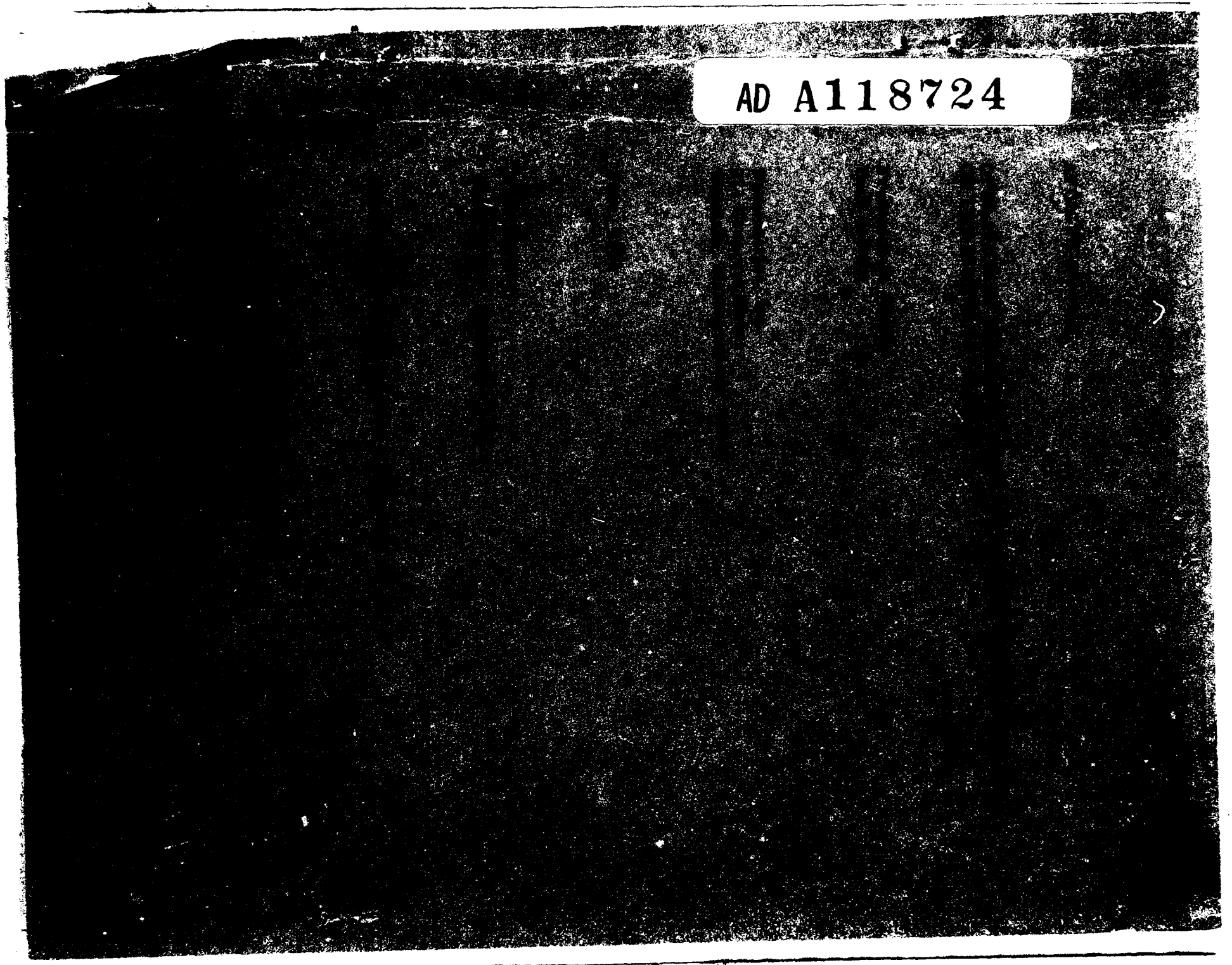

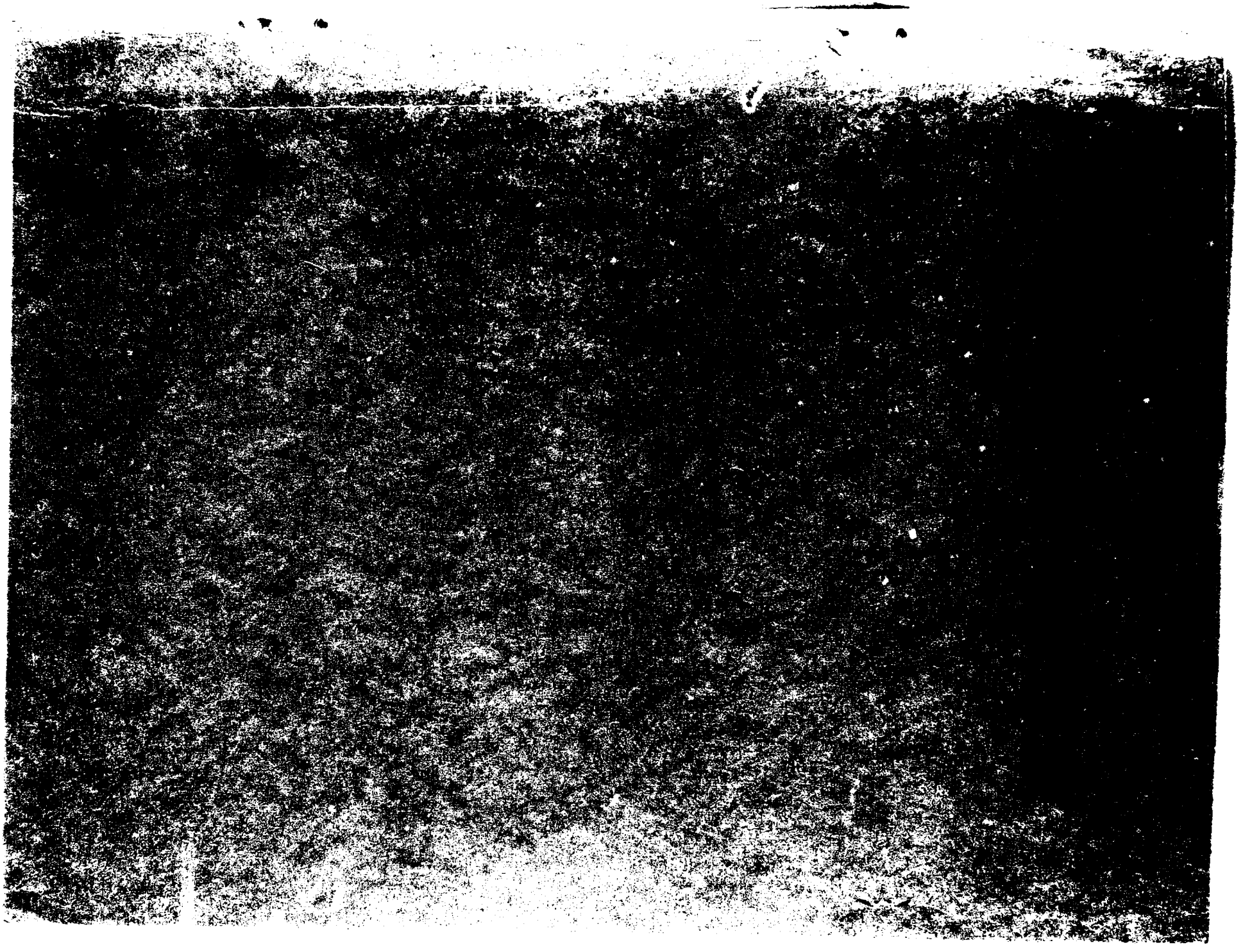

Unclassified

SECURITY CLASSIFICATION OF THIS PAGE (When Data Entered)

| REPORT DOCUMENTATION PAGE | | READ INSTRUCTIONS BEFORE COMPLETING FORM |
|---|---|---|
| 1. REPORT NUMBER<br>AFGL-TR-82-0164 | 2. GOVT ACCESSION NO.<br>AD-A118724 | 3. RECIPIENT'S CATALOG NUMBER |
| 4. TITLE (and Subtitle)<br>Operation of the Rapid Scan Particle Spectrometer SC5 on the SCATHA Satellite | | 5. TYPE OF REPORT & PERIOD COVERED<br>Final Report<br>April 1979-December 1981<br>6. PERFORMING ORG. REPORT NUMBER |
| 7. AUTHOR(s)<br>Frederick A. Hanser<br>Bach Sellers | | 8. CONTRACT OR GRANT NUMBER(s)<br>F19628-79-C-0099 |
| 9. PERFORMING ORGANIZATION NAME AND ADDRESS<br>Panametrics, Inc.<br>221 Crescent Street<br>Waltham, Massachusetts 02254 | | 10. PROGRAM ELEMENT, PROJECT, TASK AREA & WORK UNIT NUMBERS<br>62101F<br>766106 AI |
| 11. CONTROLLING OFFICE NAME AND ADDRESS<br>Air Force Geophysics Laboratory<br>Hanscom AFB, MA 01731<br>Contract Monitor: Arthur Wendle / PHG | | 12. REPORT DATE<br>June 1982<br>13. NUMBER OF PAGES<br>81 |
| 14. MONITORING AGENCY NAME & ADDRESS(if different from Controlling Office) | | 15. SECURITY CLASS. (of this report)<br>Unclassfied<br>15a. DECLASSIFICATION/DOWNGRADING SCHEDULE |

16. DISTRIBUTION STATEMENT (of this Report)

Approved for public release; distribution unlimited

17. DISTRIBUTION STATEMENT (of the abstract entered in Block 20, if different from Report)

18. SUPPLEMENTARY NOTES

19. KEY WORDS (Continue on reverse side if necessary and identify by block number)

Satellite Particle Spectrometer
Electron flux measurements
Proton flux measurements
High time resolution particle measurements
SCATHA Particle measurements

20. ABSTRACT (Continue on reverse side if necessary and identify by block number)

The SC5 Rapid Scan Particle Spectrometer on the SCATHA satellite was designed to measure electrons and protons from 0.05 to 500 keV. Electrostatic analyzers (ESA's) are used for the 0.05 to 70 KeV range, with 8 energy bins, and solid state spectrometers (SSS's) are used for the higher energy range. Two complete detector sets view in perpendicular and parallel directions to the satellite spin axis, and

DD FORM 1 JAN 73 1473 EDITION OF 1 NOV 65 IS OBSOLETE

Unclassified

SECURITY CLASSIFICATION OF THIS PAGE (When Data Entered)

a complete set of spectra is measured once per second. With a 57 second spin period, the perpendicular detector set provides pitch angle distributions with 6° resolution. The SC5 instrument can also be connected to a broad-band FM channel where the output of any one detector can be viewed with 250 microsecond time resolution.

The SCATHA satellite was launched on 30 January 1979, and SC5 was turned on on 9 February 1979. Since then it has provided a considerable amount of particle data for an environmental atlas, and much unique data, especially from the high time resolution FM band, for electron and ion gun operations. The complete detector set has operated properly for over a year, well in excess of the design life of six months. The only performance degradation is in the SEM detector gain of the ESA's, an expected and unavoidable occurrence. Most of the degradation in the result of the high count rates from the electron gun operations, which are necessary to give reasonable statistical accuracy to the high time resolution measurements. After nearly three years in orbit only the low energy perpendicular electron ESA SEM was unusable at the highest SEM bias level, so 7 of 8 SEM's have survived for this time period.

The SC5 data analysis procedure is described, and several examples of reduced spectra and pitch angle distributions are given. Some examples of FM data from the electron gun operations are also given. The ESA SEM efficiency factors for the first year of operation are shown in graphical and tabular form. The reduced spectra are in excellent mutual agreement, with different detectors giving the same flux values for the same pitch angle/energy values. The FM data from electron gun operations show the satellite response to beam operations to better than 1 millisecond time resolution. The SC5 instrument has provided a large, and in some ways unique, particle measurement data set for the near-geosynchronous environment.

## FOREWORD

The work described in this report was carried out under contract to the Air Force Geophysics Laboratory, Hanscom Air Force Base, Massachusetts. The contract monitors were Dr. David A. Hardy and Lt. Arthur Wendle of the Space Physics Group (PHG). The satellite operations for the SCATHA SC5 instrument were carried out under the supervision of Dr. Hardy, and of other personnel at the AFGL and the Air Force Satellite Control Facility in Sunnyvale, California. Data reduction and analysis were carried out in cooperation with Dr. Hardy, Mr. Gary Mullen, and other AFGL personnel. The help and cooperation of all these personnel is greatly appreciated.

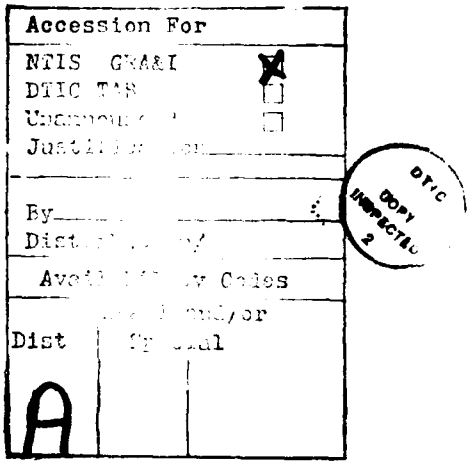

TABLE OF CONTENTS



## LIST OF ILLUSTRATIONS

LIST OF ILLUSTRATIONS (Con't)

LIST OF TABLES

# 1. INTRODUCTION

Over the past decade it has become accepted that satellites, particularly those in geosynchronous orbit, can undergo significant charging as a result of interaction with ambient particle fluxes. This charging, particularly the differential charging between various insulators and conductors on a satellite, can lead to discharges that affect satellite operation, and in severe cases can cause significant damage to sensitive electronic components. The SCATHA satellite (Ref. 1.1) was instrumented to investigate the various aspects of natural and artificial spacecraft charging in the near geosynchronous orbit region.

The SC5 payload on the SCATHA satellite was designed to provide high time resolution particle spectra. The instrument detects electrons and ions in two directions, with a complete spectrum being measured every second (Refs. 1.2, 1.3, 1.7). The Particle spectra are measured by low energy ESA's (4 energy channels covering 50 eV to 2 keV), high energy ESA's (4 energy channels covering 2 keV to 70 keV), anti-coincidence solid state spectrometers (SSS's) (5 energy ranges, 30-550 keV for electrons, 100-500 keV for protons), and coincidence SSS's (electrons to 1 MeV, protons to 8 MeV). One set of detectors views along the satellite spin axis, and one set views perpendicular to the spin axis. The SC5 instrument can also provide 250 μsec time resolution for any one detector/energy channel on a broad-band FM telemetry channel.

The SCATHA (Spacecraft Charging at High Altitudes) satellite was launched on 30 January 1979. The satellite remained in a highly elliptical transfer orbit (low altitude to geosynchronous altitude) until final orbit insertion on 2 February 1979. The final satellite orbit is elliptical and near geosynchronous, ranging from 5.3 Re to 7.8 Re (referenced to earth center), with a 7.9° inclination, and a 6°/day eastward drift. The SC5 (Rapid Scan Particle Detector) payload was turned on for the first time on 9 February 1979, successfully checked out, and thereafter remained on for most of the time.

The SCATHA satellite was originally specified for a minimum six month life, but was still in operation nearly three years later. The SC5 payload is designed for many years of operation, except for gain degradation in the SEM (Spiraltron Electron Multiplier) detectors of the ESA's. Most SEM gain degradation has taken place in the low energy electron ESA's, with a substantial fraction of the degradation caused by the high fluxes during electron gun operations, but even they have provided more than a year of useful data. After more than two years in orbit only the perpendicular low energy electron ESA had suffered severe gain degradation, with all other ESA's still providing useful data.

The operation of the SC5 instrument in orbit can be separated broadly into three categories: normal operation; eclipse season operation; and operation with the electron/ion guns. Because of the orientation of the earth's orbit and the SCATHA orbit, the satellite undergoes earth eclipses twice a year, near the equinoxes. During eclipses the satellite loses its photoelectron cloud, and thus becomes more susceptible to charging. The SC5 operations during eclipse season are thus modified to include all eclipse periods for active data taking. Operations with the electron and/or ion guns (SC4-1 and SC4-2) are generally planned in detail, with active experimenter observation in real time. This is necessary to avoid excessive damage to the ESA SEM's from the high particle fluxes that can be generated by the guns. All other operations are considered normal operations, and form the bulk of the SC5 data. A more detailed discussion of SC5 orbital operations is given in Section 2.

The major component of SC5 data reduction is the correction of the ESA data for SEM detection efficiencies. The SEM efficiencies vary with time, so this involves the use of a considerable amount of calibration data reduction. Much of the SC5 data is then used for a "data atlas" to establish a statistical particle environment for the near geosynchronous orbit region (Ref. 1.4, 1.5.) For more precise spectral determinations the ESA data must also be corrected for their broad energy resolution.

Some of the results of SC5 operation have already been presented at the "Spacecraft Charging Technology 1980" conference (Refs. 1.6, 1.8, 1.9, and some additional papers, all in Ref. 1.5). The SCATHA satellite has been observed to charge to several kV on a number of occasions in eclipse, and to hundreds of volts in sunlight, from natural particle fluxes. During gun operations the satellite has been charged to beam potential many times. Thus far, the SCATHA satellite has not been damaged by the many natural charging events that have occured, although some damage was caused by arcing during high power electron gun operations (Ref. 1.10). While SCATHA has not been significantly affected by natural charging, it should be noted that many other operational satellites in geosynchronous orbit have experienced operational anomalies correlated with magnetospheric conditions suitable for spacecraft charging. Recent data indicate that the Geostationary Operational Environmental Satellites (GOES) have experienced operational anomalies correlated with geomagnetic activity (Kp) and the midnight to dawn local time region (Ref. 1.11) indicative of a spacecraft charging cause although no on-board data are available to verify this.

Following the discussion of SC5 operations in Section 2, the data reduction procedures and ESA SEM efficiency factor histories are given in Section 3. Examples of reduced data are given in Section 4, and concluding remarks are given in Section 5. The detailed tabulation of the SEM efficiency factors used for data analysis, particularly for the data atlas (Refs. 1.4, 1.6), are given in the Appendix.

## 2. ORBITAL OPERATIONS OF SC5

### 2.1 Normal Operation

The SC5 instrument was turned on and underwent initial checkout on 9 February 1979. Thereafter, SC5 was left on continuously except for attitude maneuvers and gun operations. Details of the initial operations are

described in Ref. 1.2. The ESA SEM's can be operated in 16 different bias levels to allow the gains and efficiencies to be increased as the SEM's degrade. After first turn-on the SEM efficiencies were observed to degrade when operated in bias level 1, the lowest gain mode. This is illustrated by the efficiency plots in Fig. 2.1, which is taken from Ref. 1.2. The largest degradation took place in the low energy (LE) electron ESA's, which generally experienced the highest count rate.

After several days of operation the LE electron SEM's had only about 25% detection efficiency, so ESA operation was modified to use SEM bias level 8 for normal operation. This modified operation started on 16 Februar y 1979 (day 47). SEM gain degradation continued, so SC5 was shut off about 11 March, and turned on SSS's only on 14 March, to preserve SEM gain for the first eclipse season starting on 17 March 1979. On 17 March the ESA's were turned on again in bias level 8, and the SEM gain vs. time was measured. It was found that SEM gains decreased while on, and recovered when off, and this led to the design of operating modes with about 50% on/50% off time for the ESA's. The SSS's suffer no degradation and are left on continuously.

The SC5 ESA's also have an operating mode which allows the ESA high voltage (SEM biases, mainly) to be shut off when the perpendicular detectors sweep past the sun. The satellite spin axis is oriented perpendicular to the sun-earth line and is in the orbital plane, so the perpendicular detectors view the sun once per 57 sec spin period. Because of the high count rates from scattered solar UV, the perpendicular ESA SEM's degrade faster than the parallel ESA SEM's, so the auto-shut-off B mode was enabled to reduce this effect.

The above considerations thus led to a normal operation mode being defined as follows:

1) The SSS's are to be on at all times.
2) The ESA's are to be on in bias level 8 for all real-time passes.
3) For recorded data between passes, the ESA's are to be on for one day, in an alternating cycle. When on the SEM's are to be in bias level 8 with auto-shut-off B enabled between real-time passes.

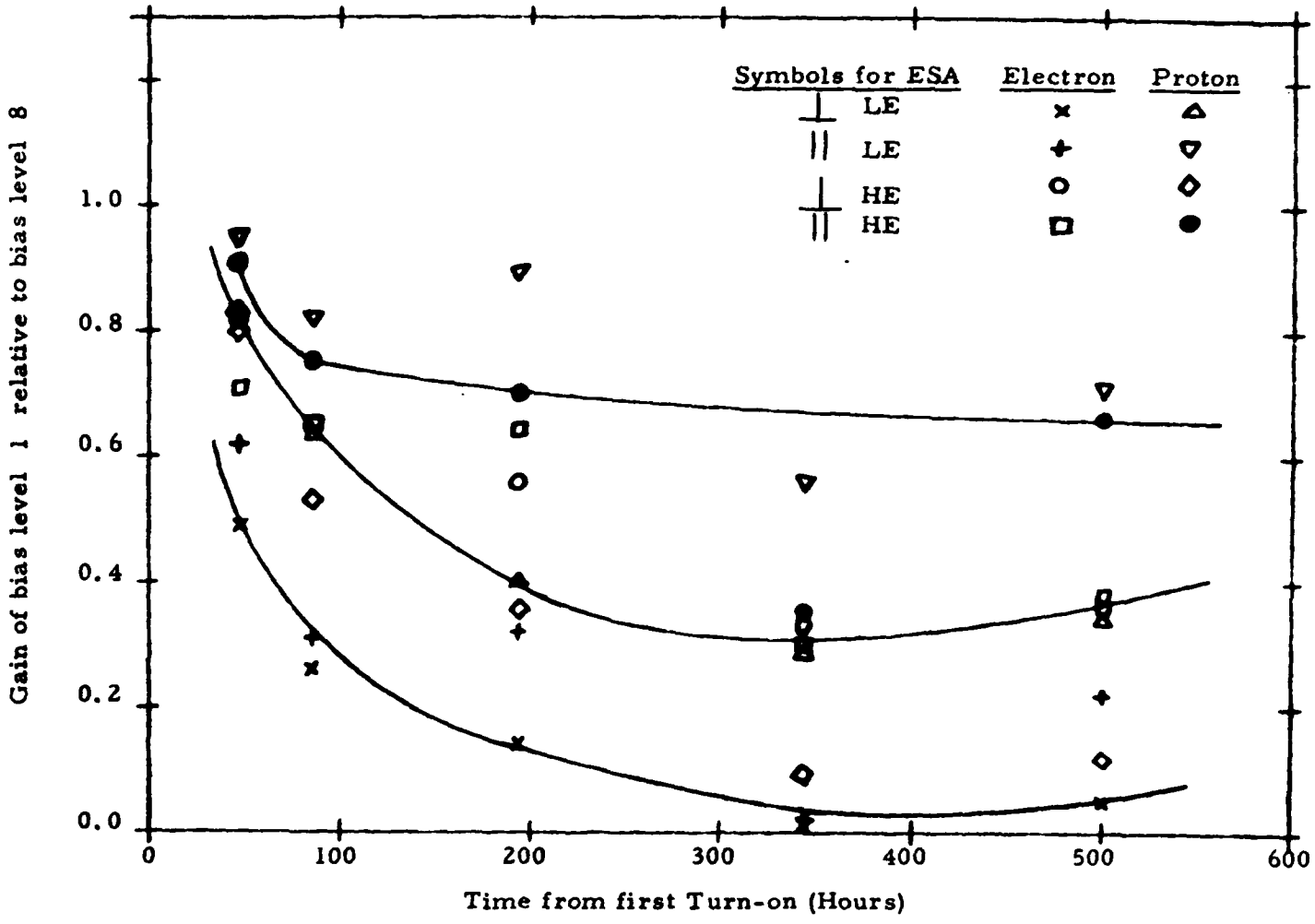


Figure 2.1 SEM Gains vs. Time After First Turn-On (From Ref. 1.2).

4) SC5 is to be off for all attitude maneuvers.

This normal mode of operation resulted in obtaining useful data from all detectors for in excess of one year. After more than two years only the perpendicular LE electron ESA had become unusable in bias level 8. The SEM efficiency histories are presented in detail in Section 3.

The SEM efficiencies are obtained from analysis of calibration cycle data. These calibration cycles consist of operating the ESA's at SEM bias levels 1, 4, 7, 10, 13, 16, and 8 for at least 70 seconds (more than one spin period) in each level. Such calibration cycles are required to be performed at least once per week, for both normal and eclipse operations.

The requirement that SC5 be off for all attitude maneuvers is to avoid possible damage to the SEM's from arcing due to the thruster gases emitted during these maneuvers. Because of the motion of the earth around the sun, the SCATHA satellite has its spin axis turning toward the sun at about $1^{o}$/day. To maintain the spin axis normal to the sun-earth line, the satellite must be torqued about once per week to undo this earth-motion drift.

## 2.2 Eclipse Season Operation

Twice each year near equinoxes the SCATHA satellite undergoes earth-eclipse once during each orbit. During eclipse the satellite's photo-electron cloud is absent and it is much more easily charged to high potentials by intense electron fluxes. Since one of the purposes of the SCATHA program is to observe the characteristics of such satellite charging, the SC5 operation mode for eclipse periods was modified to ensure complete ESA-on coverage for all eclipse periods. For the first year of SCATHA operations the eclipse periods extended from 16 March 1979 (day 75) to 30 April (day 120), and from 20 September (day 263) to 4 November (day 308).

The SC5 eclipse mode of operation was defined as follows:

1) The SSS's are on at all times.
2) The ESA's are on in bias level 8 for all real-time passes.
3) The ESA's to be turned on in the real-time pass <u>before</u> eclipse and off in the pass <u>after</u> eclipse. For between-pass tape-recorded data the ESA's are to be in SEM bias level 8 with auto-shut-off B enabled.

4) SC5 is to be off for all attitude maneuvers.

This mode of operation has worked out to several hours of continuous ESA data centered about each eclipse, plus several additional hours of ESA data from real-time passes scattered throughout the SCATHA orbit.

## 2.3 Operation with the Electron/Ion Guns

Operation of SC5 with the electron (SC4-1) and ion (SC4-2) guns on SCATHA have been approached with considerable caution. The electron gun is capable of emitting 1 μA to 13 mA of current, at 50 V to 3 kV (only to a maximum of 6 mA) potential. The ion gun is capable of emitting 0.3 to 2 mA of 1 or 2 kV energy positive $X_e$ ions. The ion gun also has a neutralizer filament capable of emitting 0.002 to 2 mA of electrons at 10 V to 1 kV energy. The SCATHA satellite is a cylinder about 1.75 m in diameter and 1.75 m high, for a total surface area of about 14.4 $m^2$. A 1 mA current of singly charged particles ($e^-$ or $X_e^+$) is $6.25 \times 10^{15}$ particles/sec, and under conditions of equilibrium satellite charge this must equal the return flux of ambient particles. For isotropic return over the entire satellite surface this gives a flux of $6.9 \times 10^9$ particles/($cm^2$-sec-sr), which for the typical peak ESA geometric factors of $10^{-4}$ $cm^2$-sr (Ref. 1.3) gives a count rate of $6.9 \times 10^5$/sec, somewhat beyond the SC5 SEM capabilities. Since much of the SCATHA surface is the insulated covering of the solar cells, the actual flux densities are likely to be much higher, and easily capable of permanently damaging the SEM's in a short period of time.

To minimize the possibility of catastrophic damage to some of the SEM's from gun operations, all of the early gun operations with SC5 were done only with SC5 data being viewed in real time. This allowed for rapid turn-off of SC5 should the data show any indications that excessive count rates were damaging any SEM. Early operations used two-station passes, with one being used for SC4 (-1 or -2) mode print-outs, and the other for the SC5 mode print-out. Later operations used single station passes with only the SC4 print-out modes, with SC5 count rates being monitored from a compressed version is the SC4 modes.

Early data showed that electron gun operations at 1 mA or above produced extremely high count rates in the LE electron ESA's, so SC5 ESA operations at these high electron beam currents were minimized. After about 3/4 of a year of operation, when most of the initally projected SC5 data had been taken, some electron gun operations at high beam currents (near 1 mA) were made. These runs used a good deal of SC5 FM high-time-resolution data, to study satellite response to beam on/off conditions. These operations also produced a rapid drop in the SEM efficiency of the LE electron ESA's, which partially recovered in the weeks after the electron gun operations. Some of the results of the SC5/gun operations are discussed in Section 4.3.

## 3. REDUCTION PROCEDURES FOR THE SC5 DATA

### 3.1 ESA Data Reduction

The ESA's measure the electron and proton spectra parallel and perpendicular to the SCATHA satellite spin axis in a total of 8 energy bins, once per second. Two dual electron/proton ESA's are used for each direction, and cover the low energy (LE) and high energy (HE) part of the total range of 50 eV to 70 keV. The principal detection characteristics of the electron and proton ESA's are given in Tables 3.1 and 3.2. For each energy channel (4 LE and 4 HE channels) the tables give the dominant energy range of the detected particles, the average detected energy, and the geometric-energy factor $G\Delta E$. The calculations are made for a flat energy spectrum, and are the zero-order response factors.

In normal operation the ESA's cycle sequentially through the four energy bins listed in Tables 3.1 and 3.2, plus a fifth background bin, staging in each bin for 0.2 second. The output counts are 12 bit words consisting of 9 bit mantissa and 3 bit exponent. A more detailed description of normal and other operation modes is given in Ref. 1.2. For normal data analysis the LE ESA's have the background count subtracted to give a net count for flux calculation. The HE ESA's usually have a negligible background contribution and so use the full count for flux calculation. The resulting counts are divided by 0.2 sec to give the count rate, and then by $G\Delta E$ to give the uncorrected flux

Table 3.1

Corrected Zero-Order Response Factors for the Electron ESA's

| | | | Parallel ESA's | | Perpendicular ESA's | |
|---|---|---|---|---|---|---|
| ESA/bin | Energy Channel # | Dominant energy range (keV) | $E_{av}$ (keV) | $G\Delta E^*$ ($cm^2$-sr-keV) | $E_{av}$ (keV) | $G\Delta E^*$ ($cm^2$-sr-keV) |
| LE/1 | 1 | 0.050-0.12 | 0.084 | 7.87-6 | 0.080 | 6.40-6 |
| LE/2 | 2 | 0.12 -0.3 | 0.210 | 2.59-5 | 0.202 | 2.45-5 |
| LE/3 | 3 | 0.3 -0.7 | 0.497 | 7.13-5 | 0.484 | 6.26-5 |
| LE/4 | 4 | 0.7 -1.8 | 1.22 | 1.56-4 | 1.24 | 1.43-4 |
| HE/1 | 5 | 1.8 -4.5 | 3.09 | 1.32-4 | 3.09 | 9.78-5 |
| HE/2 | 6 | 4.5 -11 | 7.45 | 2.27-4 | 7.44 | 1.96-4 |
| HE/3 | 7 | 11-25 | 17.8 | 5.11-4 | 18.0 | 3.98-4 |
| HE/4 | 8 | 25-70 | 45.7 | 8.51-4 | 46.1 | 7.36-4 |

*7.87-6 ≡ $7.87 \times 10^{-6}$, etc.

Table 3.2

Corrected Zero-Order Response Factors for the Proton ESA's

| | | | Parallel ESA's | | Perpendicular ESA's | |
|---|---|---|---|---|---|---|
| ESA/bin | Energy Channel # | Dominant energy range (keV) | $E_{av}$ (keV) | $G\Delta E^*$ ($cm^2$-sr-keV) | $E_{av}$ (keV) | $G\Delta E^*$ ($cm^2$-sr-keV) |
| LE/1 | 1 | 0.07-0.17 | 0.119 | 2.18-5 | 0.117 | 1.27-5 |
| LE/2 | 2 | 0.17-0.4 | 0.283 | 4.00-5 | 0.280 | 2.43-5 |
| LE/3 | 3 | 0.4-0.9 | 0.635 | 1.22-4 | 0.644 | 8.09-5 |
| LE/4 | 4 | 0.9-2.2 | 1.45 | 3.55-4 | 1.51 | 2.49-4 |
| HE/1 | 5 | 2.2-5 | 3.57 | 7.93-4 | 3.49 | 7.19-4 |
| HE/2 | 6 | 5 - 13 | 8.87 | 2.29-3 | 8.50 | 2.05-3 |
| HE/3 | 7 | 13-30 | 21.3 | 5.40-3 | 20.4 | 4.68-3 |
| HE/4 | 8 | 30-70 | 50.6 | 1.31-2 | 48.7 | 1.12-2 |

*2.18-5 $\equiv 2.18 \times 10^{-5}$, etc.

in particles/($cm^2$ - sec - sr - keV). These fluxes are then multiplied by the SEM efficiency factors (one divided by the SEM detection efficiency - a number always $\geq 1$) to give the zero order particle fluxes.

The SEM efficiency factors are derived from the weekly (or more frequent) calibration cycle data. A set of eight SEM factors is then obtained for each day by interpolation from a set of smooth curves drawn through a series of calibration results. A detailed description of the calibration results and the SEM efficiency factor histories are given in the following Section 3.1.1.

The zero order ESA fluxes are accurate for flat or near-flat energy spectra. Because of the large energy bin widths, strongly falling spectra must be corrected to give the true flux at the nominal average energy. The procedure for making this correction is described in Section 3.1.2.

### 3.1.1 SEM Efficiencies

The correct ESA fluxes can be obtained only by using the SEM detection efficiencies at the time of the measurement. The SEM efficiency factors are defined as the reciprocal of the SEM detection efficiencies, so they multiply the uncorrected fluxes to get the zero-order particle fluxes. The particle fluxes are thus given by

$$\frac{dJi}{dE} = \frac{Ni\ E_f}{T\ G\Delta E(i)} \qquad (3.1)$$

where $\frac{dJi}{dE}$ = particles/($cm^2$ - sec - sr - keV), at energy $E_{av_i}$, with $E_{av_i}$ being listed in Tables 3.1 and 3.2

$N_i$ = net counts in channel i, which is the measured count for the HE ESA's, and the measured count minus the background count for the LE ESA's

$E_f$ = the SEM efficiency factor for the ESA in question

$T$ = the count time, = 0.2 second for single counts

$G\Delta E(i)$ = the geometric-energy factor for channel i, taken from Tables 3.1 and 3.2.

The flux (3.1) is the zero-order value, which may be further corrected for spectral slope effects as described in Section 3.1.2.

The SEM efficiency factors $E_f$ are derived from calibration cycle data taken at least once per week as described in Section 2.1. The calibration cycle data are generally summed for 20 seconds midway between sun pulses to avoid solar UV contamination of the perpendicular ESA data. For each channel of each ESA (five channels/ESA, including the background channel) the relative counts as a function of bias level is calculated. The overall average for each ESA SEM is then calculated, and from the saturation value (usually bias level 16) the SEM efficiency factors for the operating bias level are calculated.

The calibration cycle data must always be checked to ensure stable particle fluxes during the 10 minute cycle. This is generally done by observing the relative flux values measured at the operating bias level before and after the calibration cycle. The typical results from a calibration cycle with stable particle fluxes is shown for the electron ESA's in Fig. 3.1. Plotted are the counts relative to a baseline count at bias level 8 before the calibration cycle starts. All four ESA's show a smooth variation of relative counts vs. bias level, with all being near full saturation (detection efficiency = 1.00 relative to the calibration geometric factors in Tables 3.1 and 3.2) at bias level 16. The averages for 3 or 4 bias level 8 counts before and after the calibration cycle are also given, and show no variations greater than 5-10%. The derived SEM efficiency factors for operation at bias level 8 are also given.

An example of a calibration cycle with varying electron fluxes is shown in Fig. 3.2. Here the data are smooth up to bias level 10, but at bias level 13 the LE electron ESA's show a large increase in flux. At bias level 16 the LE ESA's show a decrease in flux to near the earlier level, but the HE ESA's show a flux increase. Comparison of the bias level 8 counts before and after the calibration cycle show large increases from one measurement to the next. No SEM efficiency factors can be reliably derived for this calibration cycle, although the HE ESA data to bias level 10 suggest near saturation with bias level 8 efficiency factors near 1.2, in modest agreement with valid calibration data from cycles some days earlier and later.

The SEM efficiency factors can generally be obtained to 10% accuracy when the SEM's are not far from saturation at bias level 16. At times some of the SEM's are not fully saturated at bias level 16, and the efficiency

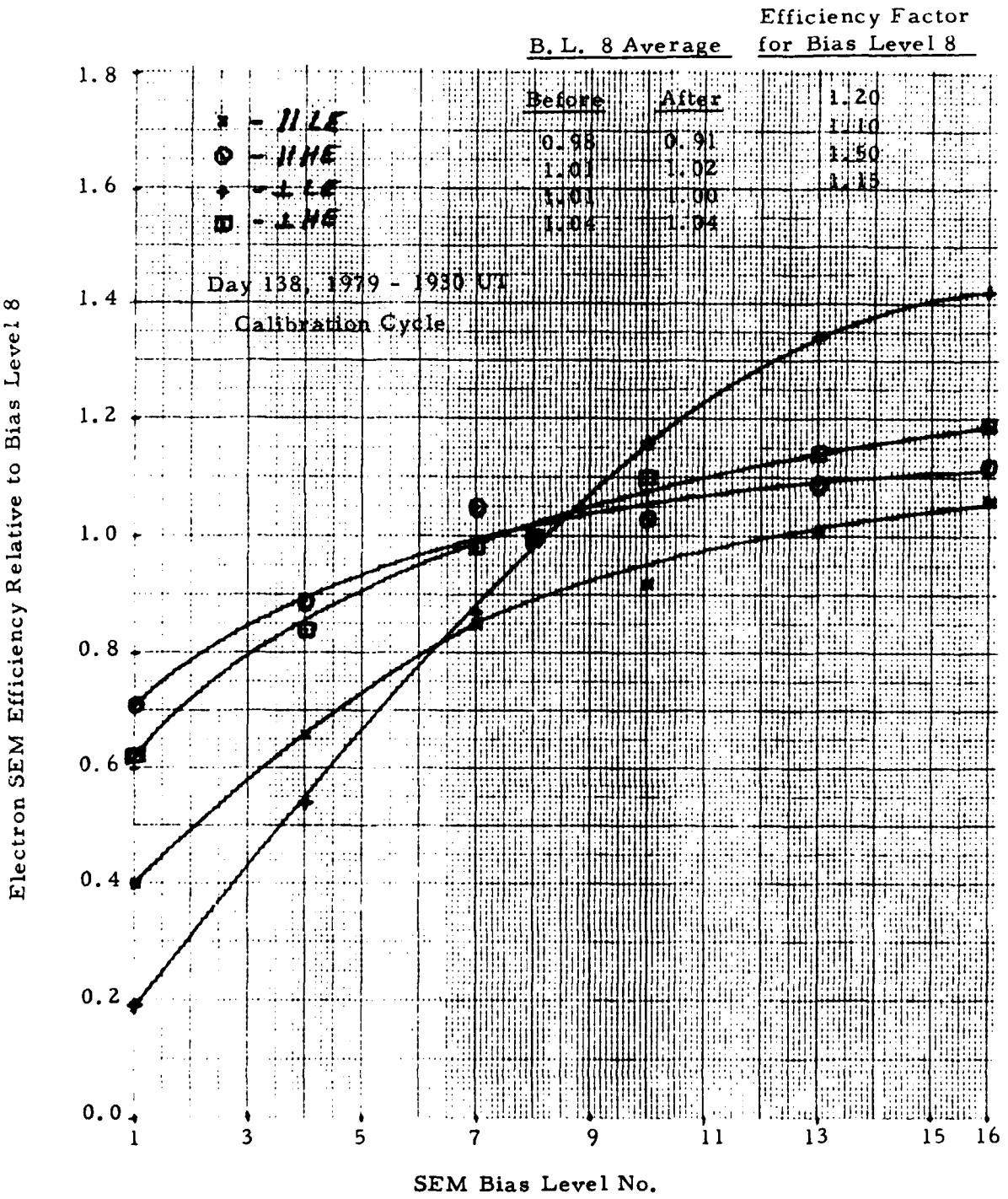


Figure 3.1. SEM Relative Efficiency vs. Bias Level for Electron FSA's on Day 138, 1979 at 1930 UT.

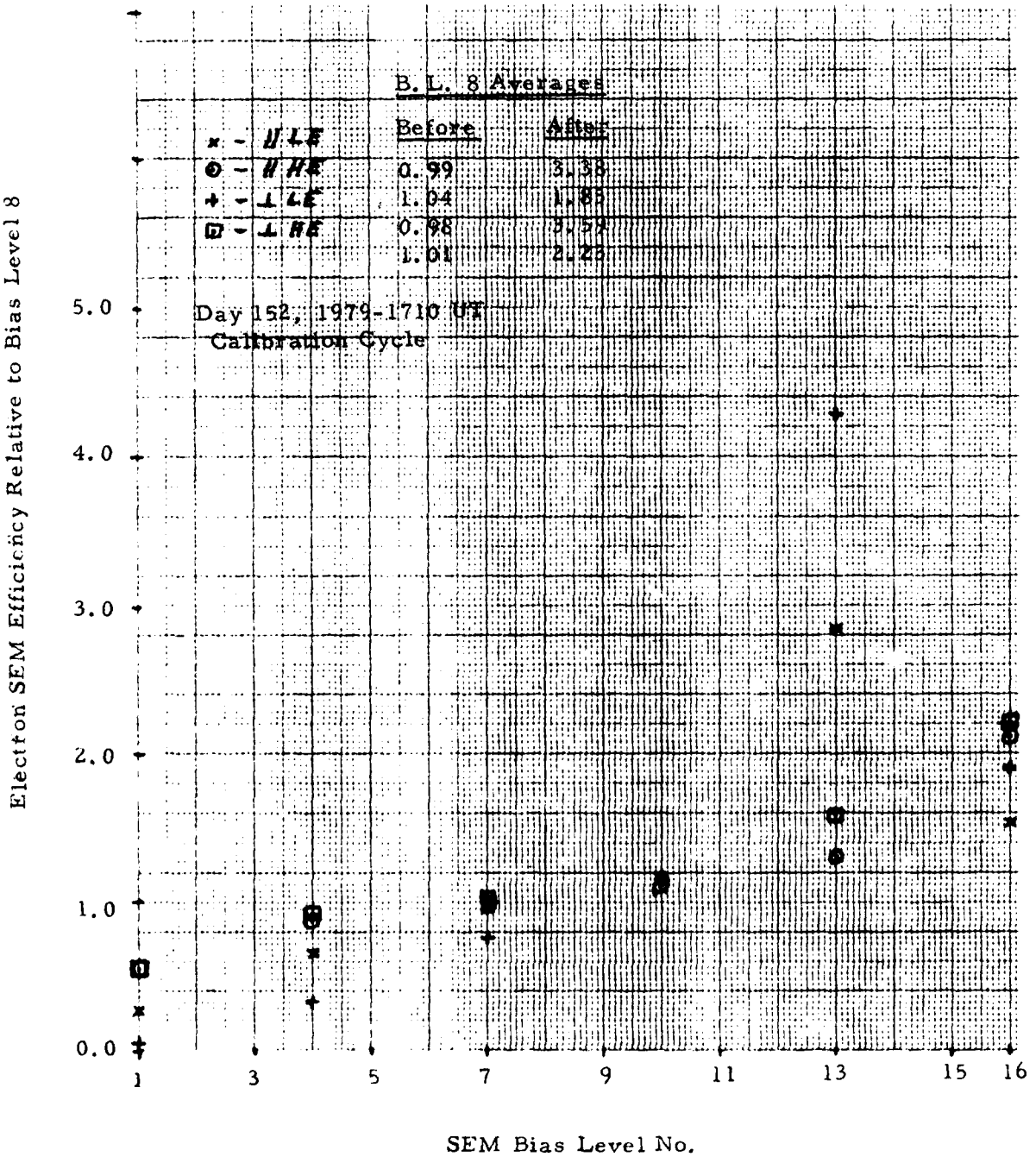


Figure 3.2. SEM Relative Efficiency vs. Bias Level for Electron ESA's on Day 152, 1979 at 1710 UT.

factor must be estimated by extrapolation of the calibration cycle data. This becomes particularly true of the $\perp$ LE electron ESA after about 200 days of operation. Under such conditions the $\perp$ LE electron ESA efficiency factor is better derived by comparison with the $\parallel$ LE ESA at equal measurement pitch angles. For operation at bias level 8, the efficiency factors can generally be derived from the calibration data for values as high as 5-10. Above 10 the accuracy of the efficiency factors worsens to 50% or more, unless comparison to another ESA is made.

The SEM efficiency factors vs. time for operation at bias level 1 are shown in Fig. 3.3 for days 40 to 48. This covers the period of operation at bias level 1, which occurred from turn-on on day 40 at 0230 UT, to day 47 at 2130 UT when bias level 8 operations began. Also shown in Fig. 3.3 are the time periods when SC5 was on, the periods of SCATHA data coverage and the times of SC4-2 ion gun operations. The double headed arrows show ion gun operations with SC5 on, and the three numbered long arrows on day 47 are the three Induced Charging Events (ICE's) for that day. As can be seen from Fig. 3.3, the perpendicular LE electron SEM efficiency factor was above 10 after day 45, and this was the primary reason for starting operations at bias level 8 on day 47.

The SEM efficiency factors for operation at bias level 8 are shown for days 48-76 in Fig. 3.4. An increase in the efficiency factors is observed from days 48 to about 56, primarily in the LE electron ESA's. This is, however, based completely on the day 45 calibration. By day 60 the SEM efficiencies had partially recovered, and the efficiency factors continued to decrease towards 1 through day 76. Data coverage, shown near the top of Fig. 3.4, was nearly continuous through day 56, after which coverage became sporadic and reduced because of problems with transmitter 1 on the SCATHA satellite. From day 63 on the SC5 ESA's were turned off more than half the time to reduce SEM efficiency degradation prior to the first eclipse season, which started with the first earth eclipse on day 75, shown by the arrow in Fig. 3.4.

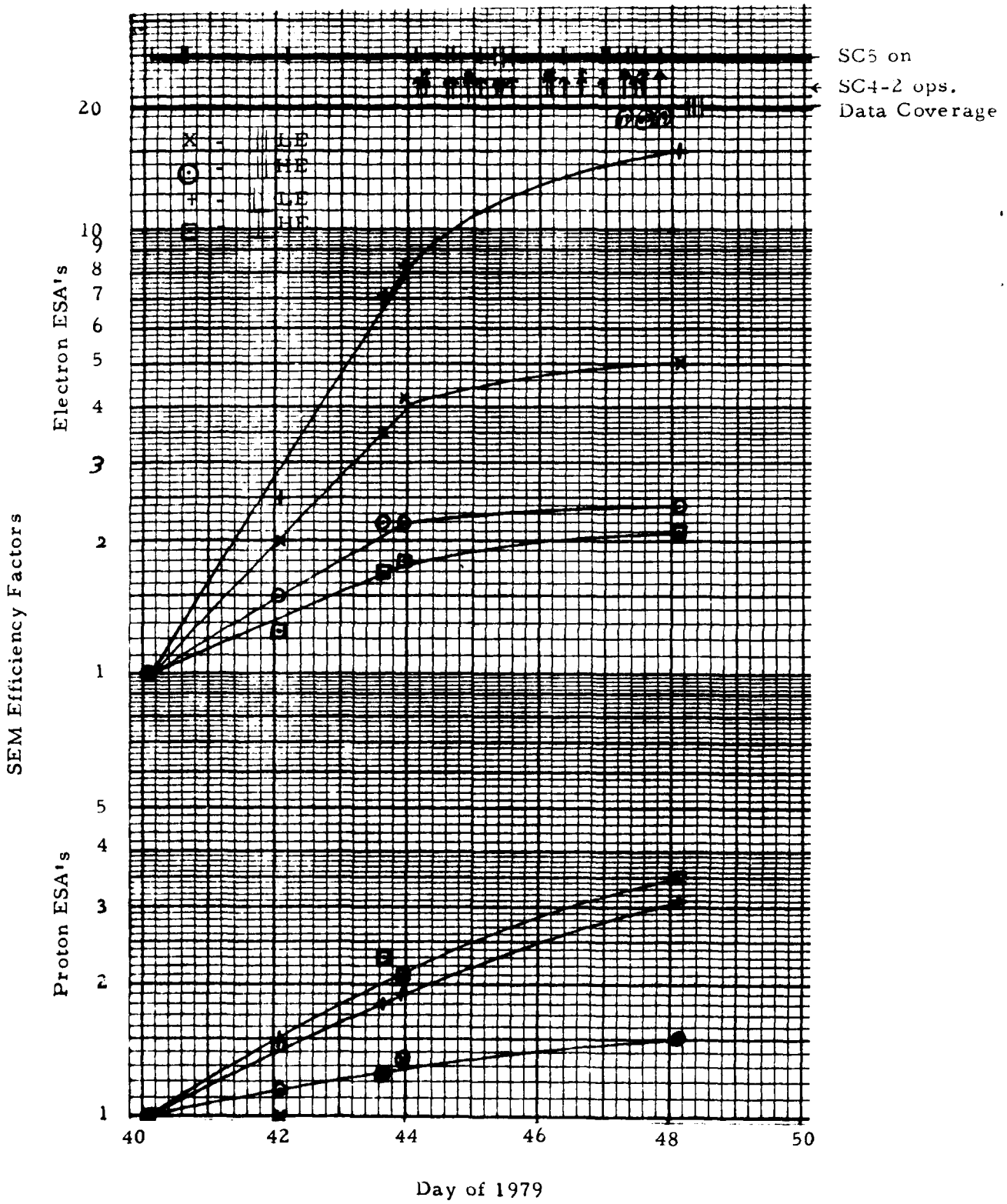


Figure 3.3. SEM Efficiency Factors for Operations at Bias Level 1 for Days 40-48, 1979.

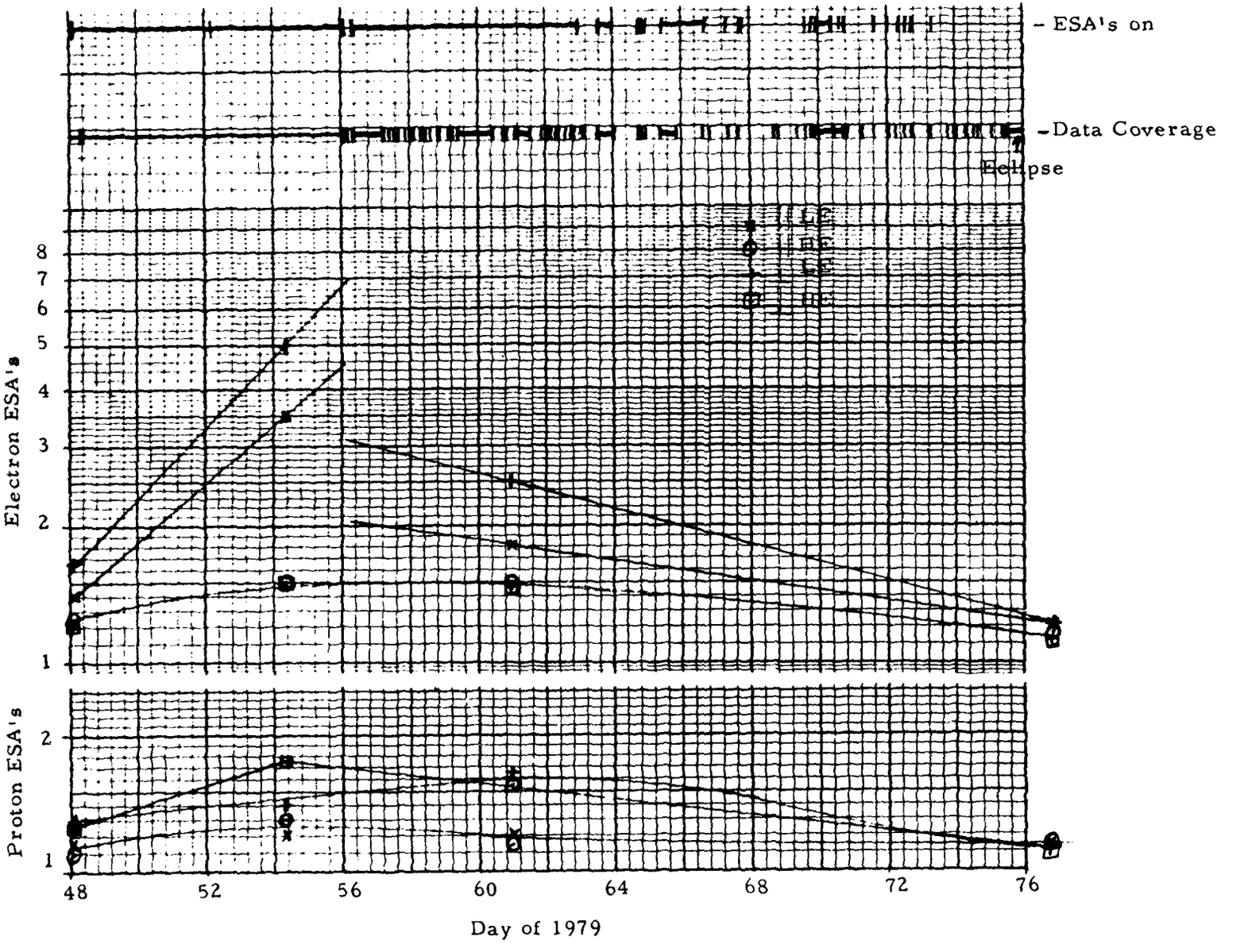


Figure 3.4. SEM Efficiency Factors for Operations at Bias Level 8 for Days 48-76, 1979.

The SCATHA transmitter 1 eventually recovered so that from day 76 on data coverage is nearly complete. The SC5 ESA's were turned on full-time again on day 76, and SEM efficiencies monitored by frequent calibration. The results are shown in Fig. 3.5, which shows the SEM efficiency factors for days 76-132, 1979, along with data coverage, ESA on times, eclipse times, and gun operation times. SC4-1 and SC4-2 gun operations are not distinguished, and the longer arrows indicate operations with the SC5 ESA's on.

The SEM efficiency factors in Fig. 3.5 show a number of significant properties about their variation with time. The initial rise on day 76 shows the moderately rapid degradation occurring after turn-on following several days of being mostly off. On day 80 the eclipse operations were modified to the 50% on/50% off mode described in Section 2.2. This seems to have halted further degradation, and perhaps even allowed for some recovery. The effect of large count rates on SEM efficiency is shown by the degradations, particularly in the LE electron ESA's, associated with the gun operations, primarily the SC4-1 electron gun.

Electron gun (SC4-1) operations started on day 89, and at about 1230 UT on day 90 the SC5 ESA's were on during SC4-1 operation at 1 mA. This operation resulted in a strong degradation in the electron ESA efficiencies, which almost completely recovered over the next few days. Additional electron gun operations on days 94 and 95 again resulted in electron ESA SEM gain degradation, most of which recovered over the next few days. A similar set of SEM gain decreases (note that this is an efficiency factor increase) and recoveries are shown by the second set of gun operations on days 110-116. Here a sharp break in SEM efficiencies is associated with electron gun operations near 0830 UT on day 112. By day 132 the SEM efficiencies had recovered to the approximate equilibrium values of day 78, after the initial decay from the day 76 turn-on.

The SEM efficiency factors for days 130-186, 1979 are shown in Fig. 3.6. Data coverage and ESA on times are shown at the top. Note that the SSS's for higher energy particles are on almost continuously. After the eclipse period ended on day 120, normal one-day-on/one-day-off operations were started. They only gun operations were with the SC4-2 ion

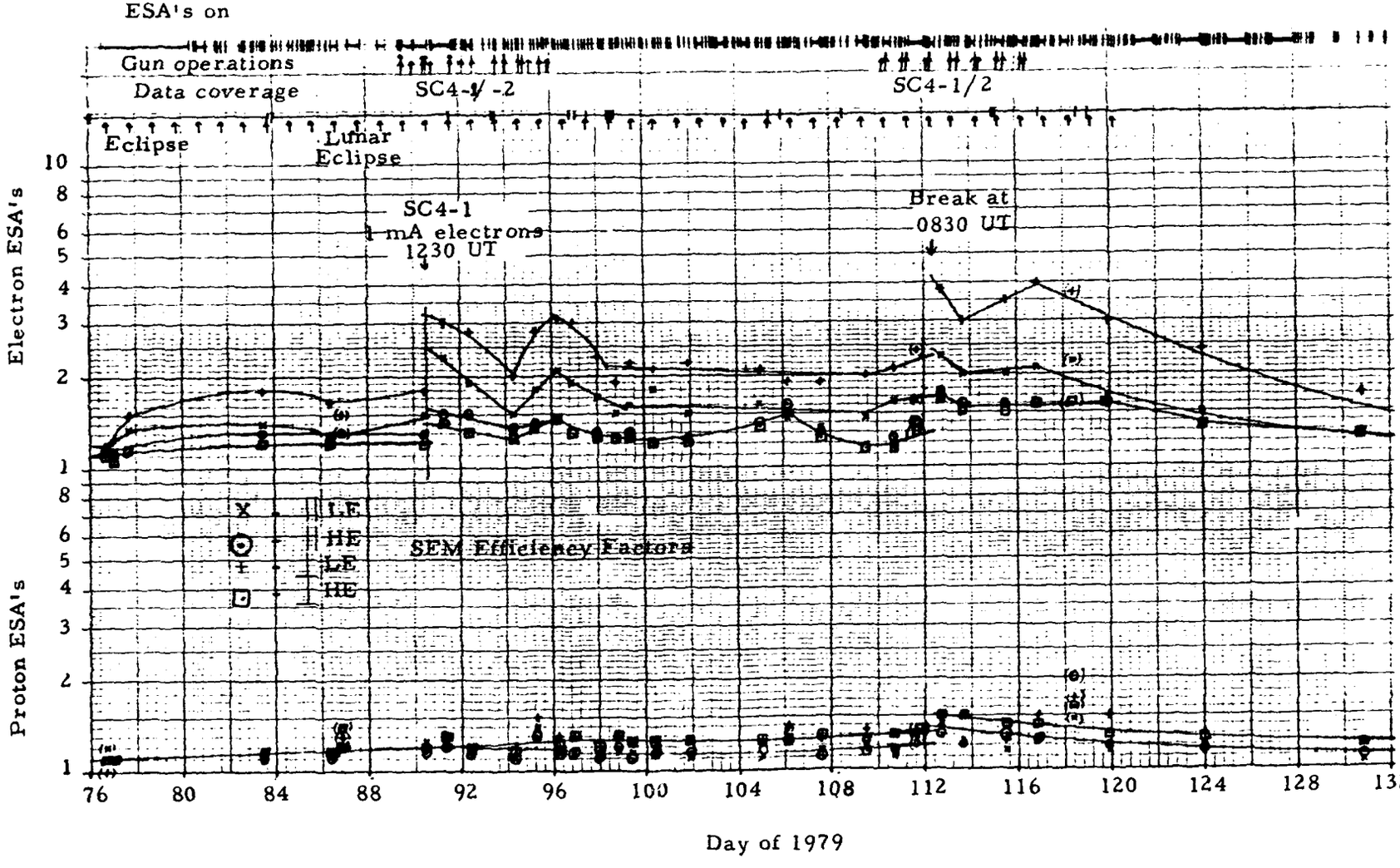


Figure 3.5 SEM Efficiency Factors for Operations at Bias Level 8 for Days 76-132, 1979.

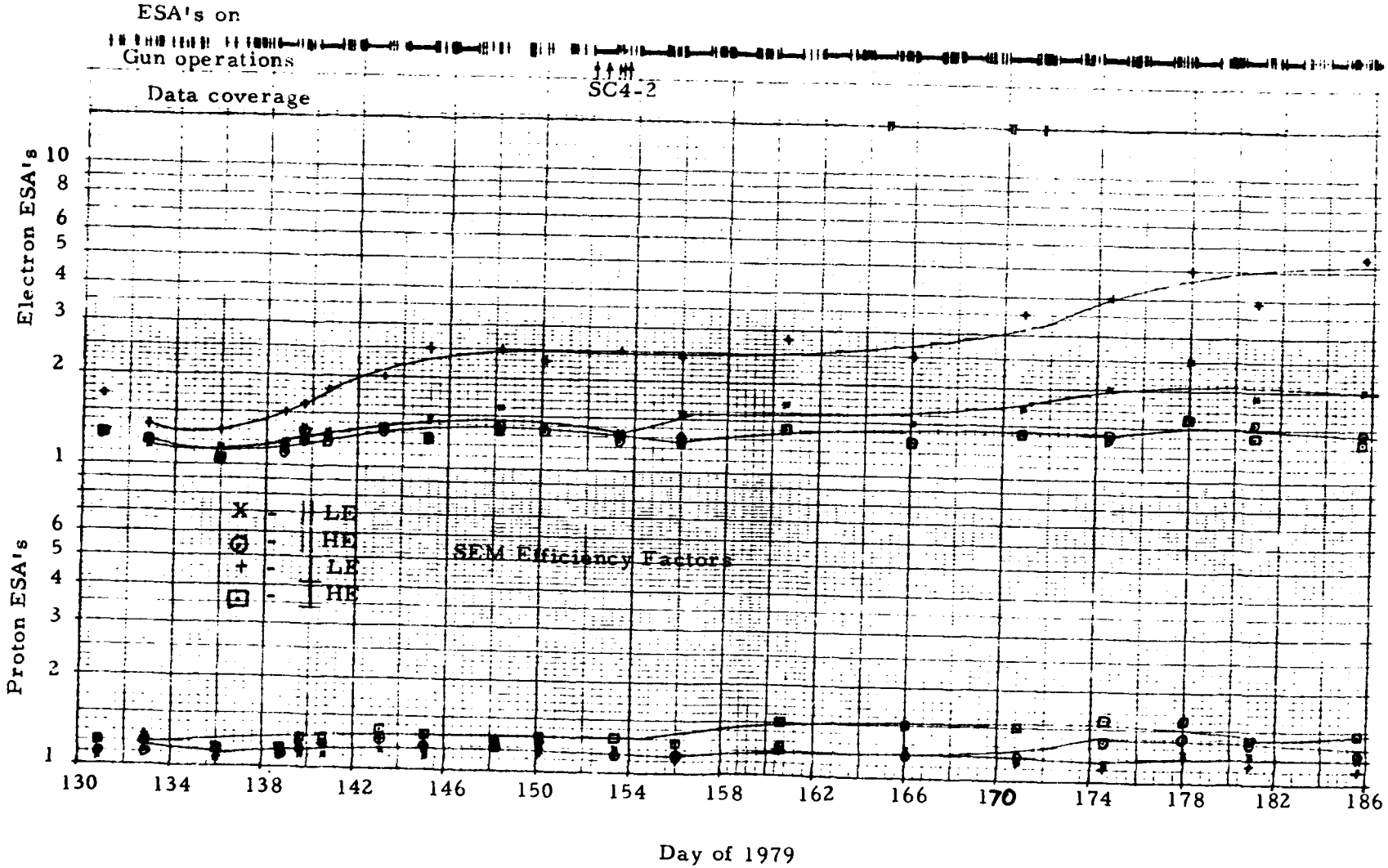


Figure 3.6. SEM Efficiency Factors for Operations at Bias Level 8 for Days 130-186, 1979.

gun on days 152-153, which had no significant effect on the SEM efficiencies. The SEM efficiencies had made the best recovery by day 135, followed by a decrease over the next 10 days and then a plateau for about 3 weeks. A further decline occurred over days 168-178, followed by a plateau and slight recovery, as shown in Fig. 3.7 which gives the SEM efficiency factors for days 184-240, 1979. Most of the changes occur in the LE electron ESA's, particularly the perpendicular ESA, which also suffers some degradation from solar UV even with the auto-shut-off B enabled.

The data in Fig. 3.7 shows some recovery in LE electron SEM efficiency up to about day 204, followed by a slow decrease in detection efficiency, mostly in the perpendicular ESA. The gun operations on days 200-203 involved no high-current/high-count-rate operations with the SC5 ESA's on, and hence caused no noticeable degradation in the SEM efficiencies. SEM efficiency factors for days 238-294, 1979 are shown in Fig. 3.8. Data coverage for this period is complete, though not shown in the figure. ESA on-time was on-one-day/off-one-day until eclipse coverage began on day 265 (actual eclipses began on day 263).

The day 238-294 period had ion gun operations on day 275, and electron/ion gun operations on days 285-293. None of these operations caused any noticeable effect on the SEM efficiencies. During this period the perpendicular LE electron ESA efficiency factor increased from about 9 to 25 at bias level 8. The other SEM efficiency factors also increased, though not as dramatically as the perpendicular LE electron SEM. Figure 3.8 also shows the perpendicular LE electron SEM efficiency factor as obtained from the parallel LE electron SEM efficiency factor and a comparison of the LE electron ESA count rates at the same pitch angle. These values are in reasonable agreement with the efficiency factors derived from the calibration cycle data.

SEM efficiency factors for days 292-352 are shown in Fig. 3.9, for operations at bias level 8. This period includes two sets of gun operations, on days 293-298 and on days 338-340. Electron gun operations on days 297, 298, and 339 were at high current levels for extended periods of time. The ESA's were operating at bias level 12 for these gun operations, and the

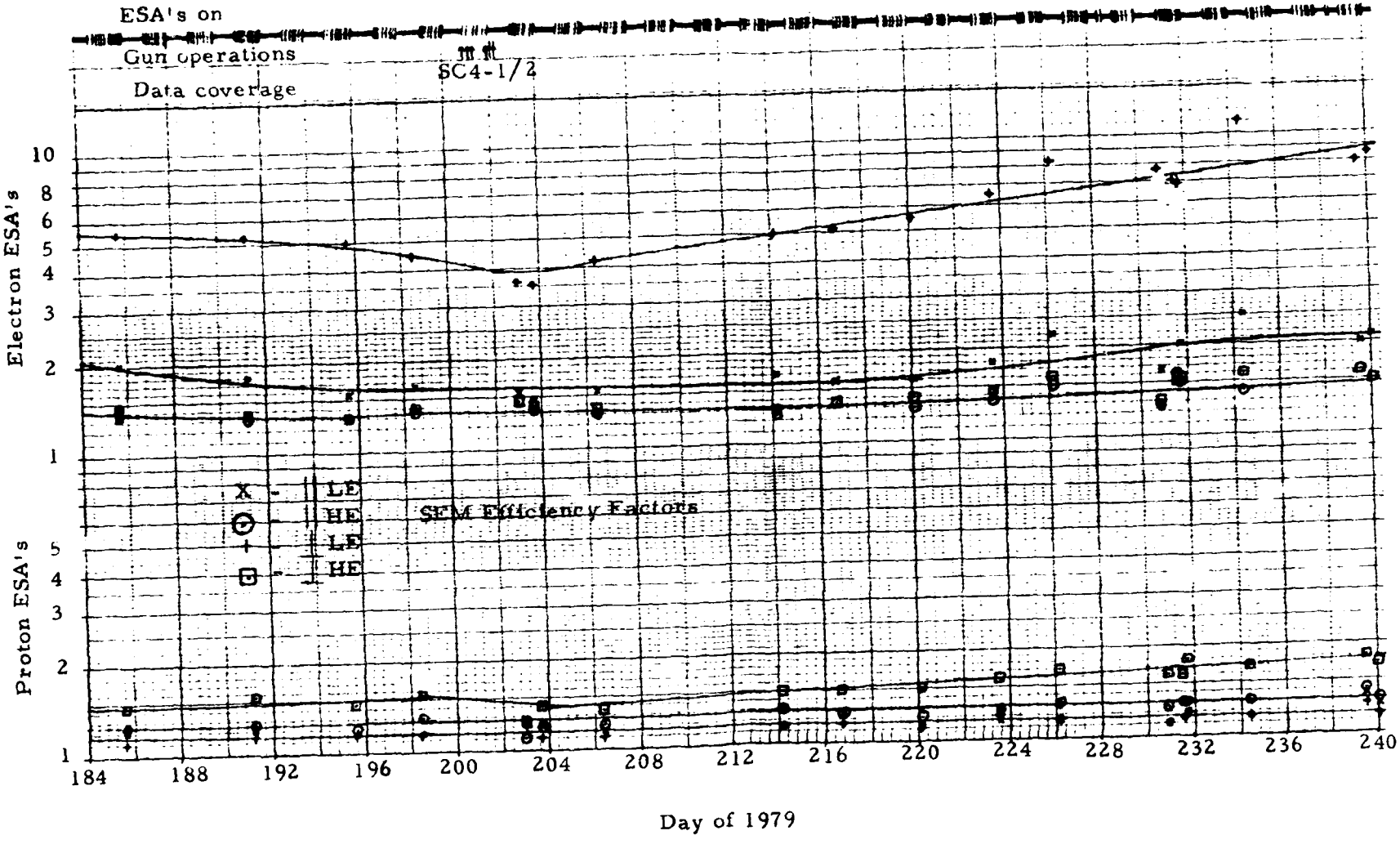


Figure 3.7. SEM Efficiency Factors for Operations at Bias Level 8 for Days 184-240, 1979.

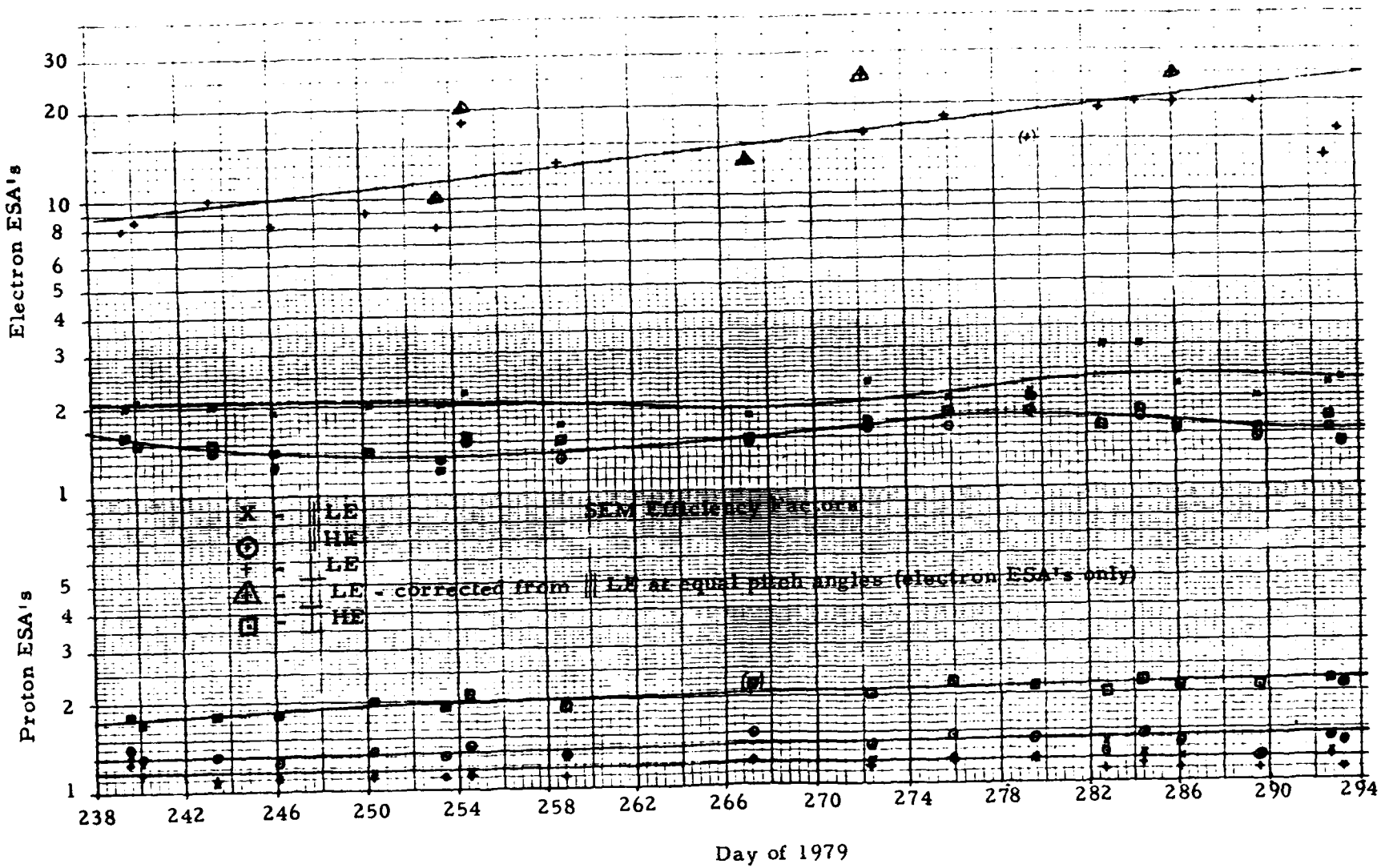


Figure 3.8. SEM Efficiency Factors for Operations at Bias Level 8 for Days 238-294, 1979.

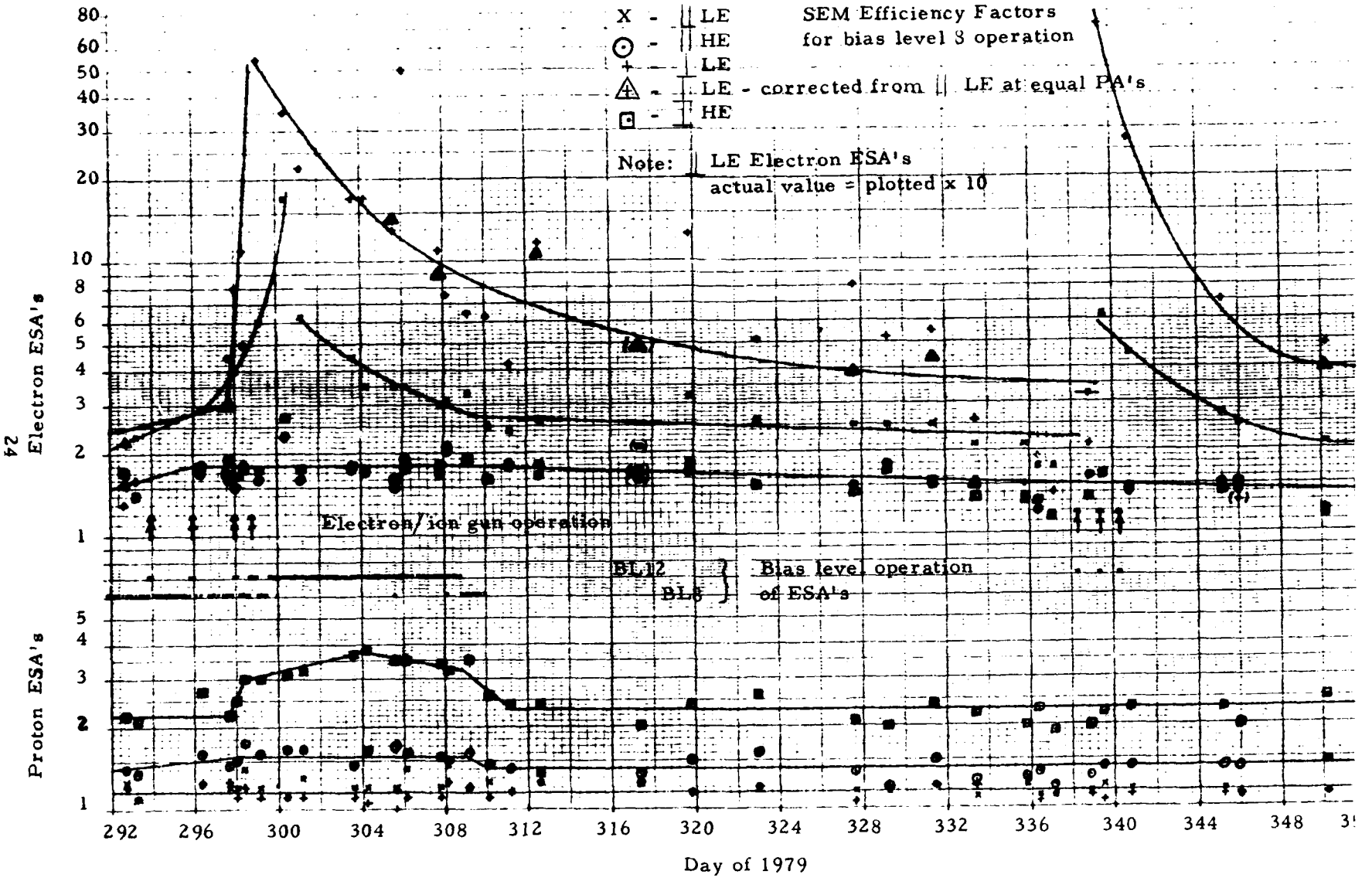


Figure 3.9. SEM Efficiency Factors for Operations at Bias Level 8 for Days 292-352, 1979.

electron ESA's had very high count rates for these operations. The strong SEM efficiency degradation resulting from these operations are apparent in Fig. 3.9, which also shows that most of the original detection efficiency was recovered within several days after the gun operations stopped. These electron gun operations were made with the ESA's on the high time resolution FM (B) band, and yielded a considerable amount of data on the rise/fall times of the satellite potential as the electron beam is turned on and off. Some of the data are discussed in Section 4.3.

Figure 3.9 shows the time periods when the SEM's were operated at bias level 12, mostly during the gun operations. The SEM efficiency factors for operation at bias level 12 for the two gun operation periods are shown in Fig. 3.10, which also shows the times when the ESA's were operated at bias level 12. For these operations the perpendicular LE electron ESA became very inefficient, particularly after the electron gun operations on days 297, 298, and 339. For bias level 8 operations this ESA was nearly unusable after days 298 and 339. The LE electron SEM's recovered moderately well in the days following gun operations, but the perpendicular SEM efficiency factor for bias level 8 did not go below 35 (detection efficiency = 0.029) for the entire period.

The SEM efficiency factors for days 348, 1979 to 37, 1980 are shown in Fig. 3.11. The efficiency factors are reasonably stable, as no gun operations occurred during this period. The perpendicular LE electron ESA is only marginally usable, with an efficiency factor of 35-60. The efficiency factors for days 35-55, 1980 are shown in Fig. 3.12. The data in Figs. 3.3 to 3.12 cover the basic operational period of the SC5 ESA's. This time period covers all of the data to be used for the AFGL data atlas, and all of the important gun operation periods. Some additional data was taken for an intense flux period for days 160-167, 1980, and the efficiency factors for this period are shown in Fig. 3.13. The factor for the perpendicular LE electron ESA is unusable, so after about 1 1/3 years in orbit 7 out of 8 ESA's in SC5 were still giving useful data. The SSS's were all operating properly, and are expected to continue proper operation almost indefinitely.

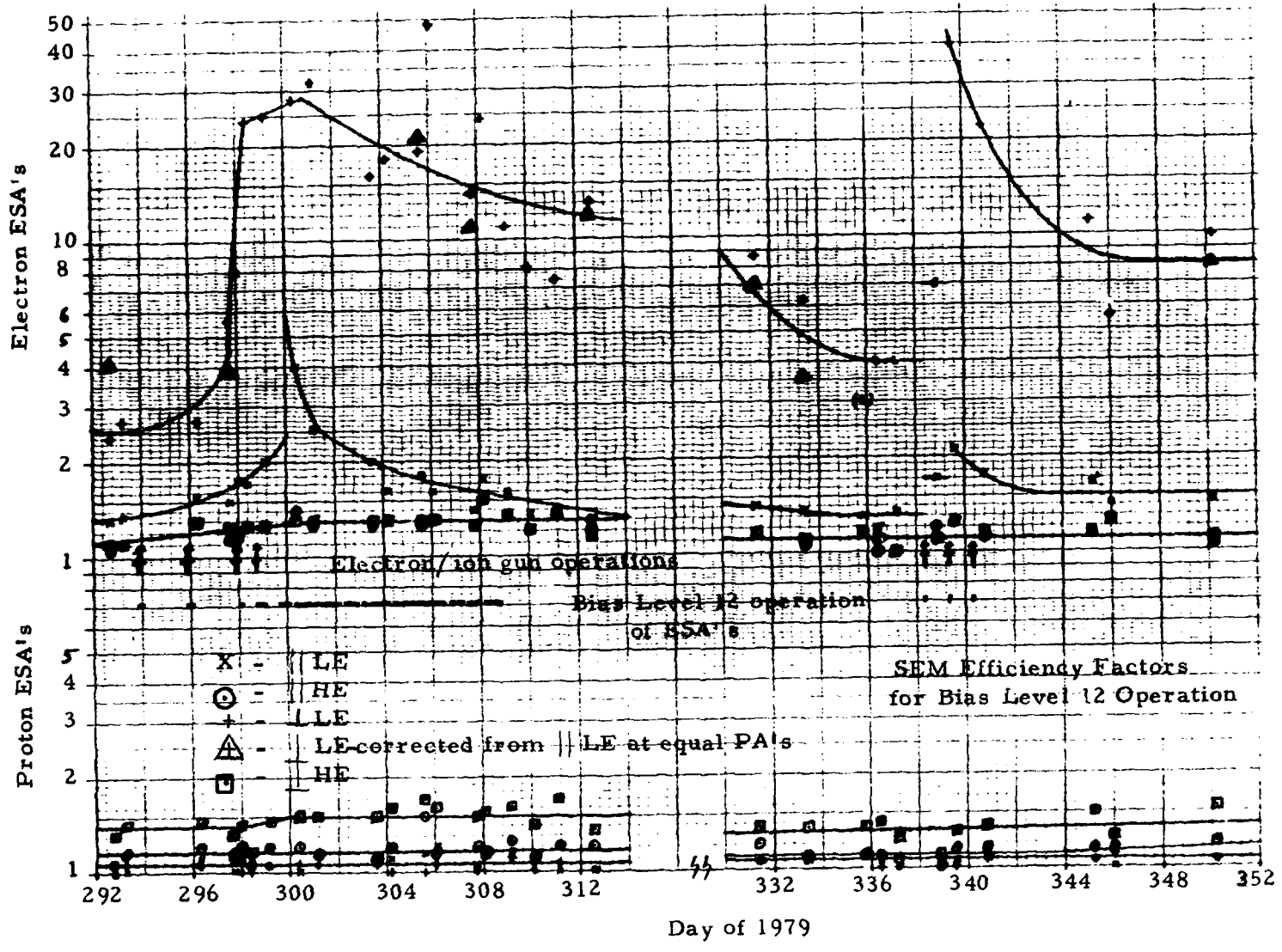


Figure 3.10. SEM Efficiency Factors for Operations at Bias Level 12 for Days 292-314 and 330-352, 1979.

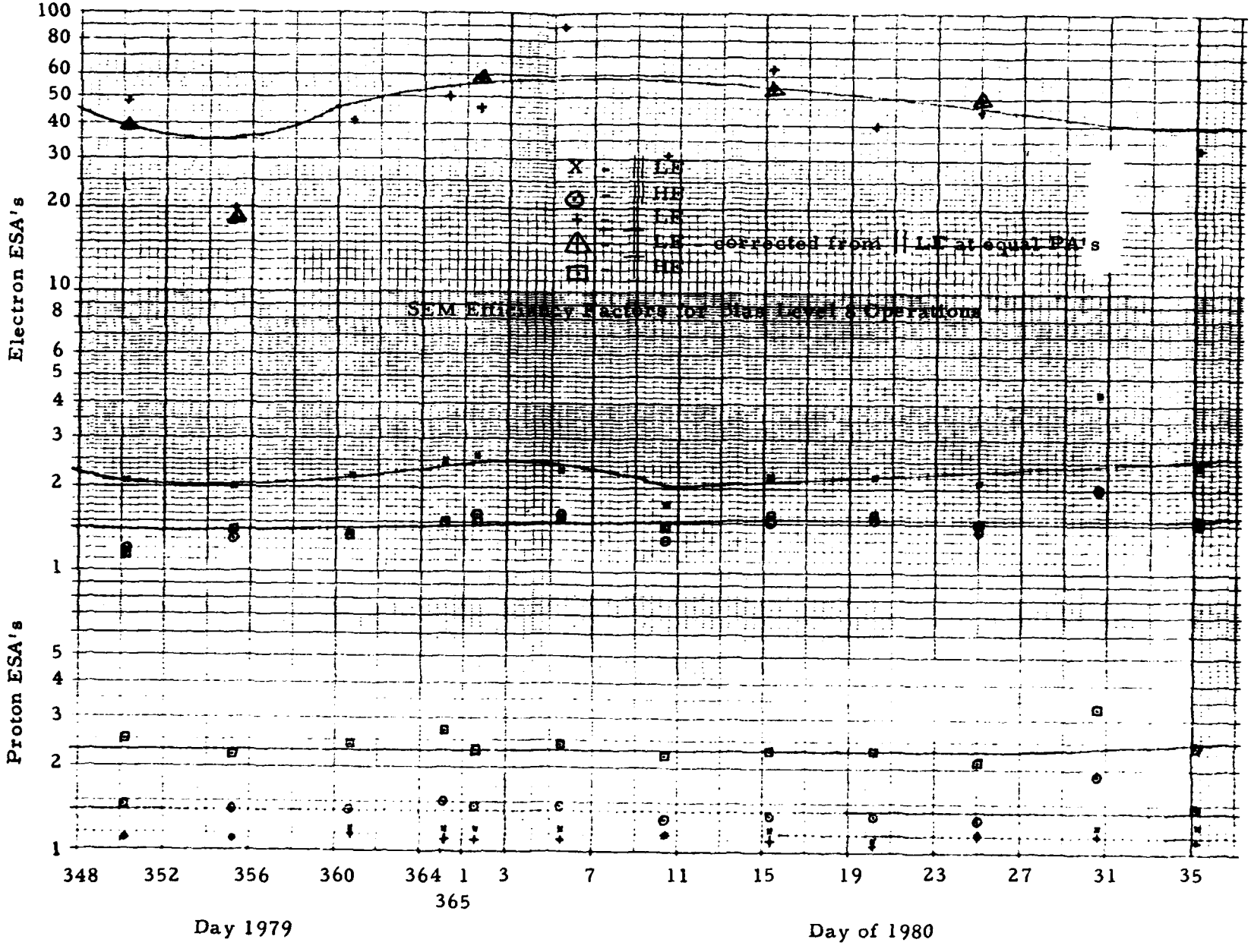


Figure 3.11. SEM Efficiency Factors for Operations at Bias Level 8 for Days 348-365, 1979 and 1-37, 1980.

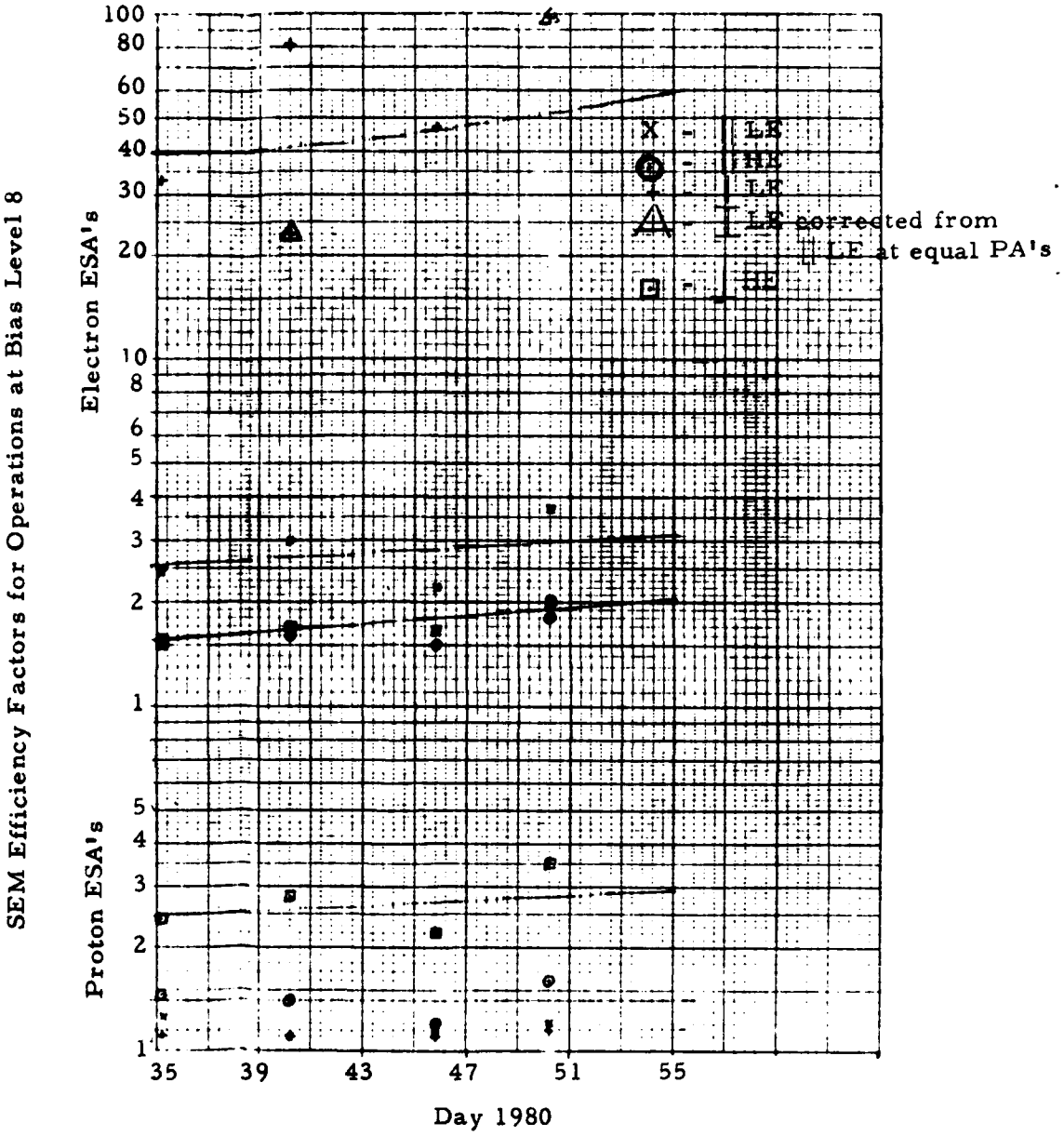


Figure 3.12. SEM Efficiency Factors for Operations at Bias Level 8 for Days 35-55, 1980.

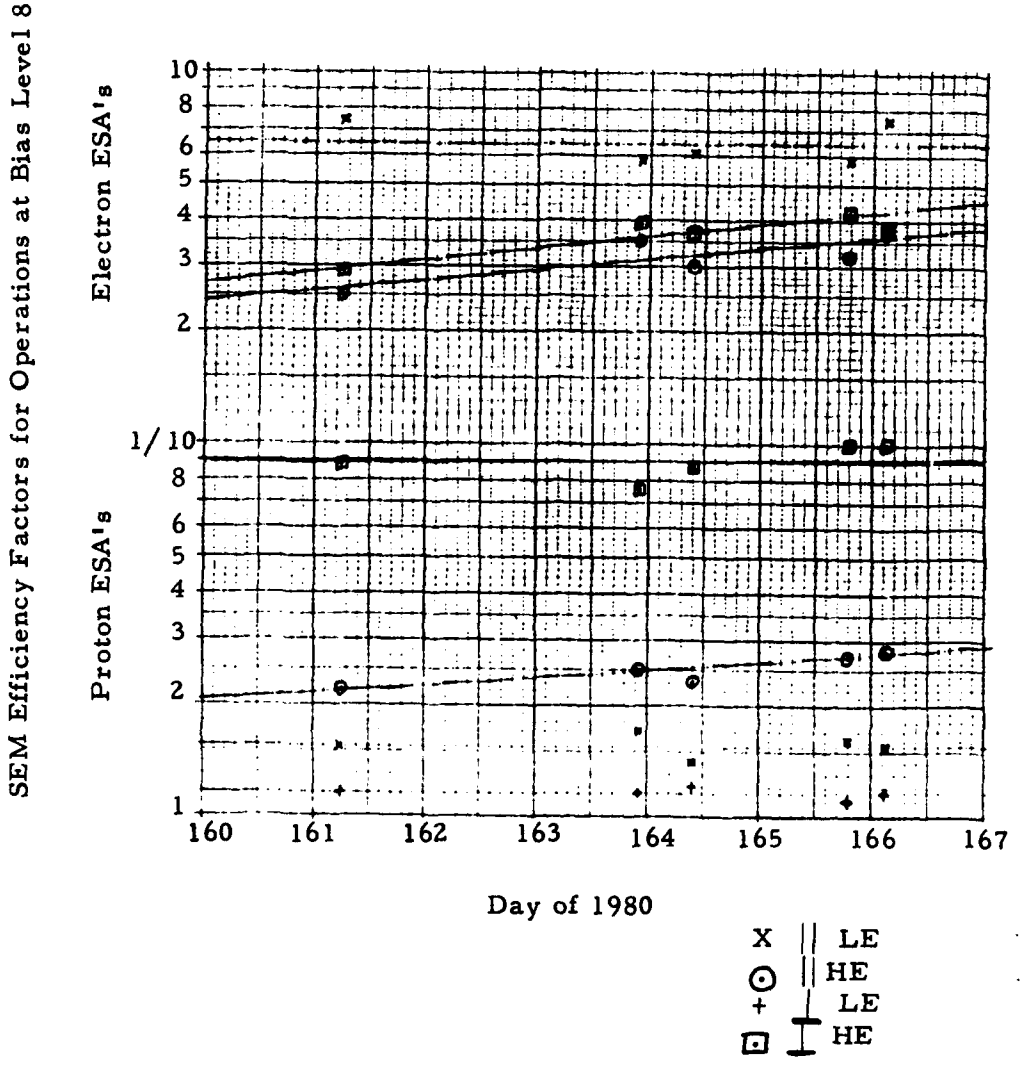


Figure 3.13. SEM Efficiency Factors for Operations at Bias Level 8 for Days 160-167, 1980

For operation at bias level 16 the perpendicular LE electron ESA efficiency factor for days 160-167, 1980 is about 16, so operation at the highest bias level could still give some moderately useful data from all 8 ESA's. However, the normal operating mode of SC5 continued to use bias level 8, except for some gun operations when bias level 12 was used. The main operational period of SC5 of concern in this report is the period covered by the data in Figs. 3.3 to 3.12 and in Fig. 3.13.

The tabulated SEM efficiency factors for days 40-47, 59, and 76-365, 1979, and for days 1-50 and 160-166, 1980, have been supplied to Air Force Geophysics Laboratory personnel for use in reducing the SC5 data. The tabulations are taken from the smoothed curves in Figs. 3.3 to 3.13, and are given in Table A.1 in Appendix A.

The SEM efficiency factors are generally the same for all energy channels of a given ESA, provided the factor is less than about 10. This is true for all ESA's except the perpendicular LE electron ESA after day 250, 1979. For this ESA the efficiency factor for channel 1 (0.080 keV) is generally larger, and the efficiency factor for channel 4 (1.24 keV) is generally smaller, than the average value, when the average value is greater than 10. The efficiency factor variations range from about $\pm 25\%$ for a factor of 20, to more than $\pm 50\%$ for a factor of 50 to 100. Under such conditions it is better to use the perpendicular LE electron ESA for the pitch angle distribution shape, and normalize the LE electron ESA fluxes to the parallel ESA values. The data in Figs. 3.3 to 3.13 and Table A.1 of Appendix A show that the neglect of this correction is less than $\pm$ 25% for days 250 to about 310, 1979, except for some post gun operations. The correction is less than $\pm$ 50% for most of the other days, except for short periods following gun operations at days 298 and 339, 1979, and for the period of days 160-166, 1980.

### 3.1.2 Energy Resolution and Background Corrections

The ESA channels on SC5 are broad (nearly 100% full width at half maximum) and overlap significantly. The zero order flux calculations (3.1) subtract background only for the low energy ESA's, and take no account of

the broad energy resolution. The proton ESA's are also sensitive to electrons, and while the low energy proton ESA's are essentially corrected for electron contamination by the background subtraction, the high energy proton ESA's may have some electron contamination in the zero order flux calculation.

The ESA's have been calibrated in detail, including the electron sensitivity of the proton ESA (Ref. 1.3). Thus the response of all ESA energy channels to given electron/proton spectra can be calculated regardless of the fine structure in the spectra. The inverse problem is more difficult, and can only give structure down to the resolution of the energy channels. Since only eight energy channels are measured over the range 0.05 to 60 keV, the corrected spectra can only give eight spectral points, each being an average over an energy range of about 100% of the central (average) energy.

The major correction to the zero order electron spectra in a shift in the flux calculated for the central bin energy for strongly energy dependent spectra. For strongly falling (or rising) electron spectra the flux calculated by dividing the count rate by $G \Delta E$ (the geometric factor in $cm^2$ - sr - keV) can differ from the true spectral $dJ/dE$ at the bin central energy by more than 50%. The higher order correction procedure includes the effects of such strongly energy dependent spectra. The corrections are calculated by assuming a power law spectrum over the range of each energy bin.

The basic procedure for correcting the ESA electron spectra is as follows:

1) The zero order spectra are calculated, along with a zero order power law exponent for each pair of adjacent channels (this gives 8 zero order fluxes and 7 zero order power law exponents).

2) The zero order power law exponents are used to calculate effective geometric factors for each energy bin, and for the high and low energy tails of each bin. Where possible, the power law exponent used is the overage between the bin in question and the adjacent higher and lower energy bins.

3) The result is an effective geometric factor matrix, in which the diagonal terms are dominant. The terms adjacent to the diagonal (adjacent energy bin overlap responses) form most of the non-zero off-diagonal terms. This geometric factor matrix is combined with the eight measured count rates (corrected for background in the low energy ESA's), and the result inverted to give the first order corrected fluxes.

4) The first order fluxes (8 values) are used to calculate the first order power law exponents (7 values).

5) Since the geometric factor matrix was calculated using the zero order power law exponents, the procedure can be reiterated by returning to step (2) above, and repeating until the fluxes change negligibly from one iteration to the next. In practice this may take several iterations. If the new power law exponents are taken as the average of input + output values, then the procedure has been found to converge more rapidly and only a few iterations are needed.

6) The proton ESA spectra are corrected after the electron spectra, and use the corrected electron spectrum to subtract a calculated electron background from the high energy proton ESA counts.

The entire correction routine has been programmed in FORTRAN and used on various types of spectra. Several examples of corrected spectra are shown in Section 4. It has been found that 5 iterations is generally sufficient to produce less than 1% change in the iterated values.

## 3.2 SSS Data Reduction

The SSS's measure the electron and proton spectra parallel and perpendicular to the spin axis in a total of 8 bins for electrons and 10 bins for protons. The electron SSS energy channels are listed in Table 3.3, and are taken directly from Ref. 1.3. The 5 anti-coincidence channels form the primary energy bins for high energy electrons. The three coincidence bins form a differential channel at 1040 keV, a threshold channel of > 950 keV, and a 70-950 keV channel. The proton SSS energy channels are listed in Table 3.4, and are also taken from Ref. 1.3. The proton SSS's have 5 anti-coincidence channels and 5 coincidence channels. One of the perpendicular proton SSS channels (#6 in Table 3.4) is very narrow because of the thin front detector (5.3 microns), since the thresholds were set to match the parallel and perpendicular anti-coincidence channel energies, and this resulted in the narrow channel #6 (see Ref. 1.3).

Table 3.3

Electron Solid State Spectrometer Response Factors

| SSS/bin | Energy Channel # | Average Energy (keV) | Bin Width (keV) | Effective GΔE ($cm^2$-sr-keV) |
|---|---|---|---|---|
| Anti-c/1 | 1 | 39 | 12 | $1.21 \times 10^{-2}$ |
| Anti-c/2 | 2 | 58 | 24 | $5.12 \times 10^{-2}$ |
| Anti-c/3 | 3 | 96 | 48 | 0.144 |
| Anti-c/4 | 4 | 335 | 430 | 1.53 |
| Anti-c/5 | 5 | 218 | 95 | 0.337 |
| Coinc/1 | - | >950 | - | $3.55 \times 10^{-3}$ * |
| Coinc/2 | - | 1040 | 120 | $4.26 \times 10^{-1}$ |
| Coinc/3 | - | 70-950 | - | $3.55 \times 10^{-3}$ * |
| Coinc/4 | - | >950 | - | $3.55 \times 10^{-3}$ * |
| Coinc/5 | - | 1040 | 120 | $4.26 \times 10^{-1}$ |

*These are G values ($cm^2$ - sr) for the threshold or energy range indicated.

Table 3.4

Proton Solid State Spectrometer Response Factors

| | | Parallel SSS | | | Perpendicular SSS | | |
|---|---|---|---|---|---|---|---|
| SSS/bin | Energy Channel # | Average Energy (keV) | Bin Width (keV) | GΔE ($cm^2$-sr-keV) | Average Energy (keV) | Bin Width (keV) | GΔE ($cm^2$-sr-keV |
| Anti-c/1 | 1 | 126 | 49 | 0.328 | 126 | 49 | 0.328 |
| Anti-c/2 | 2 | 188 | 75 | 0.502 | 188 | 75 | 0.502 |
| Anti-c/3 | 3 | 275 | 100 | 0.669 | 275 | 100 | 0.669 |
| Anti-c/4 | 4 | 388 | 125 | 0.836 | 388 | 125 | 0.836 |
| Anti-c/5 | 5 | 499 | 97 | 0.644 | 465 | 29 | 0.194 |
| Coinc/5 | 6 | 573 | 51 | 0.341 | 485 | ≈10 | ≈0.01 |
| Coinc/4 | 7 | 779 | 361 | 2.42 | 612 | 242 | 1.62 |
| Coinc/3 | 8 | 1410 | 910 | 6.07 | 1100 | 731 | 4.89 |
| Coinc/2 | 9 | 3060 | 2380 | 15.9 | 2380 | 1830 | 12.2 |
| Coinc/1 | 10 | 6430 | 4360 | 29.1 | 5020 | 3460 | 23.1 |

The SSS particle fluxes are calculated as for the ESA's, but with no efficiency factor as it is always 1.0. From (3.1) this gives

$$\frac{dJ_i}{dE} = \frac{N_i}{T\,G\Delta E\,(i)} \tag{3.2}$$

with the symbols being as defined after (3.1). The fluxes (3.2) only hold for the differential channels, 1-5 for electrons and 1-10 for protons. For the high energy electron channels (coincidence), the threshold (or wide bin) fluxes are calculated from

$$J_i\,(>E_i) = \frac{N_i}{T\,G(i)} \tag{3.3}$$

where G(i) is the geometric factor for bin i. Equation (3.3) is only needed for the electron SSS channels coinc/1, /3, and /4.

The SSS energy bin widths are a significantly smaller fraction of the average bin energy than is the case for the ESA's, so resolution corrections are not as important. The exceptions are the electron SSS energy channel #4, and the highest energy proton SSS channels. These high energy channels usually have very low count rates, so for most routine SSS data reduction the energy resolution corrections can be ignored. This is not true for the ESA's, especially the high energy channels of the electron ESA's, as is shown by some of the data presented in Section 4.

### 3.3 High Time Resolution FM Data Reduction

The SC5 detector outputs can be applied to a broadband (> 3 kHz) FM channel through a digital quasi-logarithmic count-rate circuit. These data can only be acquired in real-time, and the mode is called FM-B for the SCATHA data set. An example of the demodulated FM data is given in Fig. 3.14, where an electron beam turn-on on day 297, 1979 is shown. The general format of the FM data is a synch pulse and eight bit identification code followed by data, with the cycle repeated every 0.2 seconds. The mode shown in Fig. 3.14 has the LE parallel electron ESA, fixed in energy in channel 1, connected to the FM data channel with no cycling.

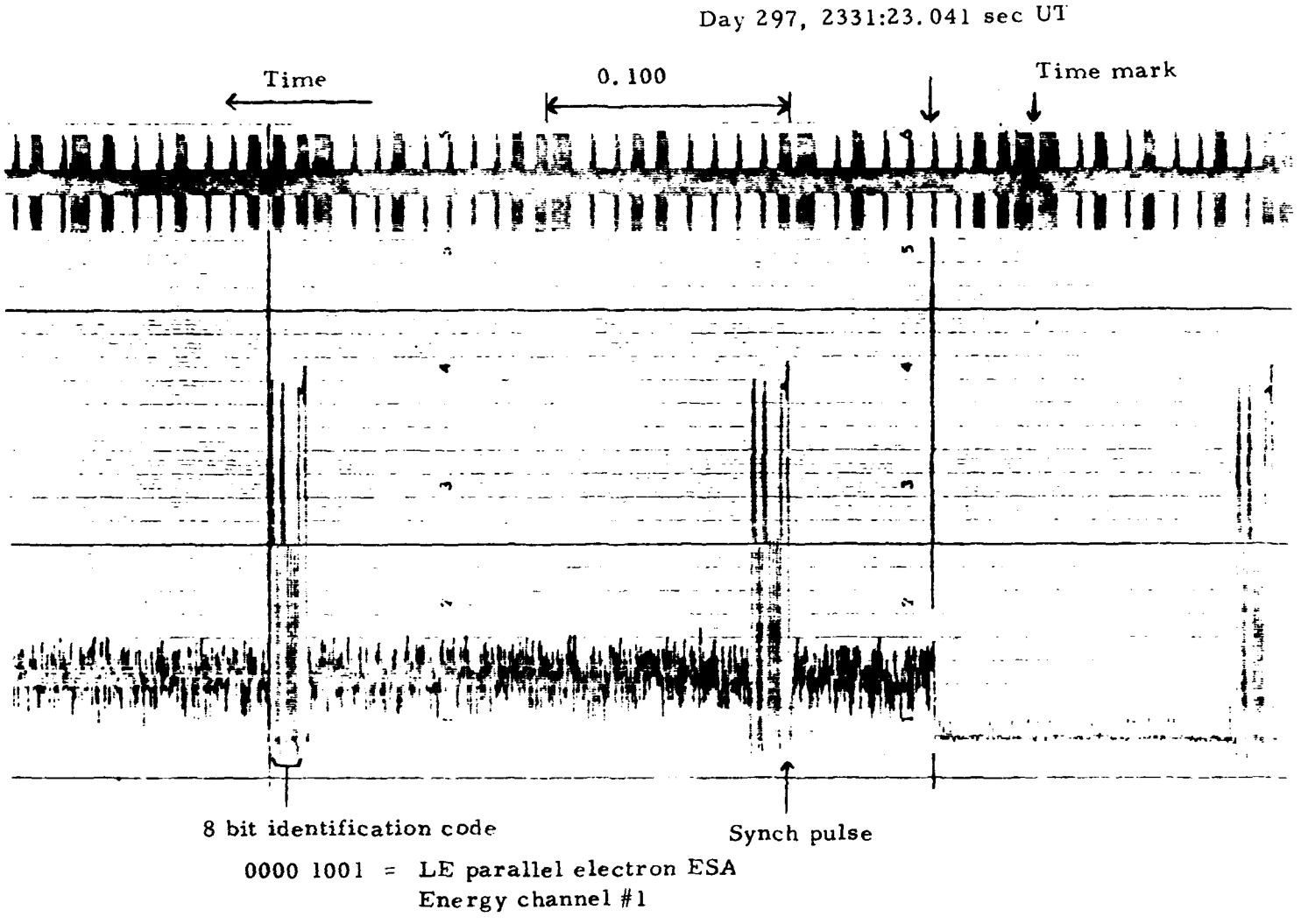


Figure 3.14. Examples of FM Data for an Electron Beam Turn-on on Day 297, 1979.

The identification code assignments are given in Table 3.5, while the output voltage level vs input counts is given in Table 3.6. Each count is for 242 microseconds, so the counts can be converted directly into count-rate. The various detector cycling modes are described in Ref. 1.2, and are needed only for commanding instrument operations. The code listing in Table 3.5 is all that is needed for data analysis.

The FM data in Fig. 3.14 show the extremely rapid response of the satellite to electron beam turn-on. The ESA channel 1 response rises to the new equilibrium value in less than 1 millisecond. The output counts after beam turn-on correspond to several input counts/digital count rate meter cycle, or to about 30,000 counts/sec. While the FM data count rates can be used to obtain particle fluxes, their primary use is in determining the rapid time variations where only relative values are needed. Additional examples of high time resolution FM data are given in Section 4.3.

## 4. SOME EXAMPLES OF REDUCED SC5 DATA

### 4.1 Comparison of the Parallel and Perpendicular Detector Spectra

The parallel detector set in the SC5 instrument has a fixed view direction which is usually near 90° to the local magnetic field direction, while the perpendicular detector set scans a pitch angle range of near 0° - 180° twice per spin period. SC5 can thus be used to measure time variations of the particle fluxes with the parallel detector set, and pitch angle distributions with the perpendicular detector set. Since the two detector sets view at the same pitch angle twice per spin period, the detectors can be cross-checked as often as desired.

The SCATHA orbit is near-geosynchronous, which places it near the edge of the predominently dipole-like region of the geomagnetic field, particularly near local midnight where tail-like field configurations may be frequently encountered. Under some conditions the perpendicular detectors may scan less than 0-180° pitch angles. Occasionally, unusual field configurations may even result in the parallel and perpendicular detector sets never viewing at the same pitch angle, at least for a short time period.

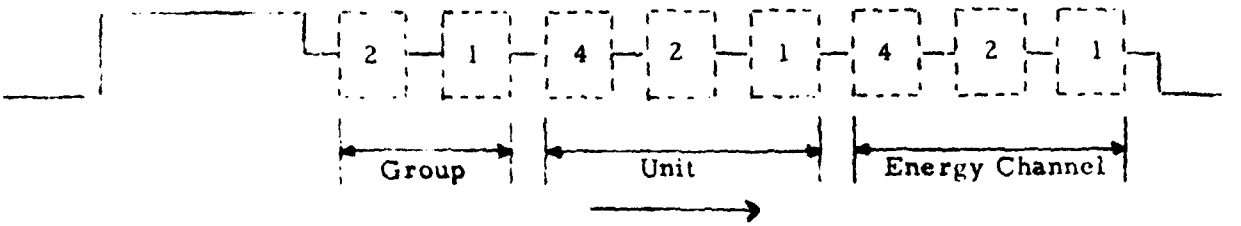


Table 3.5 - Broadband Data Identification Code Format

| Broadband Data Identification Code Assignments | | | | |
|---|---|---|---|---|
| Unit | Identification Code | | | |
| | Octal | Binary | | |
| LE ⊥ e ESA | 00X | 00 | 000 | XXX |
| LE ‖ e ESA | 01X | 00 | 001 | XXX |
| HE ⊥ e ESA | 02X | 00 | 010 | XXX |
| HE ‖ e ESA | 03X | 00 | 011 | XXX |
| LE ⊥ p ESA | 04X | 00 | 100 | XXX |
| LE ‖ p ESA | 05X | 00 | 101 | XXX |
| HE ⊥ p ESA | 06X | 00 | 110 | XXX |
| HE ‖ p ESA | 07X | 00 | 111 | XXX |
| ⊥ e SSS $\bar{c}$ | 10X | 01 | 000 | XXX |
| ‖ e SSS $\bar{c}$ | 11X | 01 | 001 | XXX |
| ⊥ e SSS c | 12X | 01 | 010 | XXX |
| ‖ e SSS c | 13X | 01 | 011 | XXX |
| ⊥ p SSS $\bar{c}$ | 14X | 01 | 100 | XXX |
| ‖ p SSS $\bar{c}$ | 15X | 01 | 101 | XXX |
| ⊥ p SSS c | 16X | 01 | 110 | XXX |
| ‖ p SSS c | 17X | 01 | 111 | XXX |
| ⊥ e SSS Th | 24X or 26X | 10 | 1X0 | XXX |
| ‖ e SSS Th | 34X or 36X | 11 | 1X0 | XXX |
| Photodiode | 25X or 27X or 35X or 37X | 1X | 1X1 | XXX |

Table 3.6

Broadband Data Output Voltage Level vs Input Counts

| Input Counts | Counter State | | Nominal Output V |
|---|---|---|---|
| | Exponent | Mantissa | |
| 0 | 00 | 000 | 0.000 |
| 1 | 00 | 001 | 0.161 |
| 2 | 00 | 010 | 0.323 |
| 3 | 00 | 011 | 0.484 |
| 4 | 00 | 100 | 0.645 |
| 5 | 00 | 101 | 0.806 |
| 6 | 00 | 110 | 0.968 |
| 7 | 00 | 111 | 1.129 |
| 8,9 | 01 | 000 | 1.290 |
| 10,11 | 01 | 001 | 1.452 |
| 12,13 | 01 | 010 | 1.613 |
| 14,15 | 01 | 011 | 1.774 |
| 16,17 | 01 | 100 | 1.935 |
| 18,19 | 01 | 101 | 2.097 |
| 20,21 | 01 | 110 | 2.258 |
| 22,23 | 01 | 111 | 2.419 |
| 24-27 | 10 | 000 | 2.581 |
| 28-31 | 10 | 001 | 2.742 |
| 32-35 | 10 | 010 | 2.903 |
| 36-39 | 10 | 011 | 3.065 |
| 40-43 | 10 | 100 | 3.226 |
| 44-47 | 10 | 101 | 3.387 |
| 48-51 | 10 | 110 | 3.548 |
| 52-55 | 10 | 111 | 3.710 |
| 56-63 | 11 | 000 | 3.871 |
| 64-71 | 11 | 001 | 4.032 |
| 72-79 | 11 | 010 | 4.193 |
| 80-87 | 11 | 011 | 4.355 |
| 88-95 | 11 | 100 | 4.516 |
| 96-103 | 11 | 101 | 4.677 |
| 104-111 | 11 | 110 | 4.839 |
| 112-119 | 11 | 111 | 5.000 |

The data reduction procedures described in Section 3 have been used to obtain several corrected ESA spectra and SSS spectra, for time periods when the perpendicular detector pitch angle is equal to the parallel detector pitch angle. Examples of different spectral shapes have been selected to show the effects of the ESA correction procedures. Figure 4.1 shows the electron spectra for 0345 UT on day 150, 1979. The data are for a pitch angle of 109°, with the perpendicular detector sun angle being 176° so that this is for a dipole-like geomagnetic field configuration. The two detector sets are in good agreement over the entire spectral range, with the differences being within the statistical errors. The triangles show the uncorrected perpendicular ESA spectra, where the differences are significant. Only the three highest energy ESA channels show significant correction effects, caused primarily by the steep spectral fall (about $E^{-3}$). Note that the corrected ESA spectra are in much better agreement with the SSS spectra.

The proton spectra for the same time period are shown in Fig. 4.2. The two lowest energy channels are dominated by the electron induced background, with the statistical errors exceeding the measured value, and so are not shown. The parallel and perpendicular detector sets are in good agreement, as are the ESA and SSS measured components of the spectra. Only the anti-coincidence SSS spectra are plotted since the higher energy coincidence data are usually very low and have poor statistical accuracy.

Electron and proton spectra for 0221:11 UT on day 59, 1979, are shown in Figs. 4.3 and 4.4. Here the electron spectrum shows a break near 30 keV, with a significant correction to the highest energy ESA channel bringing it into good agreement with the SSS data. The proton spectra show a peak at about 25 keV, with the lowest energy ESA channels all being masked by electron background. This occurs whenever a strong electron flux above 1 keV is associated with very weak proton fluxes below 1-10 keV. The spectra in Figs. 4.3 and 4.4 are for the peak of a very strong pitch angle distribution, which is described in more detail in Section 4.2.

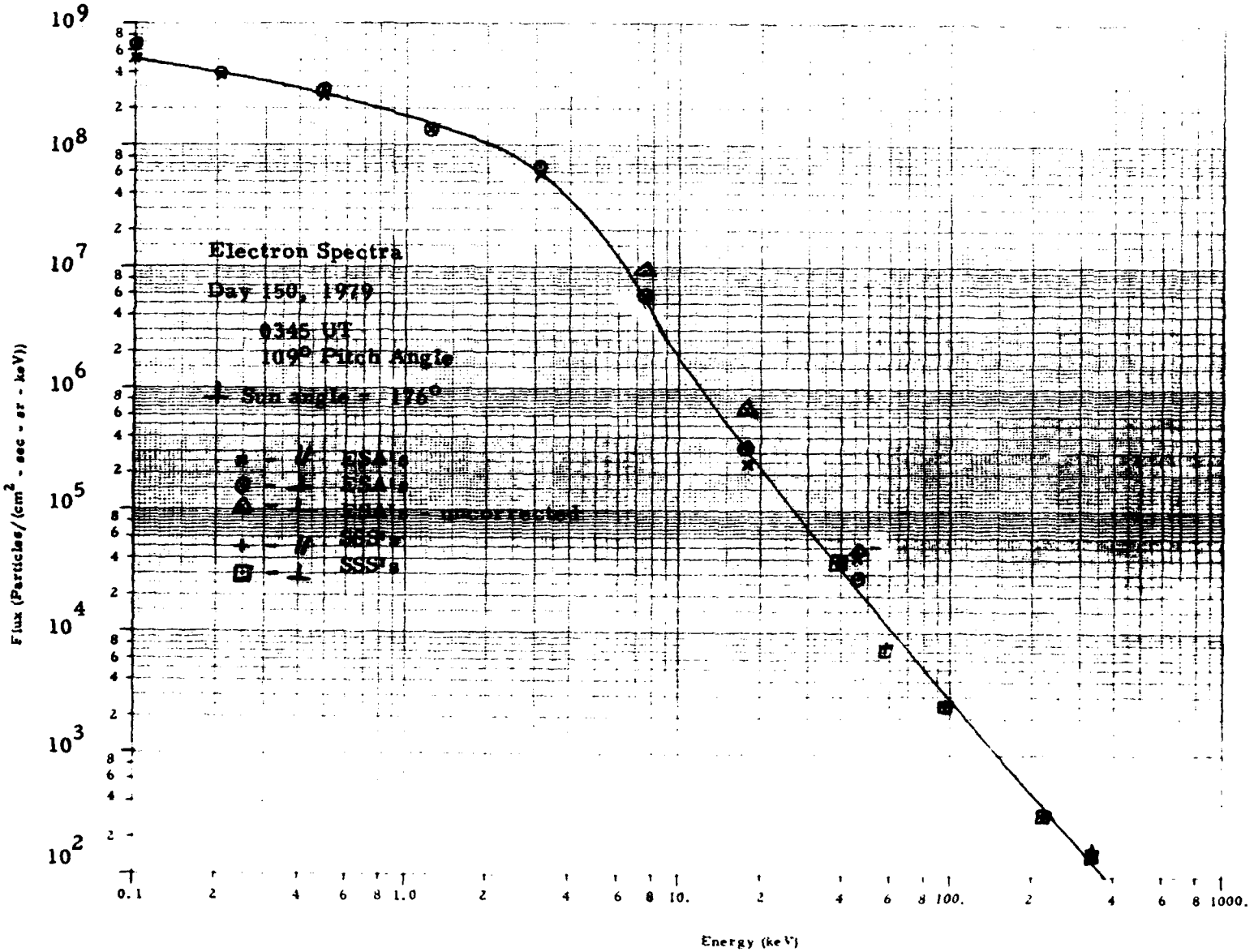


Figure 4.1. Parallel and Perpendicular Detector Electron Spectra for 0345 UT on Day 150, 1979.

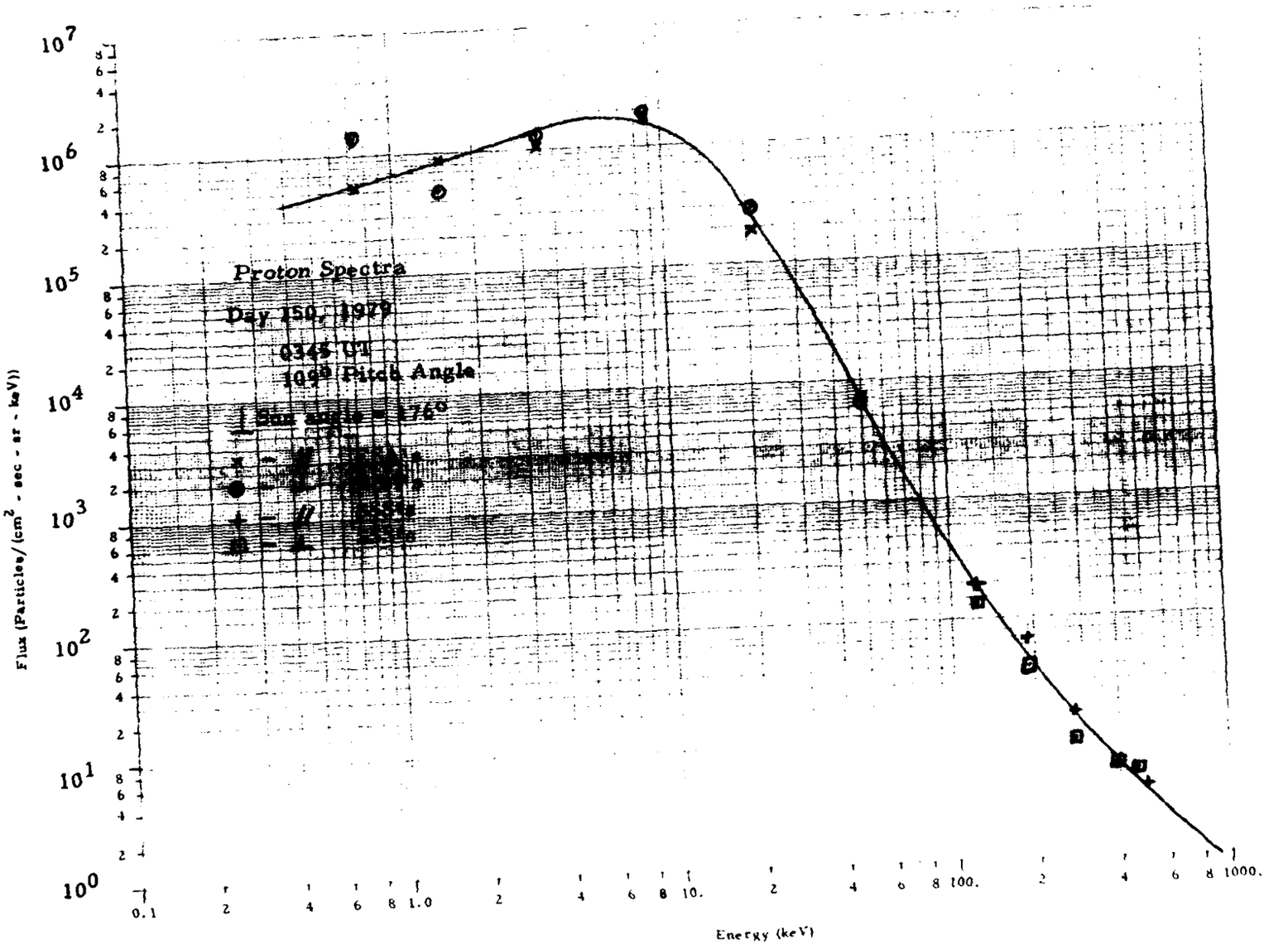


Figure 4.2. Parallel and Perpendicular Detector Proton Spectra for 0345 UT on Day 150, 1979.

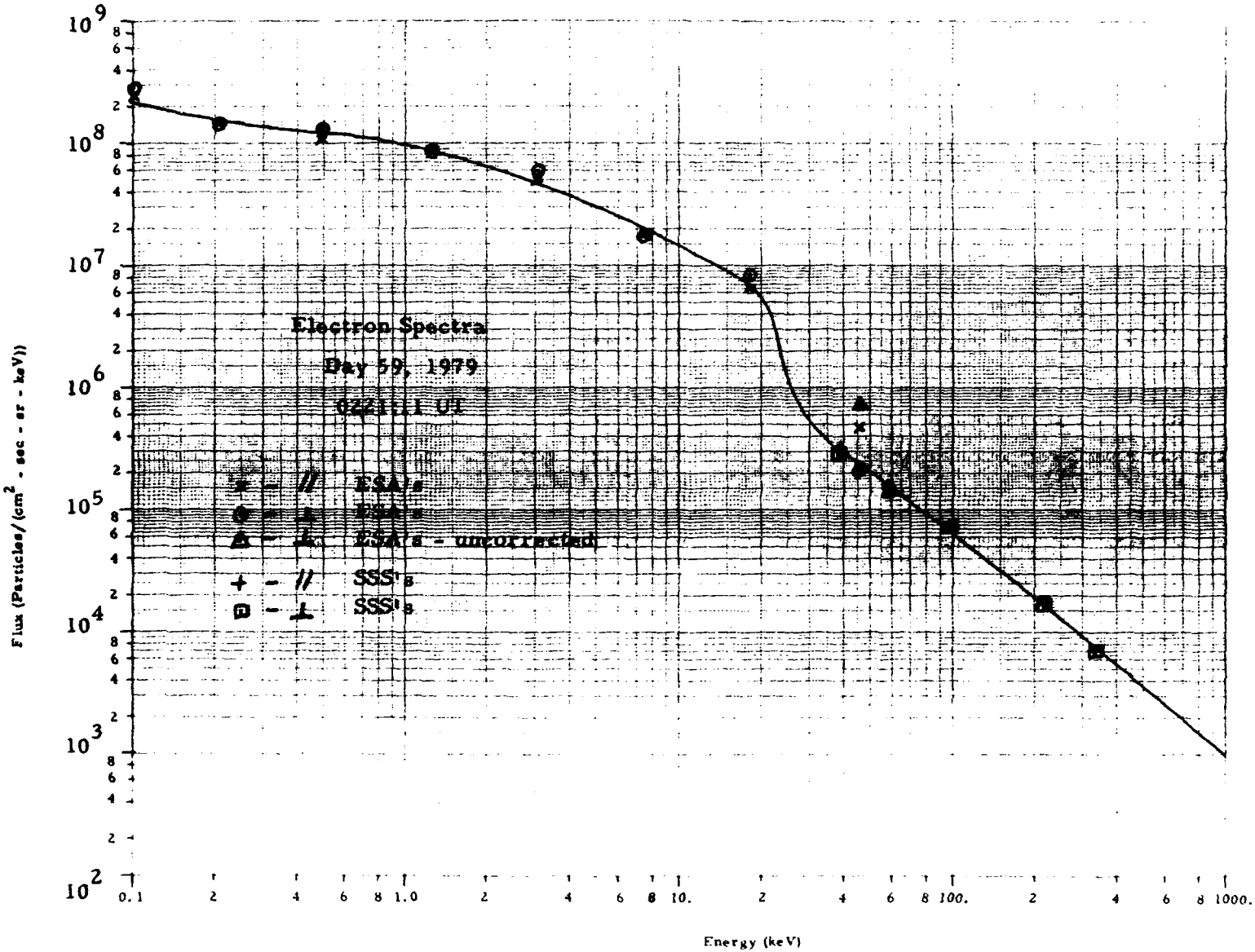


Figure 4.3. Parallel and Perpendicular Detector Electron Spectra for 0221:11 UT on Day 59, 1979.

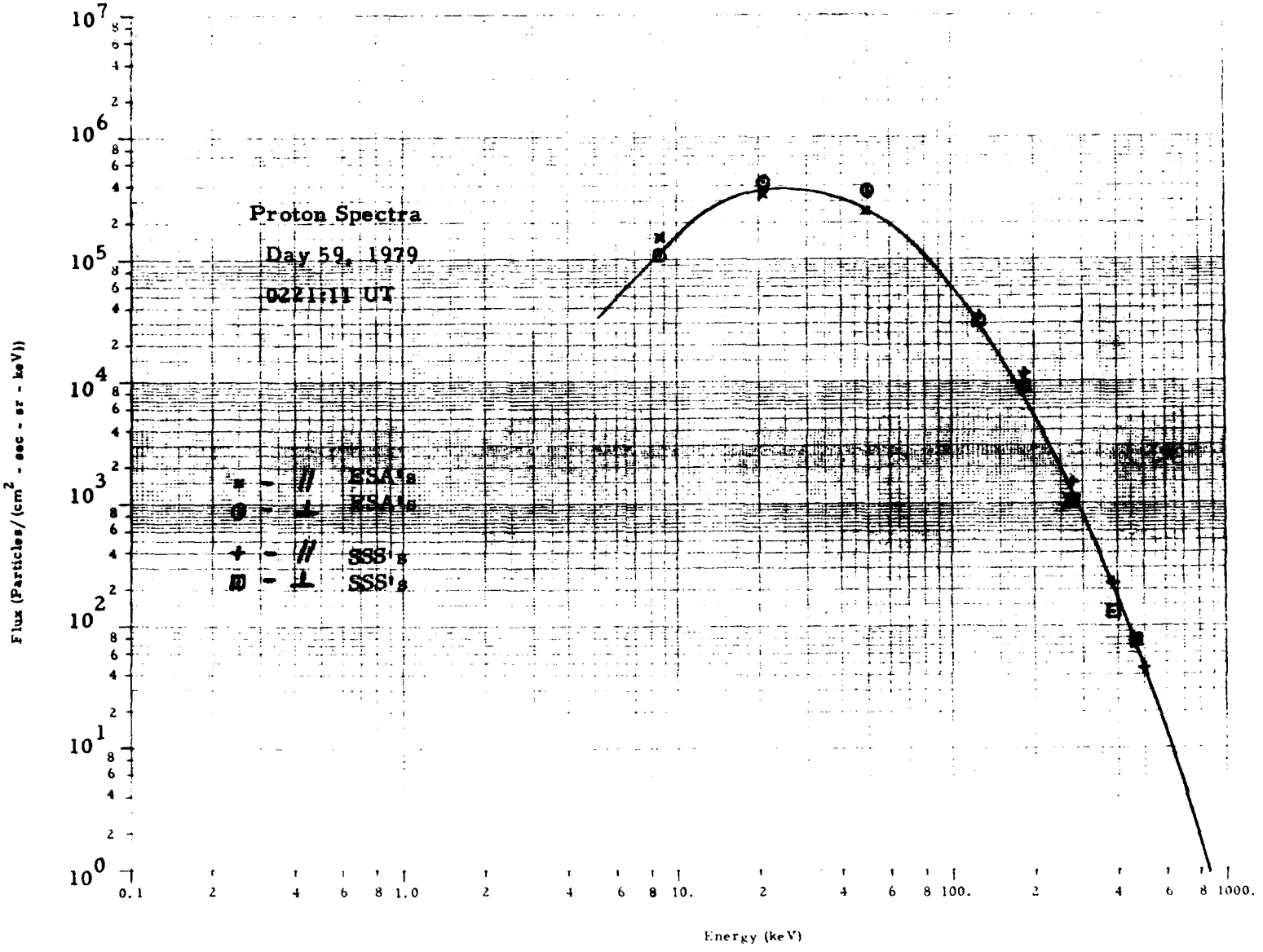


Figure 4.4. Parallel and Perpendicular Detector Proton Spectra for 0221:11 UT on Day 59, 1979.

A set of electron and proton spectra for 0907 UT on day 100, 1979 are shown in Figs. 4.5 and 4.6 The electron spectrum shows a significant drop near 8 keV, which is made stronger by the ESA corrections. The dotted extrapolations show a possible decomposition of the electron spectrum into two quasi-thermal (Maxwell-Boltzmann) distributions, as has been done for much of the particle data near geosynchronous orbit (Ref. 1.4). The proton spectra show a typical (for the SC5 proton data) broad peak in the 10-50 keV range, along with a low energy tail. The proton spectrum might also be decomposed into two quasi-thermal components. The two lowest energy proton channels are not usable because of masking by electron background.

Electron spectra for 1130 UT on day 115, 1979 are shown in Fig. 4.7. These spectra are for 109° pitch angle, with a perpendicular sun angle of 78°, a tail-type geomagnetic field configuration, and show a very hard electron spectrum. All ESA corrections are small, and the ESA and SSS spectra are in excellent agreement. The upturn at the highest energy anti-coincidence SSS channel is statistically real, and is caused by the wide energy response of the 335 keV electron anti-coincidence channel (430 keV). For strongly falling spectra this channel should be corrected in a manner similar to the ESA channels, but this has not been done since this channel usually has only a very low count rate. All the other electron SSS anti-coincidence channels are comparatively narrow, and so have small corrections for strongly varying spectra.

Electron spectra for 2207 UT on day 230, 1979 are shown in Fig. 4.8. Here the high energy break is sharp, and the two highest energy ESA channels have significant corrections. The corrected ESA spectra are in good agreement with the SSS spectra. The parallel and perpendicular detector sets also give electron spectra in excellent agreement at the same pitch angle. The data in Fig. 4.8 are for a region of dipole-like field lines, since the pitch angle is near 90° and the perpendicular detector set sun angle is near 180°.

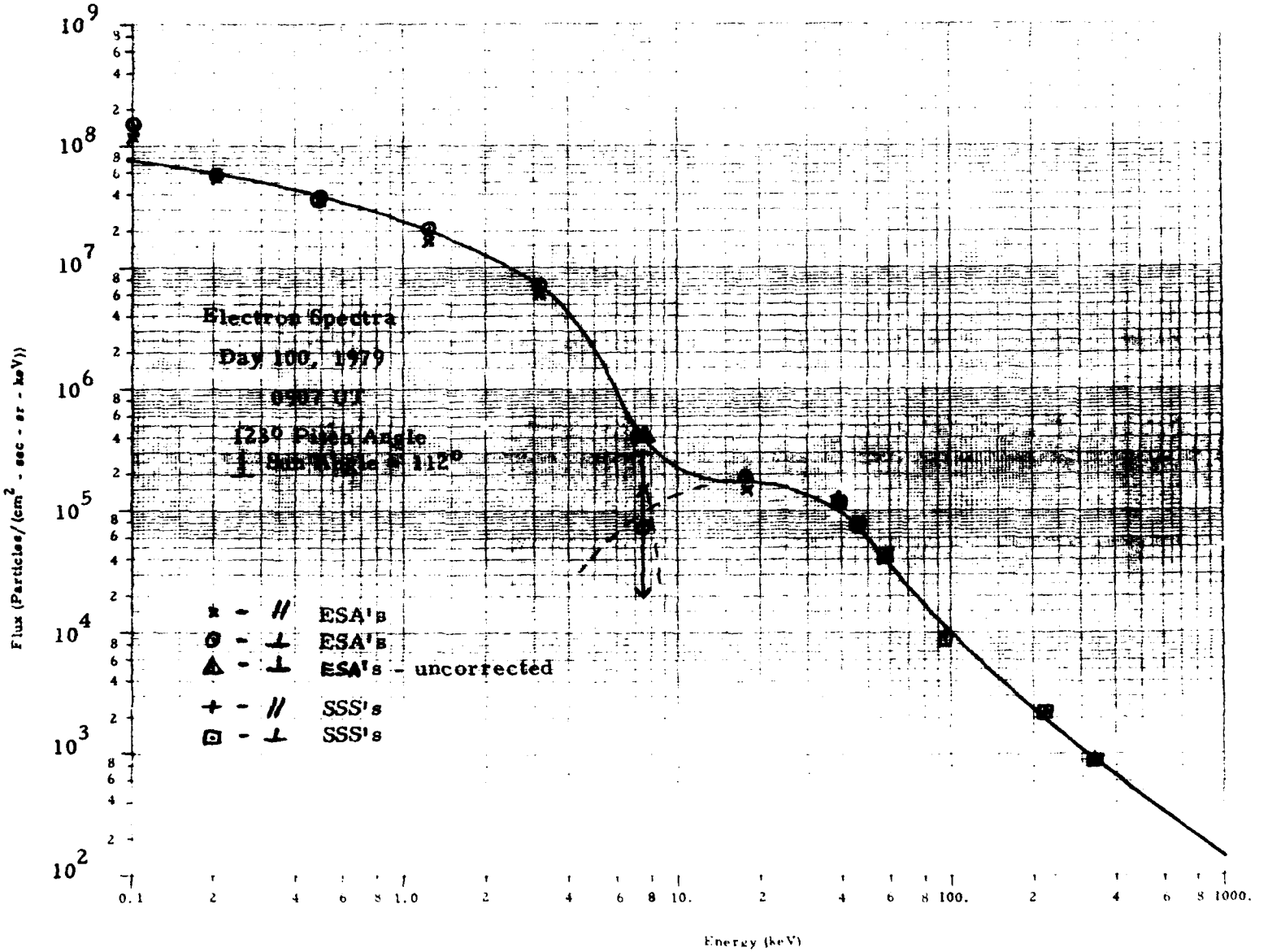


Figure 4.5. Parallel and Perpendicular Detector Electron Spectra for 0907 UT on Day 100, 1979.

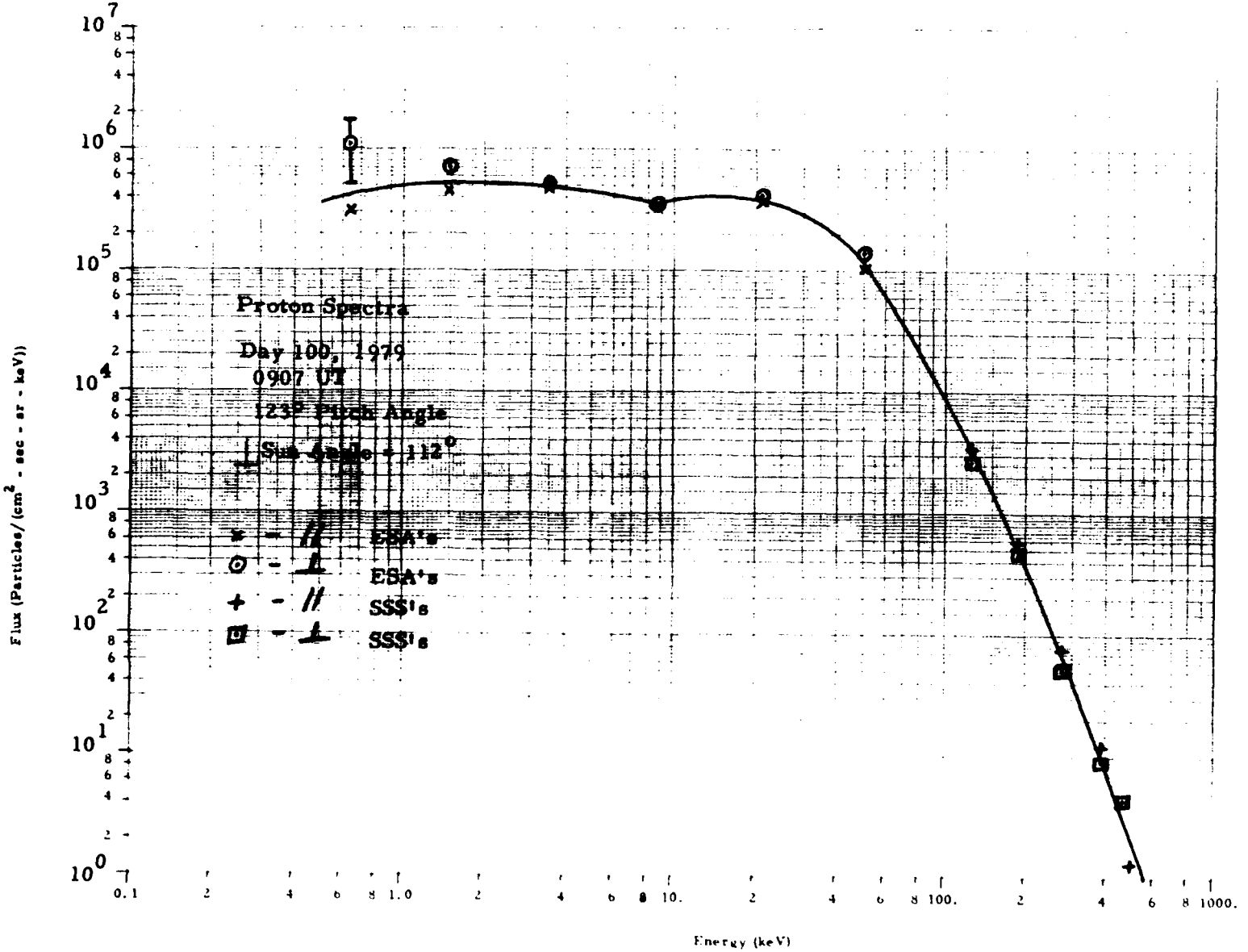


Figure 4.6. Parallel and Perpendicular Detector Proton Spectra for 0907 UT on Day 100, 1979.

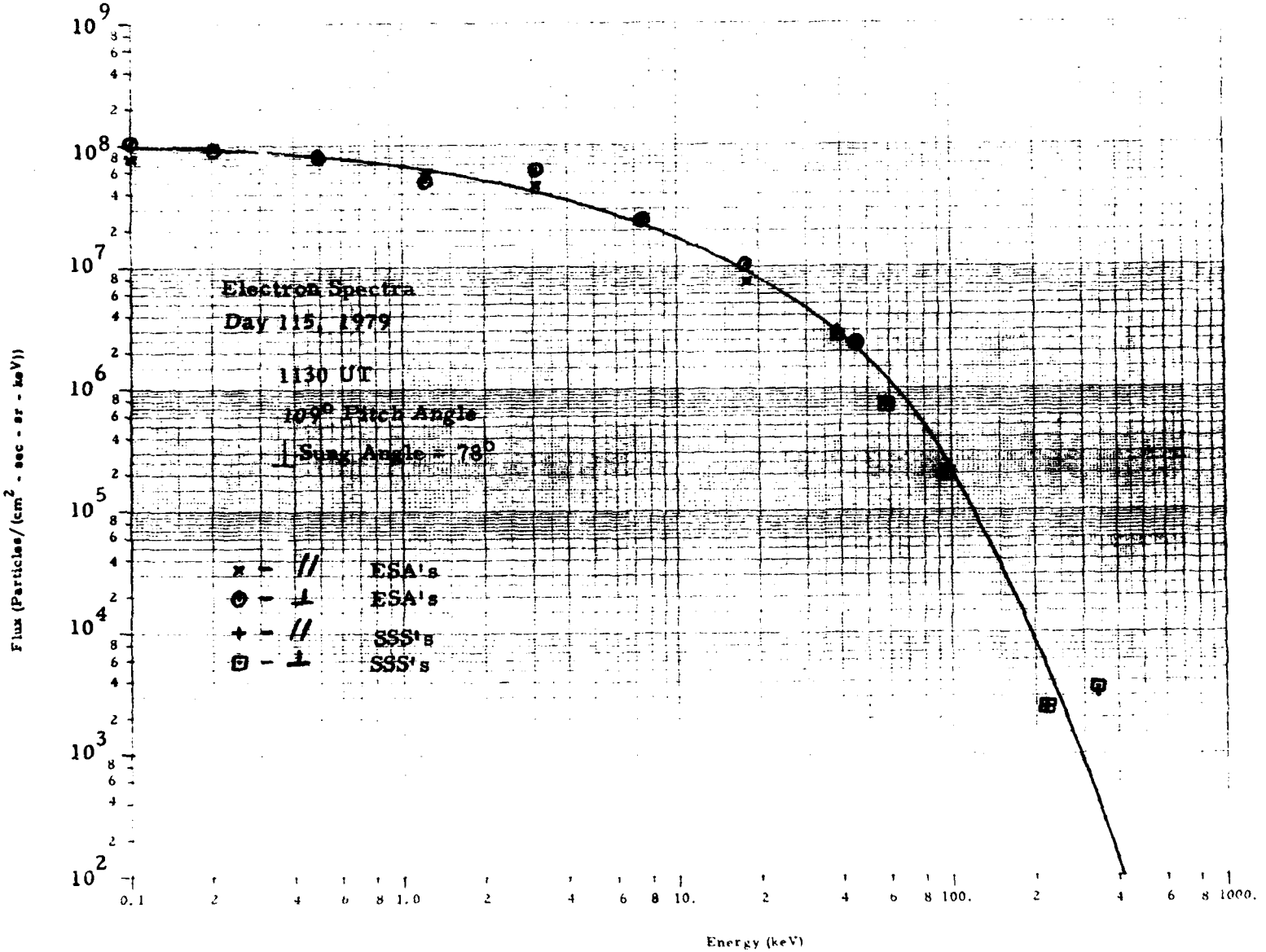


Figure 4.7. Parallel and Perpendicular Detector Electron Spectra for 1130 UT on Day 115, 1979.

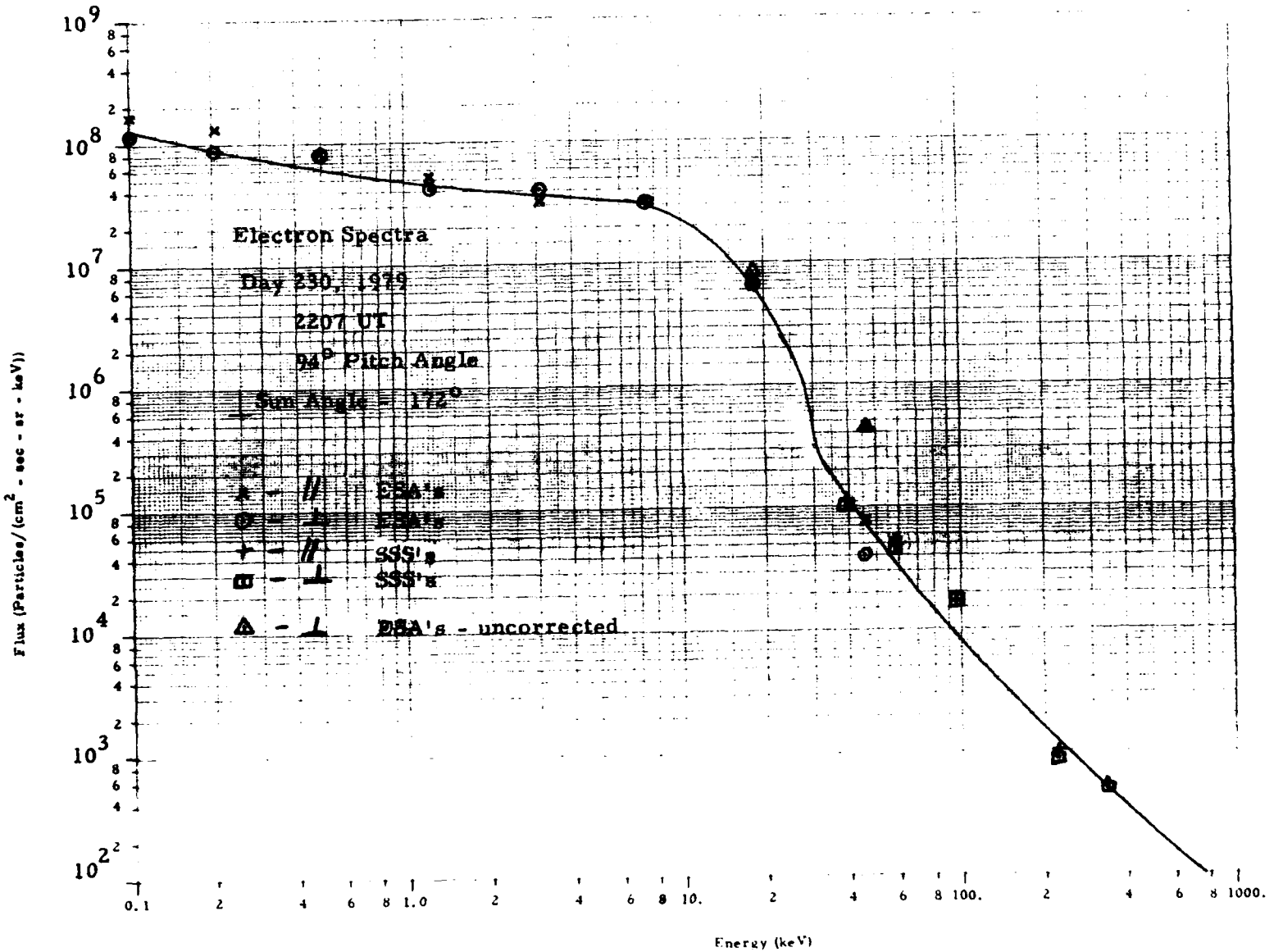


Figure 4.8. Parallel and Perpendicular Detector Electron Spectra for 2207 UT on Day 230, 1979.

The spectra shown here illustrate some of the general characteristics of the SC5 data when reduced to spectral form. Most of the zero order ESA spectra are quite good, except steeply falling portions or regions of sharp breaks. The parallel and perpendicular detector sets give spectra in excellent agreement for the same pitch angle. All the detectors, LE ESA, HE ESA, and SSS, give corrected spectra in excellent agreement.

4.2 Pitch Angle Distributions

The SC5 spectrometer makes a complete spectral measurement once every second. Since the SCATHA satellite spin period is about 57 seconds, this allows pitch angle distributions to be made with about 6° angular resolution, for all energy and particle categories. Normal operations return an immense amount of data, so detailed pitch angle analysis is likely to be done only for selected events of special interest. The pitch angle distributions are used to calculate the various particle parameters for the SCATHA Data Atlas (Refs. 1.4 and 1.6).

The SCATHA satellite orbit goes from about 5.3 $R_e$ to 7.8 $R_e$, and so samples a variety of geomagnetic field line types. This results in a variety of pitch angle distributions being measured by SC5. One of the more interesting examples is shown in Figs. 4.9 and 4.10, which give the count rate vs time for several electron and proton energy channels in the perpendicular detectors. The data are for day 59, 1979, and the spectra for the peak of the distribution, near 90° pitch angle, were shown in Figs. 4.3 and 4.4.

The electron distributions in Fig. 4.9 show a peaking at 90°, with a nearly 10:1 peak/valley ratio at 18 keV. At lower energies the peak/valley ratio decreases, as it also does at higher energies. At the highest energy shown, the distribution becomes broad and flat about 90°. The proton pitch angle distributions show a strong energy dependent form, with the lowest energies (3.5 keV) having a dip near 90°, somewhat higher energies (20.4 keV) having a flat distribution, even higher energies (49 keV) having a peak at 90°; and the highest energies (188 and 275 keV) having a double peak with a minimum at 90°.

The data in Figs. 4.9 and 4.10 illustrate the detail that is available from the SC5 perpendicular data, and do not show all of the energy channels

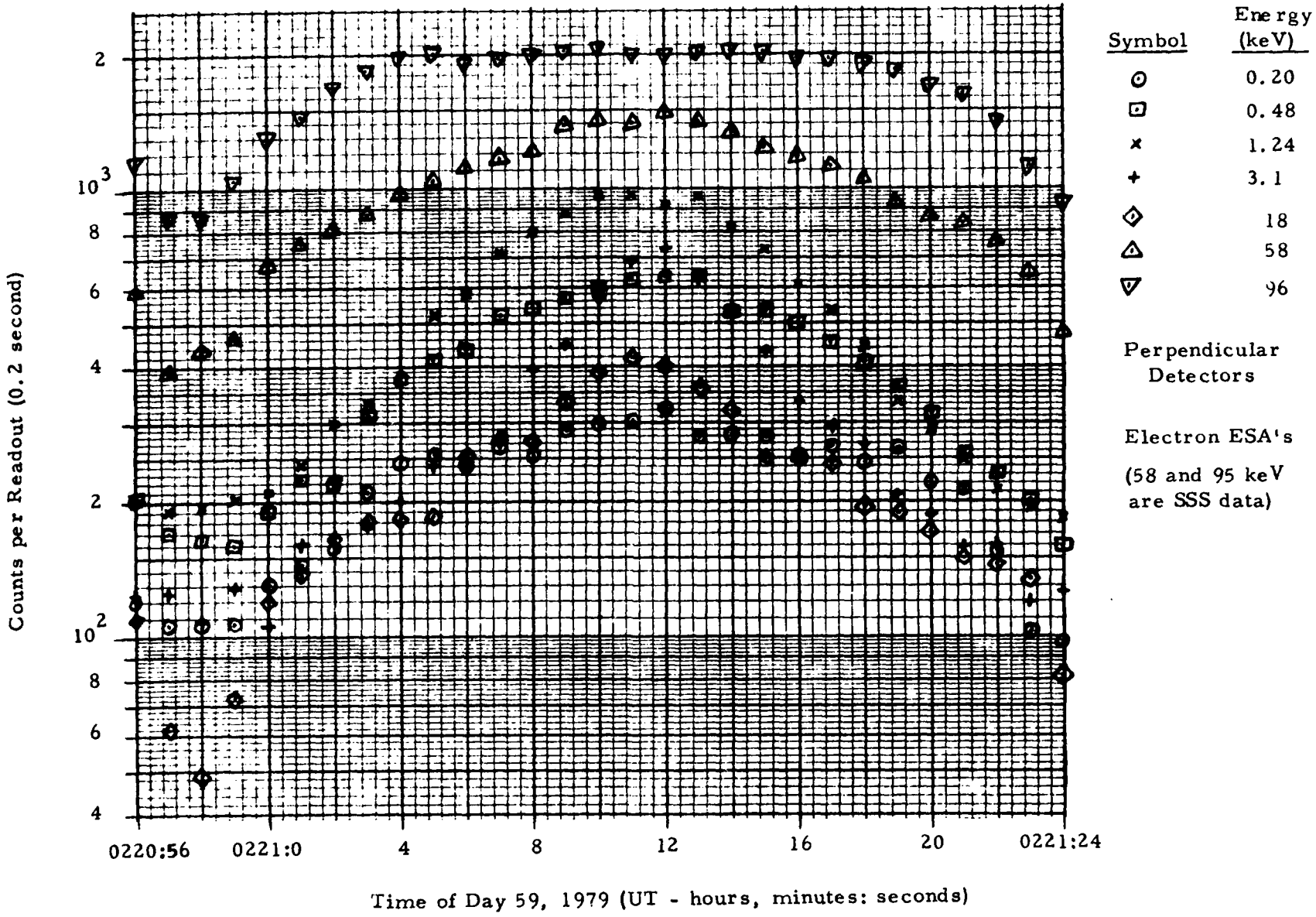


Figure 4.9. Electron Data from Day 59, 1979, Showing a Strong Pitch Angle Distribution

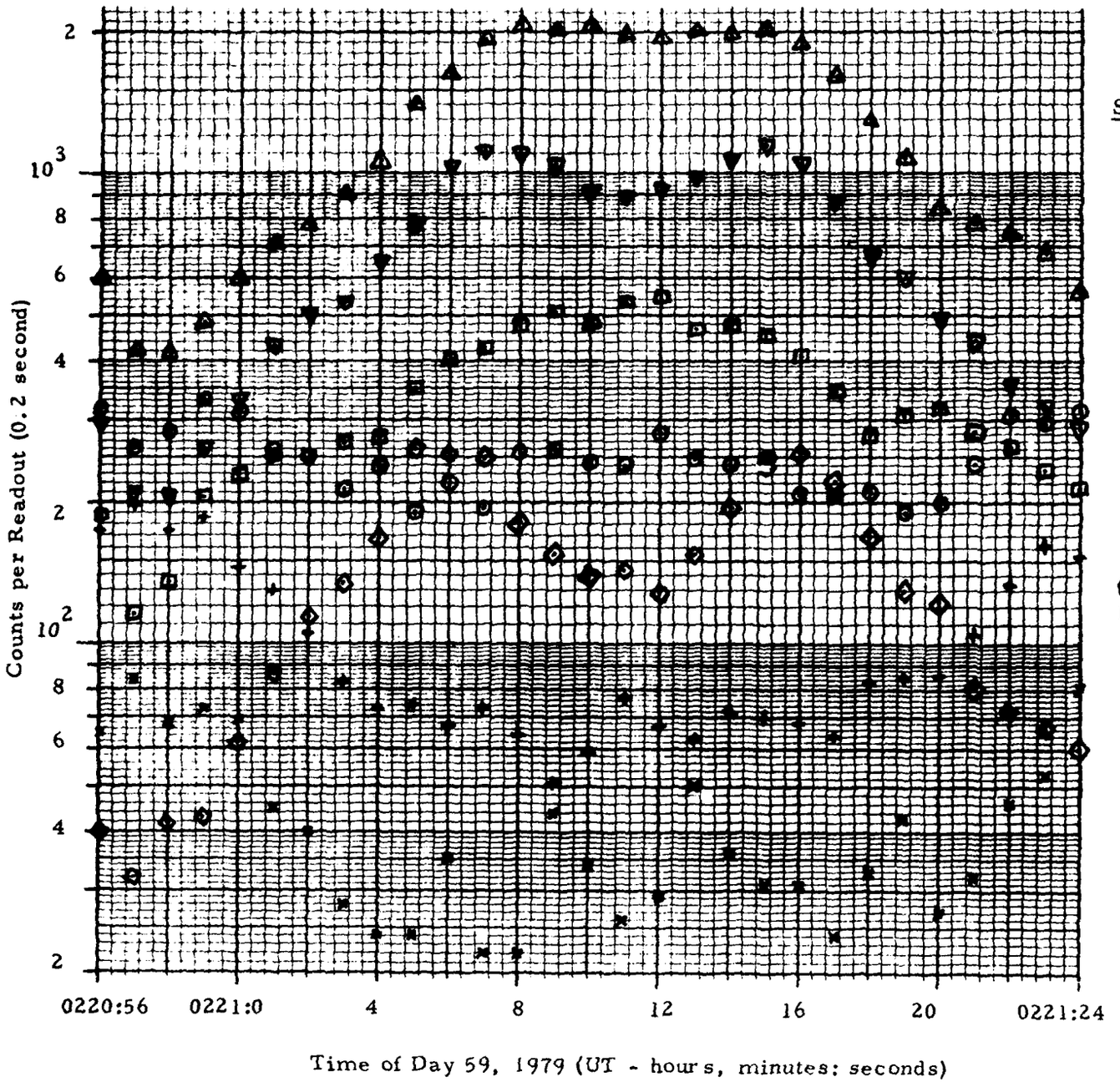


Figure 4.10. Proton Data from Day 59, 1979, Showing Energy - dependent Pitch Angle Distribution.

available. Because of the drift of the major axis of the SCATHA orbit, pitch angle distributions are available for all local time for the 5.3 to 7.8 $R_e$ region. This large data set should allow the pitch angle distributions to be used for more detailed studies of the particle populations in this near-geosynchronous orbit region.

4.3 SC5 Data During Electron Gun Operations

SC5 has been on during many electron gun operations under various ambient particle conditions. On a number of occasions the SCATHA satellite has been charged to full electron beam potential, which has been as high as 3 kV. The parallel electron ESA spectrum for one such occasion is shown in Fig. 4.11. The corrected spectrum shows a strong peak in the 3.1 keV channel, but since the actual electron spectrum contains a narrow peak near 3.0 keV, the broad energy resolution of the ESA's masks the true peak intensity. Most of the low energy tail is from backscattered and secondary electrons from the satellite surface.

Some of the most interesting SC5 data during electron gun operations comes from the 250 μsec time resolution data on the FM(B) band. An example of such data was shown earlier in Fig. 3.14. Those data are for turn-on of a 500 eV, 0.1 mA electron beam, as seen by the parallel LE electron ESA channel #1 (85 eV). Another example is shown in Fig. 4.12, where the response of channel #4 (1.25 keV) is shown for a 1.5 keV, 1 mA electron beam turn-on. Here there is a rise time constant of about 2 msec, and a subsequent partial decay with a time constant of about 0.11 second.

The response of energy channel 1 to turn-off of a 1.5 keV, 1 mA electron beam is shown in Fig. 4.13. Here there is a rise of about 1 msec with a long decay time of about 0.7 sec while the low energy ($\simeq$ 100 eV or less) electron flux returns to the initial ambient conditions. The results of some of the FM(B) data for electron gun operations on day 297, 1979 are given in Table 4.1. These comprise most of the 1 mA FM(B) data available for that series of gun operations. The FM(B) data of Figs. 3.14, 4.12, and 4.13, and the summary in Table 4.1, were presented earlier in Ref. 1.7.

The SC5 electron gun operation data are quite extensive, and have already provided some interesting results (Refs. 1.7, 1.9). At this time

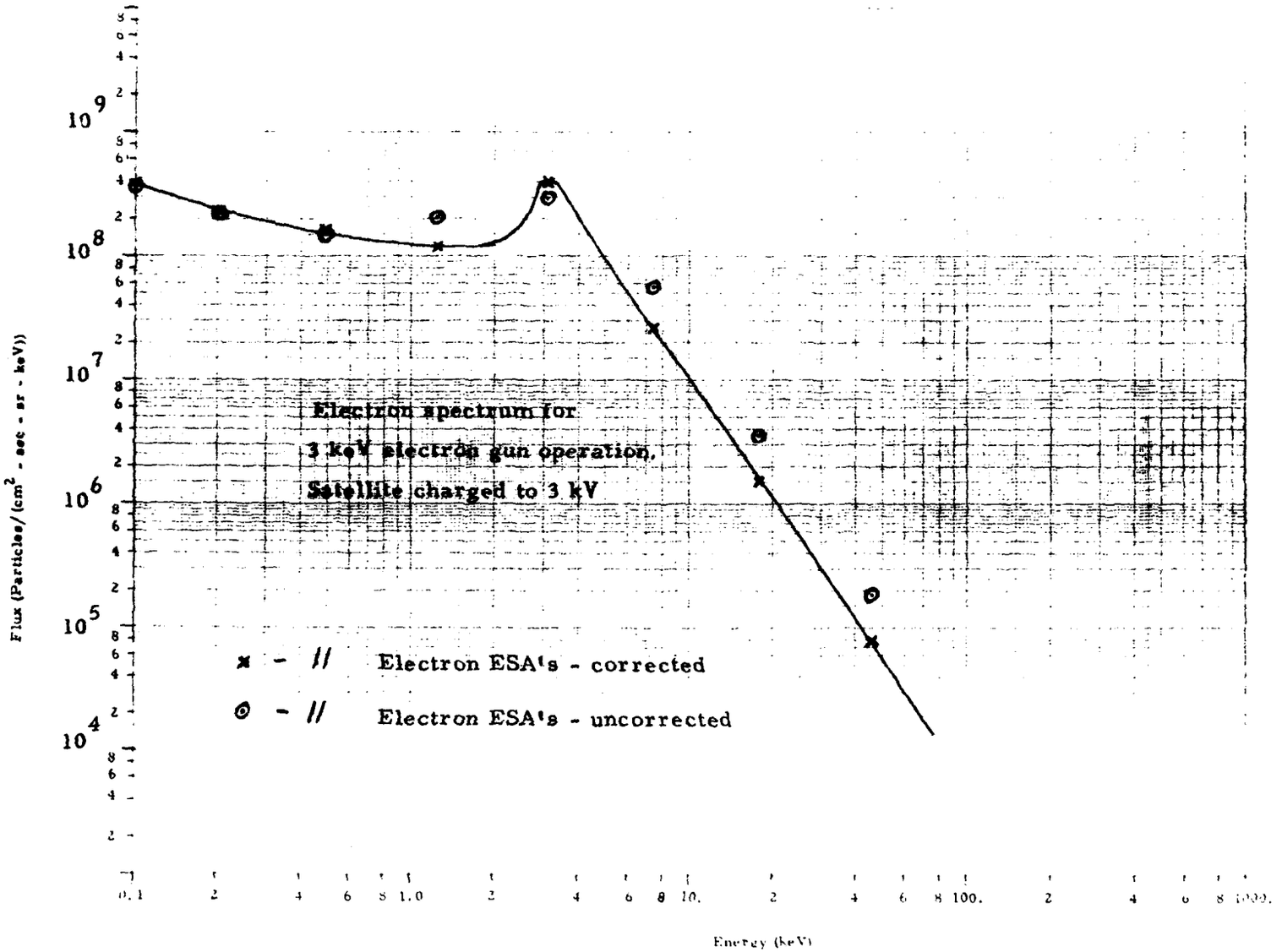


Figure 4.11. Electron Spectrum Measured During Electron Gun Operation with 3 kV Satellite Charging.

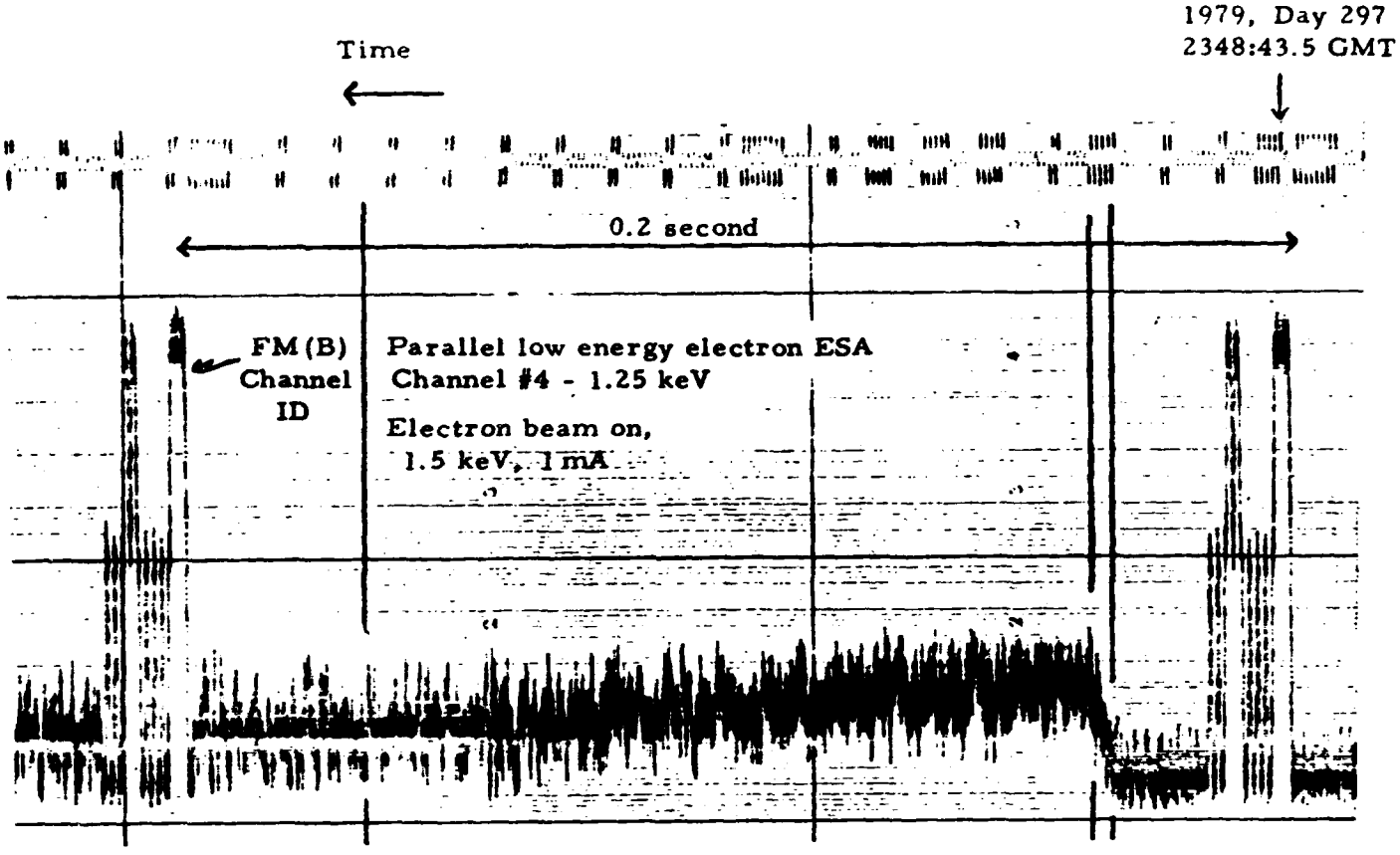


**Figure 4. 12. Response of the 1.25 keV Parallel Electron ESA Energy Channel to Electron Beam Turn-on at 1.5 keV, 1 mA, on Day 297, 1979.**

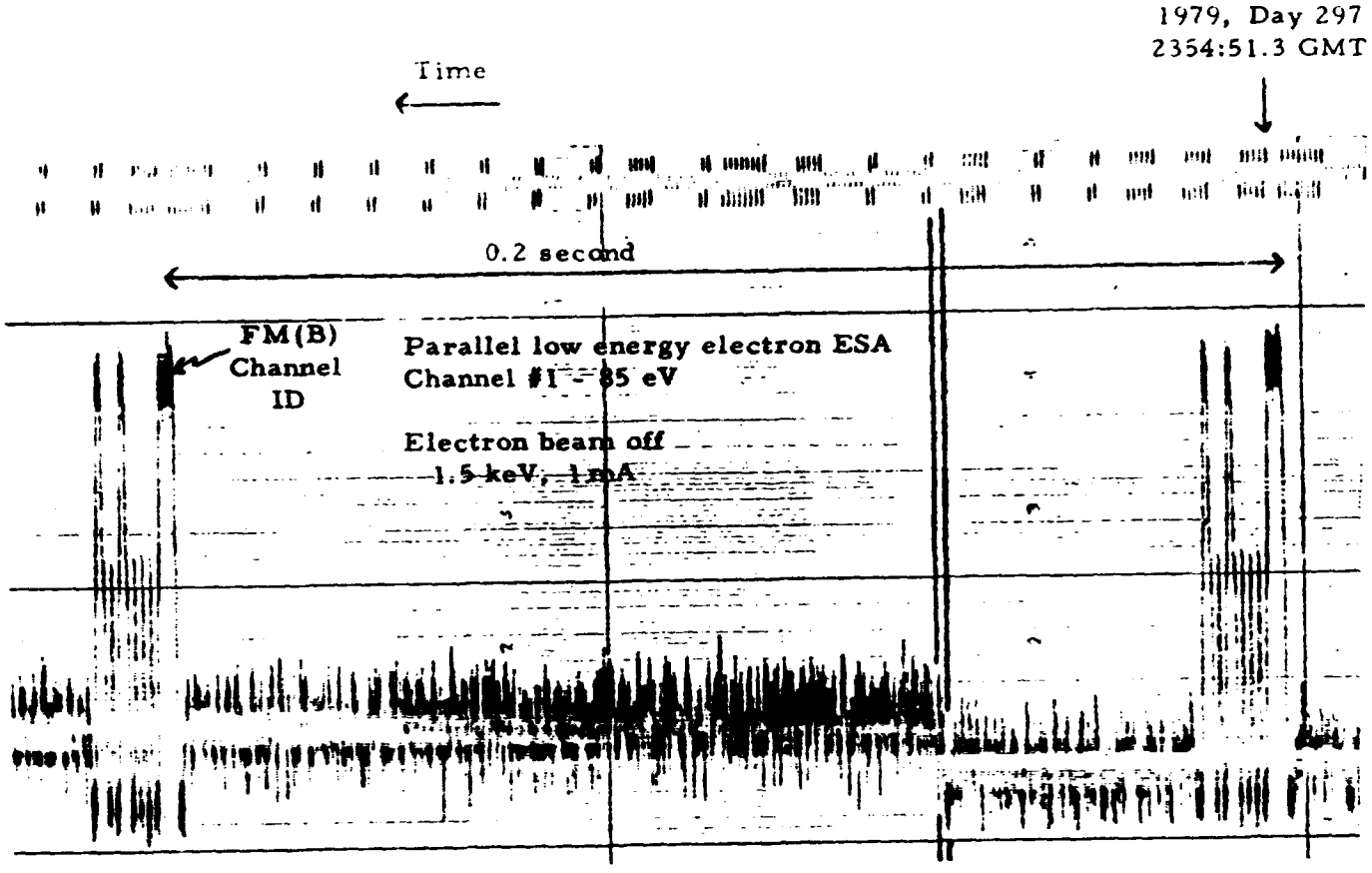


Figure 4.13 Response of the 85 eV Parallel Electron ESA Energy Channel to Electron Beam Turn-off at 1.5 keV, 1 mA, on Day 297, 1979.

Table 4.1

**Summary of Electron Beam On/Off Characteristics for Some of the Day 297, 1979 Operations**

| Electron Beam on/off | Beam Voltage (V) (Current = 1 mA) | Parallel Electron ESA Energy Channel (E in keV) | Rise/Decay Times (sec) |
|---|---|---|---|
| on | 50 | 1 (0.085) | Rise < 0.001 |
| off | 500 | 1 (0.085) | Rise $\simeq$ 0.001/Decay $\simeq$ 0.7 |
| on | 500 | 3 (0.500) | Rise $\simeq$ 0.001/Decay $\simeq$ 0.001 |
| off | 1500 | 4 (1.250) | Decay $\simeq$ 0.002 |
| on | 1500 | 4 (1.250) | Rise $\simeq$ 0.002/Fall $\simeq$ 0.11 |
| off | 1500 | 3 (0.500) | During Channel ID |
| on | 1500 | 3 (0.500) | Rise < 0.001/Fall $\simeq$ 0.001 |
| off | 1500 | 2 (0.210) | Decay $\simeq$ 0.005 |
| on | 1500 | 2 (0.210) | Rise < 0.001/Fall $\simeq$ 0.001 |
| off | 1500 | 1 (0.085) | Rise $\simeq$ 0.001/Decay $\simeq$ 0.7 |
| on | 1500 | 1 (0.085) | Rise < 0.001/Fall $\simeq$ 0.002 |

the high time resolution FM data are quite unique and provide data never before available from a satellite instrument.

## 5. CONCLUSIONS

The SC5 Rapid Scan Particle Spectrometer on the SCATHA satellite has operated properly for over one year, well in excess of the six month design life. Data show that after two years in orbit only one ESA of eight, the perpendicular low energy electron ESA, had suffered severe SEM gain degradation. Data from nearly three years after launch show that at bias level 16 all ESA's are still operating satisfactorily, except for the perpendicular LE electron ESA.

Much of the LE electron ESA degradation has come from the electron gun operations, which at times resulted in extremely high count rates. The perpendicular ESA's also suffer some degradation from scattered solar UV. The ESA geometric factors were set large to provide good statistical accuracy for high time resolution measurements, consistent with survival for a minimum of six months. The three year survival for seven of eight SEM detectors is thus quite good.

The SEM efficiency factors have been obtained from calibration cycle data for more than a year of operation. Much of the data will form the basis for a near geosynchronous orbit particle data atlas (Refs. 1.4, 1.6). Some of the data have also been used for studies of particle population behavior and of spacecraft operations (Ref. 1.7, 1.8, 1.9, 1.10). A large amount of data from SC5 have been obtained, including much FM (B) data during electron gun operations. The electron gun operation data and the detailed particle pitch angle distributions measured by SC5 form a presently unique data set.

The SCATHA satellite program has proven to be a success, with a considerable amount of data returned by the various instruments on the satellite (Ref. 1.5). The SC5 instrument has been a part of that success, and has provided large amounts of high quality data relevant to spacecraft charging.

## REFERENCES


1.1 J. R. Stevens and A. L. Vampola, editors, "Description of the Space Test Program P78-2 Spacecraft and Payloads," report SAMSO TR-78-24, 31 October 1978.

1.2 P. R. Morel, F. A. Hanser, and B. Sellers, "Design of Instrumentation Suitable for the Investigation of Charge Buildup Phenomena at Synchronous Orbit," report AFGL-TR-79-0235, October 1979.

1.3 F. A. Hanser, D. A. Hardy, and B. Sellers, "Calibration of the Rapid Scan Particle Detector Mounted in the SCATHA Satellite," report AFGL-TR-79-0167, 18 July 1979.

1.4 E. G. Mullen, H. B. Garrett, D. A. Hardy, and E. C. Whipple, "P78-2 SCATHA Preliminary Data Atlas," report AFGL-TR-80-0241, 11 August 1980.

1.5 N. J. Stevens and C. P. Pike, editors, "Spacecraft Charing Technology 1980," NASA Conference Publication 2182, AFGL-TR-81-0270 (1981).

1.6 E. G. Mullen, D. A. Hardy, H. B. Garrett, and E. C. Whipple, "P78-2 SCATHA Environmental Data Atlas," p. 802 in Ref. 1.5.

1.7 B. Sellers, F. A. Hanser, P. R. Morel, J. L. Hunerwadel, A. L. Pavel, L. Katz, and P. L. Rothwell, "A High-Time Resolution Spectrometer for 0.05 to 500 keV Electrons and Protons," p. 31 in A. Rosen, ed., Spacecraft Charging by Magnetospheric Plasmas, Progress in Astronautics and Aeronautics, Vol. 47, American Institute of Aeronautics and Astronautics (1976).

1.8 F. A. Hanser, B. Sellers, D. A. Hardy, H. A. Cohen, J. Feynman, and M. S. Gussenhoven, "Operation of SC5 Rapid Scan Particle Spectrometer on SCATHA Satellite," p. 386 in Ref. 1.5.

1.9 M. S. Gussenhoven, H. A. Cohen, D. A. Hardy, W. J. Burke, and A. Chesley, "Analysis of Ambient and Beam Particle Characteristics During the Ejection of an Electron Beam from a Satellite in Near-Geosynchronous Orbit on March 30, 1979,"p. 642 in Ref. 1.5.

1.10 H. A. Cohen, et al, "P78-2 Satellite and Payload Responses to Electron Beam Operations on March 30, 1979," p. 509 in Ref. 1.5.

1.11 W. H. Farthing, J. P. Brown, and W. C. Bryant, "Differential Spacecraft Charging on the Geostationary Operational Environmental Satellites," NASA Technical Memorandum 83908, Goddard Space Flight Center (March, 1982).

# APPENDIX A

## SEM EFFICIENCY FACTOR TABULATION

The efficiency factors plotted in Figures 3.3 to 3.13 were used to provide a tabulation of daily SEM efficiency factors for data analysis. For a few periods when the efficiency factors varied significantly in a 24 hour period, the days have been split into shorter time intervals. Most factors are for operation at SEM bias level 8, except for the initial operations at bias level 1 and some gun operation periods at bias level 12. The tabulated data are given in Table A.1, which covers most of the ESA operation time of Figs. 3.3 to 3.13. Time periods not listed in Table A.1 are not presently required for analysis, generally because of the data not being available for analysis. When no time interval is given in Table A.1, the data are for the full 24 hour period.

Table A.1

SEM Efficiency Factor Tabulation

| Day (1979) | Time range (UT) (hrs-min) | SEM Efficiency Factors: Electron ESA's LE | Electron ESA's HE | Electron ESA's LE | Electron ESA's HE | Proton ESA's LE | Proton ESA's HE | Proton ESA's LE | Proton ESA's HE |
|---|---|---|---|---|---|---|---|---|---|
| Operations at bias level 1 | | | | | | | | | |
| 40 | 0230-1200 | 1.10 | 1.05 | 1.10 | 1.05 | 1.00 | 1.00 | 1.00 | 1.00 |
| 40 | 1200-2400 | 1.25 | 1.15 | 1.40 | 1.10 | 1.05 | 1.05 | 1.10 | 1.15 |
| 41 | 0000-1200 | 1.50 | 1.25 | 1.80 | 1.15 | 1.10 | 1.10 | 1.20 | 1.25 |
| 41 | 1200-2400 | 1.80 | 1.40 | 2.5 | 1.25 | 1.10 | 1.10 | 1.30 | 1.40 |
| 42 | 0000-1200 | 2.1 | 1.55 | 3.1 | 1.35 | 1.15 | 1.15 | 1.45 | 1.55 |
| 42 | 1200-2400 | 2.5 | 1.70 | 4.1 | 1.45 | 1.20 | 1.20 | 1.55 | 1.70 |
| 43 | 0000-1200 | 3.0 | 1.90 | 5.4 | 1.60 | 1.20 | 1.20 | 1.70 | 1.90 |
| 43 | 1200-2400 | 3.7 | 2.1 | 7.2 | 1.70 | 1.25 | 1.25 | 1.80 | 2.05 |
| 44 | 0000-1200 | 4.1 | 2.2 | 9.0 | 1.80 | 1.30 | 1.30 | 1.95 | 2.2 |
| 44 | 1200-2400 | 4.3 | 2.3 | 10.0 | 1.85 | 1.30 | 1.30 | 2.1 | 2.4 |
| 45 | 0000-1200 | 4.5 | | 11.0 | 1.90 | 1.35 | 1.35 | 2.2 | 2.6 |
| 45 | 1200-2400 | 4.6 | | 12.0 | 1.95 | 1.40 | 1.40 | 2.4 | 2.7 |
| 46 | 0000-1200 | 4.8 | 2.3 | 13.0 | 2.00 | 1.40 | 1.40 | 2.6 | 2.9 |
| 46 | 1200-2400 | 4.8 | 2.4 | 13.5 | 2.0 | 1.45 | 1.45 | 2.7 | 3.1 |
| 47 | 0000-1200 | 4.9 | | 14.0 | 2.1 | 1.45 | 1.45 | 2.8 | 3.2 |
| 47 | 1200-2130 | 5.0 | 2.4 | 14.5 | 2.1 | 1.50 | 1.50 | 3.0 | 3.4 |
| Operations at bias level 8 | | | | | | | | | |
| 59 | - | 1.90 | 1.50 | 2.7 | 1.50 | 1.20 | 1.20 | 1.60 | 1.60 |
| 76 | - | 1.20 | 1.10 | 1.20 | 1.10 | 1.10 | 1.10 | 1.10 | 1.10 |
| 77 | - | 1.30 | 1.15 | 1.40 | 1.15 | | | | |
| 78 | - | 1.35 | 1.20 | 1.55 | | | | | |
| 79 | - | 1.40 | 1.25 | 1.65 | | 1.10 | 1.10 | 1.10 | 1.10 |
| 80 | - | | 1.25 | 1.70 | 1.15 | 1.15 | 1.15 | 1.15 | 1.15 |
| 81 | - | | 1.30 | 1.75 | 1.20 | | | | |
| 82 | - | | | 1.80 | | | | | |
| 83 | - | | | | | | | | |
| 84 | - | 1.40 | | 1.80 | | | | | |
| 85 | - | 1.35 | | 1.75 | | | | | |
| 86 | - | 1.30 | | 1.70 | | 1.15 | 1.15 | 1.15 | 1.15 |
| 87 | - | 1.30 | | | | 1.20 | 1.20 | 1.20 | 1.20 |
| 88 | - | 1.35 | | 1.70 | | | | | |
| 89 | - | 1.40 | 1.30 | 1.75 | 1.20 | 1.20 | 1.20 | 1.20 | 1.20 |

Table A.1 (Continued)

| Day (1979) | Time range (UT) (hrs-min) | SEM Efficiency Factors | | | | | | | |
|---|---|---|---|---|---|---|---|---|---|
| | | Electron ESA's | | | | Protons ESA's | | | |
| | | LE | HE | LE | HE | LE | HE | LE | HE |
| Operations at bias level 8 | | | | | | | | | |
| 90 | 0000-1230 | 1.45 | 1.30 | 1.80 | 1.20 | 1.20 | 1.20 | 1.20 | 1.20 |
| 90 | 1230-2400 | 2.4 | 1.55 | 3.1 | 1.40 | | | | |
| 91 | 0000-1200 | 2.3 | 1.50 | 3.0 | 1.40 | | | | |
| 91 | 1200-2400 | 2.1 | 1.50 | 2.9 | 1.35 | | | | |
| 92 | 0000-1200 | 1.95 | 1.45 | 2.8 | 1.35 | | | | |
| 92 | 1200-2400 | 1.85 | 1.40 | 2.6 | 1.30 | | | | |
| 93 | 0000-1200 | 1.70 | | 2.4 | 1.30 | | | | |
| 93 | 1200-2400 | 1.60 | 1.40 | 2.2 | 1.25 | | | | |
| 94 | 0000-1200 | 1.55 | 1.35 | 2.1 | 1.25 | | | | |
| 94 | 1200-2400 | 1.65 | 1.35 | 2.4 | 1.30 | | | 1.20 | 1.20 |
| 95 | 0000-1200 | 1.80 | 1.40 | 2.7 | 1.35 | 1.20 | 1.20 | 1.25 | 1.25 |
| 95 | 1200-2400 | 1.90 | 1.40 | 3.0 | 1.40 | 1.15 | 1.15 | | |
| 96 | 0000-1200 | 2.1 | 1.45 | 3.1 | 1.45 | | | | |
| 96 | 1200-2400 | 2.0 | 1.40 | 3.0 | 1.40 | | | | |
| 97 | 0000-1200 | 1.85 | 1.35 | 2.8 | 1.35 | | | | |
| 97 | 1200-2400 | 1.75 | 1.30 | 2.5 | 1.30 | | | | |
| 98 | - | 1.65 | | 2.2 | 1.25 | | | | |
| 99 | - | 1.60 | 1.30 | 2.1 | | | | | |
| 100 | - | | 1.25 | | | | | | |
| 101 | - | | | | | | | | |
| 102 | - | 1.60 | 1.25 | | 1.25 | | | | |
| 103 | - | 1.55 | 1.30 | | 1.30 | | | | |
| 104 | - | | 1.35 | 2.1 | 1.35 | | | | |
| 105 | - | | 1.45 | 2.0 | 1.45 | | | | |
| 106 | - | 1.55 | 1.45 | | 1.45 | | | | |
| 107 | - | 1.50 | 1.30 | | 1.30 | | | | |
| 108 | - | | 1.20 | | 1.20 | | | 1.25 | 1.25 |
| 109 | - | 1.50 | | 2.0 | | 1.15 | 1.15 | 1.30 | 1.30 |
| 110 | - | 1.60 | 1.20 | 2.1 | 1.20 | 1.20 | 1.20 | | |
| 111 | - | 1.65 | 1.25 | 2.2 | 1.25 | | | | |
| 112 | 0000-0830 | 1.70 | 1.30 | 2.3 | 1.30 | 1.20 | 1.20 | 1.30 | 1.30 |
| 112 | 0830-1200 | 2.4 | 1.70 | 4.0 | 1.70 | 1.35 | 1.35 | 1.50 | 1.50 |
| 112 | 1200-2400 | 2.3 | 1.70 | 3.8 | 1.70 | | | | |
| 113 | 0000-1200 | 2.1 | 1.60 | 3.3 | 1.60 | 1.35 | 1.35 | | |
| 113 | 1200-2400 | 2.0 | 1.55 | 3.1 | 1.55 | 1.30 | 1.30 | 1.50 | 1.50 |
| 114 | - | | | 3.2 | | | | 1.45 | 1.45 |
| 115 | - | 2.0 | 1.55 | 3.5 | 1.55 | 1.30 | 1.30 | 1.40 | 1.40 |
| 116 | - | 2.1 | 1.60 | 3.8 | 1.60 | 1.25 | 1.25 | 1.40 | 1.40 |

Table A. 1 (Continued)

| Day (1979) | Time range (UT) (hrs-min) | SEM Efficiency Factors: Electron ESA's ∥LE | ∥HE | ⊥LE | ⊥HE | Protons ESA's ∥LE | ∥HE | ⊥LE | ⊥HE |
|---|---|---|---|---|---|---|---|---|---|
| Operations at bias level 8 | | | | | | | | | |
| 117 | - | 2.0 | 1.60 | 3.7 | 1.60 | 1.25 | 1.25 | 1.40 | 1.40 |
| 118 | - | 1.90 | | 3.5 | | 1.25 | 1.25 | 1.35 | 1.35 |
| 119 | - | 1.80 | 1.60 | 3.2 | 1.60 | 1.20 | 1.20 | 1.35 | 1.35 |
| 120 | - | 1.70 | 1.55 | 2.9 | 1.55 | | | 1.30 | 1.30 |
| 121 | - | 1.60 | 1.50 | 2.7 | 1.50 | | | | |
| 122 | - | 1.55 | 1.45 | 2.5 | 1.45 | 1.20 | 1.20 | | |
| 123 | - | 1.50 | 1.40 | 2.4 | 1.40 | 1.15 | 1.15 | 1.30 | 1.30 |
| 124 | - | 1.45 | 1.35 | 2.2 | 1.35 | | | 1.25 | 1.25 |
| 125 | - | 1.40 | 1.35 | 2.1 | 1.35 | | | | |
| 126 | - | 1.35 | 1.30 | 1.95 | 1.30 | | | | |
| 127 | - | 1.30 | | 1.85 | | | | | |
| 128 | - | 1.30 | 1.30 | 1.75 | 1.30 | 1.15 | 1.15 | | |
| 129 | - | 1.25 | 1.25 | 1.65 | 1.25 | 1.10 | 1.10 | 1.25 | 1.25 |
| 130 | - | 1.25 | 1.25 | 1.55 | 1.25 | | | 1.20 | 1.20 |
| 131 | - | 1.20 | 1.20 | 1.50 | 1.20 | | | | |
| 132 | - | | | 1.45 | | | | | |
| 133 | - | | | 1.40 | | | | | |
| 134 | - | 1.20 | 1.20 | 1.35 | 1.20 | | | | |
| 135 | - | 1.15 | 1.15 | 1.30 | 1.15 | | | 1.20 | |
| 136 | - | | 1.10 | 1.35 | 1.10 | 1.10 | 1.10 | 1.10 | |
| 137 | - | 1.15 | 1.15 | 1.40 | 1.15 | 1.15 | 1.15 | 1.15 | 1.20 |
| 138 | - | 1.20 | | 1.45 | | | | | 1.25 |
| 139 | - | 1.25 | 1.15 | 1.60 | 1.15 | | | | |
| 140 | - | 1.25 | 1.20 | 1.70 | 1.20 | | | | 1.25 |
| 141 | - | 1.30 | 1.25 | 1.90 | 1.25 | | | | 1.30 |
| 142 | - | 1.35 | 1.30 | 2.0 | 1.30 | | | | |
| 143 | - | 1.40 | 1.30 | 2.1 | 1.30 | | | | |
| 144 | - | 1.40 | 1.35 | 2.2 | 1.35 | 1.15 | 1.15 | 1.15 | |
| 145 | - | 1.45 | | 2.3 | | 1.20 | 1.20 | 1.20 | |
| 146 | - | | | 2.4 | | | | | |
| 147 | - | | | 2.4 | | 1.20 | 1.20 | 1.20 | |
| 148 | - | | | 2.5 | | 1.15 | 1.15 | 1.15 | |
| 149 | - | | | | | | | | |
| 150 | - | 1.45 | | | | | | | |
| 151 | - | 1.40 | | | | | | | |
| 152 | - | 1.35 | 1.35 | | 1.35 | | | | |
| 153 | - | 1.35 | 1.30 | | 1.30 | | | | |

Table A. 1 (Continued)

| Day (1979) | Time range (UT) (hrs-min) | SEM Efficiency Factors | | | | | | | |
|---|---|---|---|---|---|---|---|---|---|
| | | Electron ESA's | | | | Proton ESA's | | | |
| | | \|\| LE | \|\| HE | ⊥ LE | ⊥ HE | \|\| LE | \|\| HE | ⊥ LE | ⊥ HE |
| Operations at bias level 8 | | | | | | | | | |
| 154 | - | 1.40 | 1.30 | 2.5 | 1.30 | 1.15 | 1.15 | 1.15 | 1.30 |
| 155 | - | 1.50 | 1.25 | | 1.25 | | | | |
| 156 | - | 1.55 | 1.25 | | 1.25 | | | | 1.30 |
| 157 | - | | 1.30 | | 1.30 | | | | 1.40 |
| 158 | - | | 1.35 | | 1.35 | 1.15 | 1.15 | 1.15 | 1.45 |
| 159 | - | 1.55 | | | | 1.20 | 1.20 | 1.20 | |
| 160 | - | 1.60 | 1.35 | | 1.35 | | | | 1.45 |
| 161 | - | | 1.40 | 2.5 | 1.40 | | | | 1.50 |
| 162 | - | | | 2.6 | | | | | |
| 163 | - | | | | | | | | |
| 164 | - | | | 2.6 | | | | | |
| 165 | - | 1.60 | | 2.7 | | | | | |
| 166 | - | 1.65 | | 2.7 | | | | | |
| 167 | - | 1.65 | | 2.8 | | | | | |
| 168 | - | 1.70 | | 2.9 | | | | | |
| 169 | - | 1.70 | | 3.0 | | | 1.20 | | 1.50 |
| 170 | - | 1.75 | | 3.1 | | | 1.25 | | 1.55 |
| 171 | - | 1.80 | | 3.2 | | | 1.25 | | |
| 172 | - | 1.85 | | 3.5 | | 1.20 | 1.30 | 1.20 | |
| 173 | - | 1.90 | | 3.7 | | 1.15 | 1.35 | 1.15 | |
| 174 | - | 1.95 | 1.40 | 4.0 | 1.40 | 1.15 | 1.35 | 1.15 | |
| 175 | - | 2.0 | 1.45 | 4.2 | 1.45 | 1.20 | 1.40 | 1.20 | |
| 176 | - | 2.0 | 1.45 | 4.4 | 1.45 | | | | |
| 177 | - | 2.1 | 1.50 | 4.6 | 1.50 | | | | 1.55 |
| 178 | - | | | 4.7 | | | 1.40 | | 1.50 |
| 179 | - | | | 4.8 | | | 1.35 | | 1.45 |
| 180 | - | 2.1 | | 5.0 | | | | | 1.45 |
| 181 | - | 2.0 | 1.50 | 5.0 | 1.50 | | | | 1.40 |
| 182 | - | | 1.45 | 5.1 | 1.45 | | | | |
| 183 | - | | | 5.2 | | | | | 1.40 |
| 184 | - | | | | | | 1.35 | | 1.45 |
| 185 | - | 2.0 | 1.45 | | 1.45 | | 1.30 | | |
| 186 | - | 1.95 | 1.40 | | 1.40 | | | | |
| 187 | - | 1.95 | | | | | | | |
| 188 | - | 1.90 | 1.40 | 5.2 | 1.40 | 1.20 | 1.30 | 1.20 | |
| 189 | - | 1.80 | 1.35 | 5.3 | 1.35 | 1.15 | 1.25 | 1.15 | |
| 190 | - | 1.75 | | 5.2 | | | | | |
| 191 | - | 1.70 | | 5.2 | | | | | |

Table A. 1 (Continued)

| Day (1979) | Time range (UT) (hrs-min) | SEM Efficiency Factors | | | | | | | |
|---|---|---|---|---|---|---|---|---|---|
| | | Electron ESA's | | | | Proton ESA's | | | |
| | | ∥LE | ∥HE | ⊥LE | ⊥HE | ∥LE | ∥HE | ⊥LE | ⊥HE |
| Operations at bias level 8 | | | | | | | | | |
| 192 | - | 1.70 | 1.35 | 5.1 | 1.35 | 1.15 | 1.25 | 1.15 | 1.50 |
| 193 | - | 1.65 | 1.30 | 5.0 | 1.30 | | | | |
| 194 | - | | | 4.9 | | | | | |
| 195 | - | 1.65 | 1.30 | 4.8 | 1.30 | | | | |
| 196 | - | 1.60 | 1.35 | 4.7 | 1.35 | | | | |
| 197 | - | | | 4.6 | | | | | |
| 198 | - | | | 4.5 | | | | | |
| 199 | - | | | 4.3 | | | | | |
| 200 | - | | | 4.2 | | | | | 1.50 |
| 201 | - | | | 4.0 | | | | | 1.45 |
| 202 | - | | | 3.9 | | | | | |
| 203 | - | | | | | | | | 1.45 |
| 204 | - | | | 3.9 | | | | | 1.40 |
| 205 | - | | | 4.0 | | | | | |
| 206 | - | | | 4.2 | | | | | |
| 207 | - | | | 4.3 | | | | | 1.40 |
| 208 | - | | | 4.4 | | | | | 1.45 |
| 209 | - | | 1.35 | 4.5 | 1.35 | | 1.25 | | |
| 210 | - | | 1.30 | 4.6 | 1.30 | | 1.30 | | |
| 211 | - | | | 4.7 | | | | | 1.45 |
| 212 | - | | | 4.8 | | | | | 1.50 |
| 213 | - | | | 4.9 | | | | | |
| 214 | - | | | 5.0 | | | | | |
| 215 | - | | | 5.1 | | | | | |
| 216 | - | | | 5.2 | | | | | 1.50 |
| 217 | - | | 1.30 | 5.4 | 1.30 | | | | 1.55 |
| 218 | - | 1.60 | 1.35 | 5.5 | 1.35 | | | | |
| 219 | - | 1.65 | | 5.6 | | | | | |
| 220 | - | | | 5.7 | | | | | |
| 221 | - | 1.65 | | 5.9 | | | | | 1.55 |
| 222 | - | 1.70 | | 6.0 | | | | | 1.60 |
| 223 | - | 1.70 | | 6.1 | | | | | |
| 224 | - | 1.75 | | 6.2 | | | | | |
| 225 | - | 1.75 | | 6.4 | | | | | 1.60 |
| 226 | - | 1.80 | 1.35 | 6.6 | 1.35 | | | | 1.65 |
| 227 | - | 1.80 | 1.40 | 6.7 | 1.40 | | | | |
| 228 | - | 1.85 | | 6.8 | | | | | |

Table A. 1 (Continued)

| Day (1979) | Time range (UT) (hrs-min) | SEM Efficiency Factors | | | | | | | |
|---|---|---|---|---|---|---|---|---|---|
| | | Electron ESA's | | | | Proton ESA's | | | |
| | | ∥LE | ∥HE | ⊥LE | ⊥HE | ∥LE | ∥HE | ⊥LE | ⊥HE |
| Operations at bias level 8 | | | | | | | | | |
| 229 | - | 1.90 | 1.40 | 7.0 | 1.40 | 1.15 | 1.30 | 1.15 | 1.65 |
| 230 | - | 1.95 | | 7.2 | | | | | 1.70 |
| 231 | - | 2.0 | | 7.4 | | | | | |
| 232 | - | | | 7.5 | | | | | |
| 233 | - | 2.0 | 1.40 | 7.6 | 1.40 | | | | |
| 234 | - | 2.1 | 1.45 | 7.8 | 1.45 | | | | 1.70 |
| 235 | - | | | 8.0 | | | | | 1.75 |
| 236 | - | | | 8.2 | | | | | |
| 237 | - | | | 8.4 | | | | | |
| 238 | - | | | 8.6 | | | | | 1.75 |
| 239 | - | | | 8.8 | | | | | 1.80 |
| 240 | - | | | 9.0 | | | | | |
| 241 | - | | 1.45 | 9.2 | 1.45 | | | | |
| 242 | - | | 1.50 | 9.4 | 1.50 | | | | 1.80 |
| 243 | - | | | 9.6 | | | | | 1.85 |
| 244 | - | | 1.50 | 9.8 | 1.50 | | | | |
| 245 | - | | 1.40 | 10.0 | 1.40 | | | | |
| 246 | - | | 1.40 | 10.0 | 1.40 | | | | 1.85 |
| 247 | - | | 1.35 | 10.5 | 1.35 | | | | 1.90 |
| 248 | - | | | | | | | | |
| 249 | - | | | 10.5 | | | | | 1.90 |
| 250 | - | | | 11.0 | | | 1.30 | | 1.95 |
| 251 | - | | | | | | 1.35 | | |
| 252 | - | | | 11.0 | | | | | 1.95 |
| 253 | - | 2.1 | | 11.5 | | | | | 2.0 |
| 254 | - | 2.0 | | 11.5 | | | | | |
| 255 | - | | | 12.0 | | | | | |
| 256 | - | | | 12.0 | | | | | |
| 257 | - | | | 12.5 | | | | | |
| 258 | - | | 1.35 | 12.5 | 1.35 | | | | |
| 259 | - | | 1.40 | 13.0 | 1.40 | 1.15 | | 1.15 | |
| 260 | - | | | 13.0 | | 1.20 | | 1.20 | |
| 261 | - | 2.0 | | 13.5 | | | | | |
| 262 | - | 1.95 | 1.40 | 13.5 | 1.40 | | | | |
| 263 | - | 1.90 | 1.45 | 14.0 | 1.45 | | | | |
| 264 | - | | | 14.0 | | | | | |
| 265 | - | | | 14.5 | | | | | |

Table A. 1 (Continued)

| Day (1979) | Time range (UT) (hrs-min) | SEM Efficiency Factors | | | | | | | |
|---|---|---|---|---|---|---|---|---|---|
| | | Electron ESA's | | | | Proton ESA's | | | |
| | | \|\| LE | \|\| HE | ⊥ LE | ⊥ HE | \|\| LE | \|\| HE | ⊥ LE | ⊥ HE |
| **Operations at bias level 8** | | | | | | | | | |
| 266 | - | 1.90 | 1.50 | 14.5 | 1.50 | 1.20 | 1.40 | 1.20 | 2.1 |
| 267 | - | \| | 1.50 | 15.0 | 1.50 | \| | \| | \| | \| |
| 268 | - | \| | 1.55 | 15.0 | 1.55 | \| | \| | \| | \| |
| 269 | - | 1.90 | 1.55 | 15.5 | 1.55 | \| | \| | \| | \| |
| 270 | - | 1.95 | 1.60 | 15.5 | 1.60 | \| | \| | \| | \| |
| 271 | - | 1.95 | 1.60 | 16.0 | 1.60 | \| | \| | \| | \| |
| 272 | - | 2.0 | 1.65 | 16.5 | 1.65 | \| | \| | \| | \| |
| 273 | - | \| | 1.65 | 16.5 | 1.65 | \| | \| | \| | \| |
| 274 | - | 2.0 | 1.70 | 17.0 | 1.70 | \| | \| | \| | \| |
| 275 | - | 2.1 | 1.75 | 17.0 | 1.75 | \| | \| | \| | \| |
| 276 | - | 2.1 | \| | 17.5 | \| | \| | \| | \| | \| |
| 277 | - | 2.2 | \| | 18.0 | \| | \| | \| | \| | \| |
| 278 | - | 2.2 | \| | 18.0 | \| | \| | \| | \| | \| |
| 279 | - | 2.3 | \| | 18.5 | \| | \| | \| | \| | \| |
| 280 | - | \| | \| | 19.0 | \| | \| | \| | \| | \| |
| 281 | - | 2.3 | \| | 19.5 | \| | \| | \| | \| | 2.1 |
| 282 | - | 2.4 | 1.75 | 20. | 1.75 | \| | \| | \| | 2.2 |
| 283 | - | \| | 1.70 | 20. | 1.70 | \| | \| | \| | \| |
| 284 | - | \| | 1.70 | 21. | 1.70 | \| | \| | \| | \| |
| 285 | - | \| | 1.65 | \| | 1.65 | \| | \| | \| | \| |
| 286 | - | \| | 1.65 | 21. | 1.65 | \| | \| | \| | \| |
| 287 | - | \| | 1.60 | 22. | 1.60 | \| | 1.40 | \| | \| |
| 288 | - | \| | 1.60 | 22. | 1.60 | \| | 1.45 | \| | \| |
| 289 | - | \| | 1.55 | 23. | 1.55 | \| | \| | \| | \| |
| 290 | - | 2.4 | \| | \| | \| | \| | \| | \| | \| |
| 291 | - | 2.3 | \| | 23. | \| | \| | \| | \| | \| |
| 292 | - | 2.3 | 1.55 | 24. | 1.55 | 1.20 | \| | 1.20 | \| |
| 293 | 0000-2022 | 2.4 | 1.60 | 20. | 1.60 | 1.15 | \| | 1.15 | \| |
| **Operations at bias level 12** | | | | | | | | | |
| 293 | 2022-2400 | 1.35 | 1.15 | 2.6 | 1.15 | 1.05 | 1.15 | 1.05 | 1.40 |
| 294 | 0000-0057 | 1.35 | 1.15 | 2.6 | 1.15 | 1.05 | 1.15 | 1.05 | 1.40 |
| **Operations at bias level 8** | | | | | | | | | |
| 294 | 0057-2400 | 2.5 | 1.70 | 2 0 | 1.70 | 1.15 | 1.50 | 1.15 | 2.2 |
| 295 | 0000-1941 | 2.7 | 1.70 | 2 5 | 1.70 | 1.15 | 1.50 | 1.15 | 2.2 |

Table A.1 (Continued)

| Day (1979) | Time range (UT) (hrs-min) | SEM Efficiency Factors | | | | | | | |
|---|---|---|---|---|---|---|---|---|---|
| | | Electron ESA's | | | | Proton ESA's | | | |
| | | \|\|LE | \|\|HE | ⊥LE | ⊥HE | \|\|LE | \|\|HE | ⊥LE | ⊥HE |
| Operations at bias level 12 | | | | | | | | | |
| 295 | 1941-2400 | 1.50 | 1.20 | 3.0 | 1.20 | 1.05 | 1.15 | 1.05 | 1.40 |
| 296 | 0000-0133 | 1.50 | 1.20 | 3.0 | 1.20 | 1.05 | 1.15 | 1.05 | 1.40 |
| Operations at bias level 8 | | | | | | | | | |
| 296 | 0133-2400 | 3.0 | 1.80 | 3.0 | 1.80 | 1.15 | 1.50 | 1.15 | 2.2 |
| 297 | 0000-2256 | 3.5 | 1.80 | 3.0 | 1.80 | 1.15 | 1.55 | 1.15 | 2.2 |
| Operations at bias level 12 | | | | | | | | | |
| 297 | 2256-2400 | 1.70 | 1.20 | 10. | 1.20 | 1.05 | 1.15 | 1.05 | 1.40 |
| 298 | 0000-0152 | 1.70 | 1.20 | 10. | 1.20 | 1.05 | 1.15 | 1.05 | 1.40 |
| Operations at bias level 8 | | | | | | | | | |
| 298 | 0152-1627 | 4.5 | 1.80 | 200 | 1.80 | 1.15 | 1.55 | 1.15 | 2.8 |
| Operations at bias level 12 | | | | | | | | | |
| 298 | 1627-2400 | 1.9 | 1.25 | 25 | 1.25 | 1.05 | 1.15 | 1.05 | 1.45 |
| 299 | 0000-0007 | 1.9 | 1.25 | 25 | 1.25 | 1.05 | 1.15 | 1.05 | 1.45 |
| Operations at bias level 8 | | | | | | | | | |
| 299 | 0007-1502 | 6.5 | 1.80 | 500 | 1.80 | 1.15 | 1.55 | 1.15 | 3.1 |
| Operations at bias level 12 | | | | | | | | | |
| 299 | 1502-2252 | 2.5 | 1.25 | 25 | 1.25 | 1.05 | 1.15 | 1.05 | 1.50 |
| Operations at bias level 8 | | | | | | | | | |
| 299 | 2252-2400 | 9.0 | 1.80 | 450 | 1.80 | 1.15 | 1.55 | 1.15 | 3.2 |
| 300 | 0000-0108 | 9.0 | 1.80 | 450 | 1.80 | 1.15 | 1.55 | 1.15 | 3.2 |

Table A. 1 (Continued)

| Day (1979) | Time range (UT) (hrs-min) | SEM Efficiency Factors: Electron ESA's ‖LE | ‖HE | ⊥LE | ⊥HE | Proton ESA's ‖LE | ‖HE | ⊥LE | ⊥HE |
|---|---|---|---|---|---|---|---|---|---|
| **Operations at bias level 12** | | | | | | | | | |
| 300 | 0108-1200 | 4.5 | 1.25 | 30 | 1.25 | 1.05 | 1.15 | 1.05 | 1.50 |
| 300 | 1200-2400 | 3.5 | 1.30 | 30 | 1.30 | | | | |
| 301 | 0000-1200 | 2.6 | | 25 | | | | | |
| 301 | 1200-2400 | 2.4 | | | | | | | |
| 302 | 0000-1200 | 2.3 | | | | | | | |
| 302 | 1200-2400 | 2.1 | | 25 | | | | | |
| 303 | 0000-1200 | 2.0 | | 20 | | | | | |
| 303 | 1200-2400 | 1.9 | | | | | | | |
| 304 | - | 1.8 | | 20 | | | | | |
| 305 | 0000-1350 | 1.8 | 1.30 | 18 | 1.30 | 1.05 | 1.15 | 1.05 | 1.50 |
| **Operations at bias level 8** | | | | | | | | | |
| 305 | 1350-1457 | 3.5 | 1.8 | 130 | 1.8 | 1.15 | 1.55 | 1.15 | 3.5 |
| **Operations at bias level 12** | | | | | | | | | |
| 305 | 1457-2400 | 1.7 | 1.30 | 17 | 1.30 | 1.05 | 1.15 | 1.05 | 1.50 |
| 306 | - | 1.65 | | 16 | | | | | |
| 307 | - | 1.60 | | 15 | | | | | |
| 308 | 0000-0326 | 1.60 | 1.30 | 15 | 1.30 | 1.05 | 1.15 | 1.05 | 1.50 |
| **Operations at bias level 8** | | | | | | | | | |
| 308 | 0326-0347 | 2.9 | 1.8 | 95 | 1.8 | 1.15 | 1.55 | 1.15 | 3.3 |
| **Operations at bias level 12** | | | | | | | | | |
| 308 | 0347-2256 | 1.60 | 1.30 | 14 | 1.30 | 1.05 | 1.15 | 1.05 | 1.50 |
| **Operations at bias level 8** | | | | | | | | | |
| 308 | 2256-2400 | 2.9 | 1.8 | 90 | 1.8 | 1.15 | 1.55 | 1.15 | 3.2 |
| 309 | - | 2.7 | | 85 | | | 1.45 | | 2.9 |
| 310 | - | | 1.8 | 80 | 1.8 | | 1.40 | | 2.6 |
| 311 | - | | 1.75 | 75 | 1.75 | | | | 2.3 |
| 312 | - | | | 70 | | | | | |
| 313 | - | | | 65 | | | | | |

Table A. 1 (Continued)

| Day (1979) | Time range (UT) (hrs-min) | SEM Efficiency Factors | | | | | | | |
|---|---|---|---|---|---|---|---|---|---|
| | | Electron ESA's | | | | Proton ESA's | | | |
| | | \|\| LE | \|\| HE | ⊥ LE | ⊥ HE | \|\| LE | \|\| HE | ⊥ LE | ⊥ HE |
| **Operations at bias level 8** | | | | | | | | | |
| 314 | - | 2.6 | 1.70 | 60 | 1.70 | 1.15 | 1.40 | 1.15 | 2.3 |
| 315 | - | | | 58 | | | | | |
| 316 | - | | | 54 | | | | | |
| 317 | - | | | 52 | | | | | |
| 318 | - | | 1.70 | 50 | 1.70 | | | | |
| 319 | - | 2.6 | 1.65 | 48 | 1.65 | | | | |
| 320 | - | 2.5 | | 46 | | | | | |
| 321 | - | | | 44 | | | | | |
| 322 | - | | | 44 | | | | | |
| 323 | - | | | 42 | | | | | |
| 324 | - | | 1.65 | 42 | 1.65 | | | | |
| 325 | - | 2.5 | 1.60 | 40 | 1.60 | | | | |
| 326 | - | 2.4 | | 40 | | | | | |
| 327 | - | | | 38 | | | | | |
| 329 | - | | 1.60 | | 1.60 | | | | |
| 330 | - | | 1.55 | | 1.55 | | | | |
| 331 | - | 2.4 | | 38 | | | | | |
| 332 | - | 2.3 | | 36 | | | | | |
| 333 | - | | | | | | | | |
| 334 | - | | 1.55 | | 1.55 | | | | |
| 335 | - | | 1.50 | | 1.50 | | | | |
| 336 | - | | | | | | | | |
| 337 | - | 2.3 | | 36 | | | | | |
| 338 | 0000-0811 | 2.2 | | 34 | | | | | |
| **Operations at bias level 12** | | | | | | | | | |
| 338 | 0811-0851 | 1.30 | 1.10 | 4.0 | 1.10 | 1.05 | 1.10 | 1.05 | 1.30 |
| **Operations at bias level 8** | | | | | | | | | |
| 338 | 0851-2400 | 3.2 | 1.50 | 50 | 1.50 | 1.15 | 1.40 | 1.15 | 2.3 |
| 339 | 0000-0746 | 3.2 | 1.50 | 50 | 1.50 | 1.15 | 1.40 | 1.15 | 2.3 |
| **Operations at bias level 12** | | | | | | | | | |
| 339 | 0746-0902 | 1.70 | 1.10 | 6.0 | 1.10 | 1.05 | 1.10 | 1.05 | 1.30 |

Table A.1 (Continued)

| Day (1979) | Time range (UT) (hrs-min) | SEM Efficiency Factors: Electron ESA's: ∥LE | ∥HE | ⊥LE | ⊥HE | Proton ESA's: ∥LE | ∥HE | ⊥LE | ⊥HE |
|---|---|---|---|---|---|---|---|---|---|
| Operations at bias level 8 | | | | | | | | | |
| 339 | 0902-1200 | 5.5 | 1.50 | 800 | 1.50 | 1.15 | 1.40 | 1.15 | 2.3 |
| 339 | 1200-2400 | 5.5 | | 600 | | | | | |
| 340 | 0000-0741 | 5.0 | 1.50 | 450 | 1.50 | 1.15 | 1.40 | 1.15 | 2.3 |
| Operations at bias level 12 | | | | | | | | | |
| 340 | 0741-0906 | 1.85 | 1.10 | 28 | 1.10 | 1.05 | 1.10 | 28 | 1.10 |
| Operations at bias level 8 | | | | | | | | | |
| 340 | 0906-1200 | 5.0 | 1.50 | 400 | 1.50 | 1.15 | 1.40 | 1.15 | 2.3 |
| 340 | 1200-2400 | 4.5 | | 350 | | | | | |
| 341 | 0000-1200 | 4.5 | | 250 | | | | | |
| 341 | 1200-2400 | 4.0 | 1.50 | 200 | 1.50 | | | | |
| 342 | 0000-1200 | 3.8 | 1.45 | 150 | 1.45 | | | | |
| 342 | 1200-2400 | 3.6 | | 130 | | | | | |
| 343 | - | 3.2 | | 100 | | | | | |
| 344 | - | 2.9 | | 75 | | | | | |
| 345 | - | 2.7 | | 60 | | | | | |
| 346 | - | 2.5 | | 50 | | | | | |
| 347 | - | 2.3 | 1.45 | 46 | 1.45 | | | | |
| 348 | - | 2.2 | 1.40 | 43 | 1.40 | | | | |
| 349 | - | 2.1 | | 40 | | | | | |
| 350 | - | | | 38 | | | | | |
| 351 | - | 2.1 | | 37 | | | | | |
| 352 | - | 2.0 | | 36 | | | | | |
| 353 | - | | | 35 | | | | | |
| 354 | - | | | 35 | | | | | |
| 355 | - | 2.0 | | 36 | | | | | |
| 356 | - | 2.1 | | 37 | | | | | |
| 357 | - | | | 38 | | | | | |
| 358 | - | | | 40 | | | | | |
| 359 | - | 2.1 | | 44 | | | | | |
| 360 | - | 2.2 | | 46 | | | | | |

Table A. 1 (Continued)

| Day (1979) | Time range (UT) (hrs-min) | SEM Efficiency Factors | | | | | | | |
|---|---|---|---|---|---|---|---|---|---|
| | | Electron ESA's | | | | Proton ESA's | | | |
| | | \|\|LE | \|\|HE | ⊥LE | ⊥HE | \|\|LE | \|\|HE | ⊥LE | ⊥HE |
| Operations at bias level 8 | | | | | | | | | |
| 361 | - | 2.2 | 1.45 | 48 | 1.45 | 1.15 | 1.40 | 1.15 | 2.3 |
| 362 | - | 2.2 | \| | 50 | \| | \| | \| | \| | \| |
| 363 | - | 2.3 | \| | 52 | \| | \| | \| | \| | \| |
| 364 | - | 2.3 | \| | 54 | \| | \| | \| | \| | \| |
| 365 | - | 2.4 | 1.45 | 54 | 1.45 | 1.15 | 1.40 | 1.15 | 2.3 |
| Day (1980) | | | | | | | | | |
| 1 | - | 2.5 | 1.45 | 56 | 1.45 | 1.15 | 1.40 | 1.15 | 2.3 |
| 2 | - | \| | 1.45 | 56 | 1.45 | \| | \| | \| | \| |
| 3 | - | \| | 1.50 | 58 | 1.50 | \| | \| | \| | \| |
| 4 | - | 2.5 | \| | \| | \| | \| | \| | \| | \| |
| 5 | - | 2.4 | \| | \| | \| | \| | \| | \| | \| |
| 6 | - | 2.4 | \| | \| | \| | \| | \| | \| | \| |
| 7 | - | 2.3 | \| | \| | \| | \| | \| | \| | \| |
| 8 | - | 2.2 | \| | \| | \| | \| | \| | \| | \| |
| 9 | - | 2.1 | \| | \| | \| | \| | \| | \| | \| |
| 10 | - | 2.0 | \| | \| | \| | \| | \| | \| | \| |
| 11 | - | 2.0 | 1.50 | 58 | 1.50 | \| | \| | \| | \| |
| 12 | - | 2.1 | 1.55 | 56 | 1.55 | \| | \| | \| | \| |
| 13 | - | \| | \| | \| | \| | \| | \| | \| | \| |
| 14 | - | \| | \| | 56 | \| | \| | \| | \| | \| |
| 15 | - | \| | \| | 54 | \| | \| | \| | \| | \| |
| 16 | - | 2.1 | \| | \| | \| | \| | \| | \| | \| |
| 17 | - | 2.2 | \| | 54 | \| | \| | \| | \| | \| |
| 18 | - | \| | \| | 52 | \| | \| | \| | \| | \| |
| 19 | - | \| | \| | 52 | \| | \| | \| | \| | \| |
| 20 | - | \| | \| | 50 | \| | \| | \| | \| | \| |
| 21 | - | 2.2 | \| | 50 | \| | \| | \| | \| | \| |
| 22 | - | 2.3 | \| | 48 | \| | \| | \| | \| | \| |
| 23 | - | \| | \| | 48 | \| | \| | \| | \| | \| |
| 24 | - | \| | \| | 46 | \| | \| | \| | \| | \| |
| 25 | - | \| | \| | 46 | \| | \| | \| | \| | \| |
| 26 | - | 2.3 | \| | 44 | \| | \| | \| | \| | \| |
| 27 | - | 2.4 | \| | 44 | \| | \| | \| | \| | \| |
| 28 | - | \| | \| | 42 | \| | \| | \| | \| | \| |
| 29 | - | \| | \| | 42 | \| | \| | \| | \| | \| |

Table A.1 (Continued)

| Day (1980) | Time range (UT) (hrs-min) | SEM Efficiency Factors | | | | | | | |
|---|---|---|---|---|---|---|---|---|---|
| | | Electron ESA's | | | | Proton ESA's | | | |
| | | \|\| LE | \|\| HE | ⊥ LE | ⊥ HE | \|\| LE | \|\| HE | ⊥ LE | ⊥ HE |
| Operations at bias level 8 | | | | | | | | | |
| 30 | - | 2.4 | 1.55 | 42 | 1.55 | 1.15 | 1.40 | 1.15 | 2.4 |
| 31 | - | 2.5 | | 40 | | | | | |
| 32 | - | | | | | | | | |
| 33 | - | | | | | | | | 2.4 |
| 34 | - | 2.5 | | | | | | | 2.5 |
| 35 | - | 2.6 | 1.55 | | 1.55 | | | | |
| 36 | - | | 1.60 | | 1.60 | | | | |
| 37 | - | | | | | | | | |
| 38 | - | 2.6 | 1.60 | | 1.60 | | | | 2.5 |
| 39 | - | 2.7 | 1.65 | 40 | 1.65 | | | | 2.6 |
| 40 | - | | 1.65 | 42 | 1.65 | | | | |
| 41 | - | | 1.70 | | 1.70 | | | | |
| 42 | - | 2.7 | 1.70 | 42 | 1.70 | | | | |
| 43 | - | 2.8 | 1.75 | 44 | 1.75 | | | | 2.6 |
| 44 | - | | 1.75 | 44 | 1.75 | | | | 2.7 |
| 45 | - | 2.8 | 1.80 | 46 | 1.80 | | | | |
| 46 | - | 2.9 | 1.80 | 46 | 1.80 | | | | |
| 47 | - | | 1.85 | 48 | 1.85 | | | | 2.7 |
| 48 | - | | 1.85 | 50 | 1.85 | | | | 2.8 |
| 49 | - | 2.9 | 1.90 | 50 | 1.90 | | | | |
| 50 | - | 3.0 | 1.90 | 52 | 1.90 | 1.15 | 1.40 | 1.15 | 2.8 |
| 160 | - | 6.5 | 2.5 | 650 | 2.8 | 1.55 | 2.1 | 1.15 | 9.0 |
| 161 | - | | 2.6 | | 3.0 | | 2.2 | | |
| 162 | - | | 2.8 | | 3.2 | | 2.3 | | |
| 163 | - | | 3.0 | | 3.5 | | 2.4 | | |
| 164 | - | | 3.2 | | 3.7 | | 2.5 | | |
| 165 | - | | 3.5 | | 4.0 | | 2.7 | | |
| 166 | - | 6.5 | 3.7 | 650 | 4.4 | 1.55 | 2.8 | 1.15 | 9.0 |

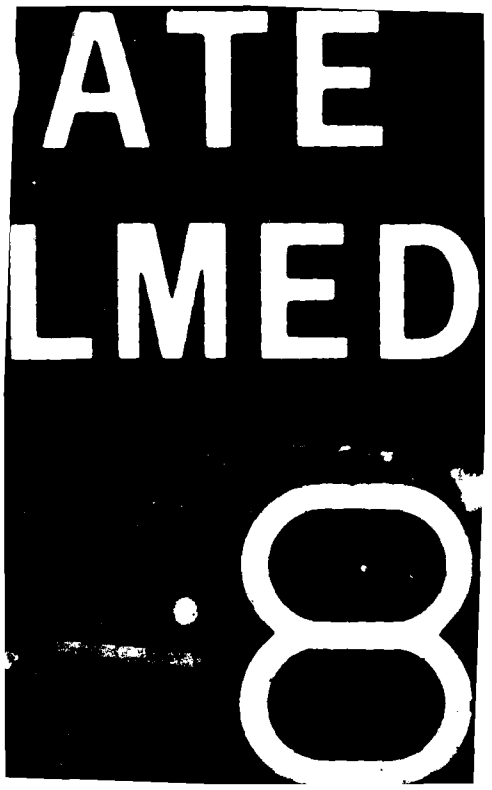
ATE
LMED
8